

THOMAS S BEDWELL
DEVELOPMENT OF MOLECULARLY
IMPRINTED ASSAYS TARGETING
PEPTIDES AND PROTEINS

Thesis submitted for the degree of Doctor of Philosophy
Department of Chemistry, University of Leicester
September, 2018

ABSTRACT

Many efforts have been made to produce artificial materials with bio-mimetic properties for diagnostics and life science applications. Among these efforts the technique of molecular imprinting has received much attention, however challenges regarding imprinting of biologically relevant analytes are important to overcome if the technology is to reach its full potential. The lack of generality amongst current molecularly imprinted assay formats is a further discouraging factor against the adoption of molecularly imprinted assays over conventional immunoassays. Whilst many elegant methods for specific templates have been devised, a simple, universal format applicable to any analyte of interest would be a far more attractive prospect.

The work presented in this thesis aims to address these challenges. A novel screening tool for optimisation of polymerisation mixtures taking advantage of solid-phase imprinting has been developed and applied to both peptides and proteins. The molecularly imprinted polymers (MIPs) generated in this manner have then been applied to a number of assay formats, with the intention of designing a biologic-free assay for target peptides. The potential application of these techniques has then been demonstrated using a model protein, acetylcholinesterase (AChE). A novel epitope mapping approach has been utilised to identify peptide sequences useful as templates for MIP generation for site specific binding to AChE. Changes in structure and enzymatic activity as a result of binding interactions have been investigated, presenting an opportunity for development of novel allosteric MIP based enzyme activators. The site specific binding has been further exploited in the final application in detection of AChE in a novel sandwich assay format.

In this way, it has been demonstrated that this process can be used to identify unknown binding sites on a protein, generate high affinity recognition materials for these sites, and then use these in a generic assay format for detection of the original protein of interest.

ACKNOWLEDGEMENTS

First and foremost I would like to thank Prof Sergey Piletsky for all the support and guidance he has given me throughout the duration of my PhD, despite my frequent reluctance to accept that he is always right. I would also like to thank Dr Mike Whitcombe for offering me the opportunity to work on such an exciting project, and Dr Jonathan Wingfield for hosting me during my time working at AstraZeneca. This research would not have been possible without funding from the Biotechnology and Biological Sciences Research Council (BBSRC) and from the industrial partner for the project, AstraZeneca, and so I am very thankful for their generosity.

I would like to express my gratitude to Francesco Canfarotta, Joanna Czulak and Antonio Guerreiro for always being willing to share their extensive practical experience despite being far too busy helping every other member of the lab. Your selflessness is greatly appreciated. Thank you to all of the students who have worked with me over the years; in particular Xi Jin, Nadeem Anjum, Yifeng Ma, and Justine Foiret. Without your hard work there would certainly be parts of this thesis left unfinished, and so I am very grateful to you all.

To the many friends who have passed through our lab over the years, those scattered throughout the department of chemistry, and those further afield; there are too many to name you all, but my thanks go to all of you. It has not always been easy, and I truly appreciate the support I have received from so many people.

Finally, I would like to express my sincerest gratitude to my family, who have always supported me throughout all of my endeavours.

CONTENTS

CHAPTER 1: INTRODUCTION.....	1
1.1. Molecularly imprinted polymers as synthetic receptors	1
1.2. Development of molecularly imprinted assays.....	3
1.3. Radio-labelled MIAs	7
1.4. Fluorescence-based MIAs	8
1.4.1. Heterogeneous fluorescent assays.....	9
1.4.2. Homogenous fluorescent assays	10
1.5. Enzyme-linked MIAs	13
1.6. Other MIA formats.....	16
1.7. MIAs targeting peptides and proteins	22
1.8. Prospects for diagnostic applications	24
1.9. Aims of the project.....	25
CHAPTER 2: MOLECULAR IMPRINTING OF PEPTIDES AND PROTEINS	26
2.1. Introduction.....	27
2.2. Small scale synthesis screening strategy.....	30
2.3. Polymer composition for imprinting of peptides	31
2.4. Polymer composition for imprinting of proteins.....	36
2.5. Conclusions.....	38
CHAPTER 3: DEVELOPMENT OF A GENERIC HOMOGENOUS ASSAY FORMAT	39
3.1. Introduction.....	40
3.2. Fluorescence polarisation molecularly imprinted assay.....	44
3.3. Molecularly imprinted magnetic nanoparticle assay.....	48
3.4. Conclusions.....	53
CHAPTER 4: APPLICATION TO A MODEL SYSTEM - ACETYLCHOLINESTERASE	55
4.1. Introduction.....	56

4.2. Identification of EeAChE epitopes for synthesis of MIP NPs	61
4.3. Synthesis and characterisation of MIP NPs	63
4.4. Modulation of enzyme activity	65
4.5. Prevention and regeneration following inhibition	69
4.6. Sandwich MINA for the detection of AChE	72
4.7. Conclusions.....	76
CHAPTER 5: FINAL CONCLUSIONS AND FUTURE WORK	77
CHAPTER 6: EXPERIMENTAL.....	79
6.1. General information	79
6.2. Preparation of template-derivatised solid phase.....	80
6.2.1. Activation of glass microspheres.....	80
6.2.2. Silanisation of glass microspheres.....	80
6.2.3. Immobilisation of peptides	81
6.2.4. Immobilisation of proteins	81
6.3. Solid phase synthesis of MIP NPs	82
6.4. Analysis of the size of MIP NPs	82
6.5. MIP affinity measurements by SPR	83
6.6. Small scale synthesis screen with filtration microplates	83
6.7. Fluorescent labelling of EPEGIpYGV-KKK-C	84
6.8. FPMIA for EPEGIpYGV-KKK-C	85
6.9. Preparation of template-derivatised mNPs.....	85
6.10. MINA for FRFSFVPV-GG-C	85
6.11. Epitope mapping of AChE.....	86
6.12. Structural modelling of AChE.....	87
6.13. Circular dichroism measurements.....	87
6.14. Enzyme activity assays	87
6.15. Synthesis of mMIPs	88
6.16. Sandwich MINA for AChE	88
CHAPTER 7: REFERENCES	89

ABBREVIATIONS

β -CD	β -cyclodextrin
2,4-D	2,4-dichlorophenoxyacetic acid
AAc	Acrylic acid
AAm	Acrylamide
AChE	Acetylcholinesterase
AD	Alzheimer's disease
AFP	α -fetoprotein
APMA	<i>N</i> -(3-aminopropyl)methacrylamide
APS	Ammonium persulfate
BIS	<i>N,N</i> -methylenebisacrylamide
BSA	Bovine serum albumin
CAP	Chloramphenicol
CEA	Carcinoembryonic antigen
DDV	Dichlorvos
DLS	Dynamic light scattering
EeAChE	<i>Electrophorus electricus</i> acetylcholinesterase
ELISA	Enzyme-linked immunosorbent assay
FP	Fluorescence polarisation
FPMIA	Fluorescence polarisation molecularly imprinted assay
hAChE	Human acetylcholinesterase
HBS	HEPES buffered saline
HEPES	4-(2-hydroxyethyl)-1-piperazineethanesulfonic acid
HRP	Horseradish peroxidase
IPP	Imprinted photonic polymers
LOD	Limit of detection
mAbs	Monoclonal antibodies

MIA	Molecularly imprinted [sorbent] assay
MINA	Molecularly imprinted nanoparticle assay
MIN	Molecularly imprinted nanoparticle
MIP	Molecularly imprinted polymer
MIP NP	Molecularly imprinted polymer nanoparticle
mMIP	Magnetic molecularly imprinted polymer
mNP	Magnetic nanoparticle
mP	Millipolarisation unit
MS	Mass spectrometry
NIPAm	<i>N</i> -isopropylacrylamide
OP	Organophosphate
PAS	Peripheral anionic site
PBS	Phosphate buffered saline
PenG	Penicillin G
QCM	Quartz crystal microbalance
QD	Quantum dot
SIA	Succinimidyl iodoacetate
SPR	Surface plasmon resonance
TBA _m	<i>N-tert</i> -butylacrylamide
TEM	Transmission electron microscopy
TEMED	<i>N,N,N',N'</i> -tetramethylethylenediamine
TMB	3,3',5,5'-tetramethylbenzidine

CHAPTER 1: INTRODUCTION

1.1. Molecularly imprinted polymers as synthetic receptors

Specific receptor–ligand interactions are a fundamental process in biological systems, essential for the generation of physiological responses to substances such as hormones, proteins, cellular markers, antigens etc. The specific nature of biological recognition, in particular of antibodies and enzymes, has led to their exploitation as the recognition element of choice in many assay systems and biosensors. However, despite possessing high specificity and sensitivity for their respective ligands, biomolecules suffer the disadvantages of fragility and high cost. The ability to mimic the highly specific nature of antibodies and enzymes in more robust and lower cost materials has been of great interest to researchers in the field. Consequently, much effort has been expended in the design and synthesis of artificial materials with biomimetic properties. Among these, the technique of molecular imprinting has received much attention because of the high selectivity obtainable for molecules of interest. Coupled with the advantages of short synthesis time, robustness, regeneration (and consequently cost efficiency), as well as cheap initial production, molecularly imprinted polymers (MIPs) provide an attractive alternative to conventional biological receptors.

The process of molecular imprinting involves the synthesis of a polymeric material in the presence of a template, producing complementary recognition sites in the imprinted polymer that are specific for the template molecule (Figure 1). This is achieved by addition of the template to a polymerisation mixture comprising functional monomer, cross-linking agent, and solvent (sometimes referred to as the porogen). A prepolymerisation complex is initially formed, with functional monomers arranging themselves around the template in a manner influenced by the shape and chemical properties of the template. Subsequent polymerisation of this complex fixes the monomers in this arrangement, and removal of the template affords a complementary recognition site for the template molecule. In this way, an imprinted polymer is constructed with molecular memory for the substrate of interest by a self-assembly process.¹⁻⁶

This simple concept is applicable to a large variety of target molecules, ranging from ions and small molecules to macromolecules (e.g. proteins) and microorganisms. As a

result, molecular imprinting has been utilised in a number of applications, including purification and separation,^{7, 8} sensing,⁹ catalysis,¹⁰ drug delivery,¹¹ and of particular importance to this work, in a variety of assay formats.¹²

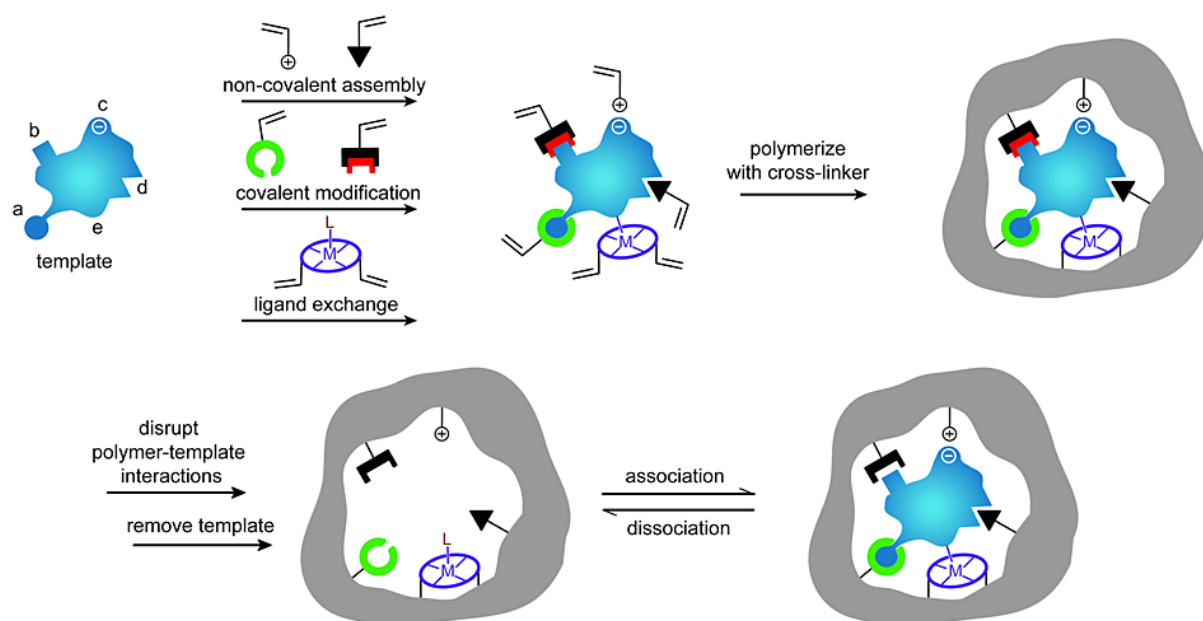


Figure 1. A schematic representation of the molecular imprinting process. The formation of reversible interactions between the template and polymerisable functionality may involve one or more of the following interactions: reversible covalent bonds (a), covalently attached polymerisable binding groups that are activated for non-covalent interaction by template cleavage (b), electrostatic interactions (c), hydrophobic or van der Waals interactions (d), or co-ordination with a metal centre (e); each formed with complementary functional groups or structural elements of the template. Reproduced from Alexander et al.¹ with permission from John Wiley and Sons.

1.2. Development of molecularly imprinted assays

Once imprinted polymers could be generated with affinity and selectivity comparable to biological antibodies, the potential to compete as a genuine synthetic alternative in assays became possible. In 1993, Vlatakis et al. described such an assay, coining the term “molecularly imprinted [sorbet] assay” (MIA).¹³ Imprinted polymers of ethylene dimethacrylate-co-methacrylic acid were prepared by bulk polymerisation against two chemically unrelated drugs, theophylline (a bronchodilator) and diazepam (a tranquilizer). The MIPs were successfully employed in assays analogous to competitive radiolabelled immunoassays, achieving impressive results: for theophylline, measurements were linear over the range of 14-224 μM , the results of analysis of serum samples from 32 patients showed excellent correlation with those obtained using the enzyme-multiplied immunoassay technique, and cross-reactivity against other major metabolites and structurally similar compounds was shown to be similar to that observed with biological antibodies. Whilst these results were encouraging, the MIA method was more cumbersome than the enzyme-multiplied immunoassay technique as a consequence of the necessary extraction of analyte from the biological sample prior to analysis, due to the polymers giving optimal binding and selectivity only in organic solvents.

Molecular imprinting of morphine and the endogenous neuropeptide [Leu5]-enkephalin in methacrylic acid-ethylene glycol dimethacrylate copolymers and their application to a similar radioactive ligand binding assay were described by Andersson et al. in 1995.¹⁴ These MIPs demonstrated high binding affinity and selectivity in aqueous buffers as well as organic solvents, presenting a major breakthrough for molecular imprinting technology since the binding reactions were now occurring under conditions relevant to biological systems. Although efficient rebinding was possible in aqueous buffers, the affinities and selectivities obtained were lower than those obtained in the best organic solvents.

The influence of parameters affecting ligand binding in water were subject to further study, and an optimisation of the assay conditions for (S)-propranolol afforded similarly high sensitivity under both organic and aqueous conditions, with limits of detection (LOD) as low as 5.5 and 6.0 nM, respectively.¹⁵ This represented a 100- to 1000-fold improvement compared to LODs previously achieved with MIPs, placing both aqueous and organic solvent-based MIAs on the same level as immunoassays using biological antibodies.

Having developed analyte-MIP systems that may be utilised equally well using an aqueous buffer or an organic solvent, progression into direct assay of biological samples was next to be reported. Using (S)-propranolol MIPs prepared in the same manner as the aforementioned study, a radiolabelled assay for direct determination of the

concentration of (S)-propranolol in human plasma and urine was accomplished over the range of 20 to 1000 nM with accuracies of 89%-107% and 91%-125%, respectively.¹⁶ These results demonstrated that it was possible to carry out molecular imprint-based assays of biological samples without prior sample clean up.

Whilst attempting to develop a detection system for the herbicide 2,4-dichlorophenoxyacetic acid (2,4-D), Haupt et al., following limited success imprinting in the presence of nonpolar solvents, investigated whether specific noncovalent molecular imprints could be obtained in the presence of polar solvents using a combination of the hydrophobic effect and ionic interactions.¹⁷ The template 2,4-D functioned well in this role owing to its hydrophobic aromatic ring and ionisable carboxyl group. Polymers synthesised using 4-vinylpyridine as functional monomer and ethylene glycol dimethacrylate as cross-linker demonstrated an appreciable binding specificity and sensitivity comparable to indirect enzyme-linked immunosorbent assay (ELISA) or radioimmunoassay. These findings extended the potential applicability of noncovalent molecular imprinting to assays in cases where either the use of polar solvents may be required, or the target molecule may lack the functionality required for imprinting in nonpolar solvents.

Despite the undeniable advantage provided by the possibility of using radiolabelled tracers with identical chemical structure to the analyte of interest, issues concerning the commercial unavailability of isotopic-labelled tracers for many compounds of interest coupled with apprehensions over the handling and disposal of radionuclides made the development of assays based on other labelling and detection methods an attractive proposition. The first MIA to remove the necessity for radiolabelling was developed by Piletsky et al., who utilised competition between a fluorescein-labelled triazine analogue and unlabelled triazine for specific binding sites in an imprinted polymer to achieve an optical sensor based on fluorescence measurement.¹⁸ This assay exhibited sensitivity for triazine over the range 0.01–100 mM, demonstrating that highly sensitive optical assays based on safe fluorescent labels could offer a promising alternative to the currently adopted radiolabelling approach.

An alternative approach to utilise changes in fluorescence as the detection mechanism led to the design of a fluorescent functional monomer: *trans*-4-[p-(*N,N*-dimethylamino)styryl]-*N*-vinylbenzenepyridinium chloride.¹⁹ This monomer combined microenvironmental sensitive fluorescence, attributable to intramolecular charge-transfer behaviour, with a positive charge capable of association with negatively charged nucleotides, together with a vinyl group, necessary for incorporation into the polymer matrix. With these characteristics, the monomer was incorporated within a methacrylate polymer, where it acted as both the recognition and detection element for the fluorescence determination of adenosine 3',5'-cyclic monophosphate in aqueous media. The binding led to a quantifiable quenching of fluorescence, whereas almost no effect was observed in the presence of the structurally similar molecule guanosine 3'5'-cyclic monophosphate. Whilst this demonstrated the utility of modifying the MIP rather than analyte in order to elicit a response to binding, the use of fluorophores which act

simultaneously as both recognition element and detection element means that new monomers will need to be specifically designed for each class of analyte.

Another substitute to radiolabelling commonly employed in immunoassays involves the incorporation of enzyme labels; however, these initially seemed less suitable in MIAs for two reasons: firstly, enzymes often only work in aqueous buffers, and secondly the hydrophobic nature and highly cross-linked structure of the polymers was proposed to limit the access of large protein molecules to the imprinted sites. As previously discussed, MIPs which perform well in aqueous solvents had been developed, however the second problem of binding site accessibility could not be circumvented until the technique of MIP synthesis via precipitation polymerisation to yield monodisperse, spherical polymer particles in the micron-scale range was realised.

Following their initial application to radiolabelled assays against theophylline and 17β -estradiol, where the imprinted microspheres demonstrated higher binding site densities and more rapid kinetics as a direct consequence of their small bead diameter²⁰, the potential use of molecularly imprinted microspheres in ELISA-like assays was tested. The assay developed by Surugiu et al. was specific for the herbicide 2,4-D and used the enzyme label tobacco peroxidase as a conjugate tracer for colorimetric and chemiluminescence detection, with calibration curves ranging from 40-600 $\mu\text{g mL}^{-1}$ and 1-200 $\mu\text{g mL}^{-1}$, respectively.²¹ Even though this assay was still less sensitive than some antibody-based assays, the findings showed for the first time that imprinted polymers could be compatible with enzyme labels, broadening the potential for the application of MIPs in immunoassay-type applications.

Identifying the ever-increasing demand for automated, high-throughput assaying and screening of natural products, as well as of biological and chemical combinatorial libraries, the same group decided to adapt their ELISA-type MIP-based imaging assay for this purpose.²² Microtiter plates (96 or 384 wells) were coated with polymer microspheres imprinted with 2,4-D, which were fixed in place using poly(vinyl alcohol) as glue. Using a competitive format, the amount of polymer-bound 2,4-D-peroxidase conjugate was quantified using luminol as the chemiluminescent substrate. Light emission was consequently measured in a high-throughput imaging format with a CCD camera-based imaging system, allowing simultaneous measurement of a large number of samples. The detection limit of 2,4-D in this assay was 34 nM, with a useful range from 68 nM to 680 μM —a dynamic range only slightly narrower than that reported for antibody-based assays (although the antibody-based assays did have lower detection limits).

Further optimisation for high throughput screening purposes led to a novel assay aimed at eliminating the requirement for a separation step prior to quantification of the target analyte, in order to greatly increase sample throughput.²³ Generation of the binding signal was based on the principle of proximity scintillation between a scintillation fluor covalently incorporated into the MIP microparticles during preparation and the tritium-labelled analyte. Following radiolabelled ligand binding, the scintillation fluor converts incident β -radiation into a fluorescent signal, removing any

need for separation of bound and unbound analyte prior to signal quantification (Figure 2). Although this was the first demonstration of a homogenous MIP assay, the use of radiolabelled tracers was a step back from recent advances, where their usage was largely replaced by that of fluorescent and enzymatic tracers for reasons previously discussed.

The aforementioned examples demonstrate the landmark events in MIA developments; establishing the core labelling strategies, advances in solvent compatibility, and adaptations to high-throughput and homogenous assay formats. Of the MIAs developed since the initial work of Vlatakis et al., the majority can be classified into one of three categories determined by the type of label used for signalling: radio-labelled, fluorescence-labelled, or enzyme-linked. Recent years have seen the emergence of numerous novel assay types that do not fall into these categories; however, as each is seemingly unique in its approach, these have been grouped as “other” for simplicity.

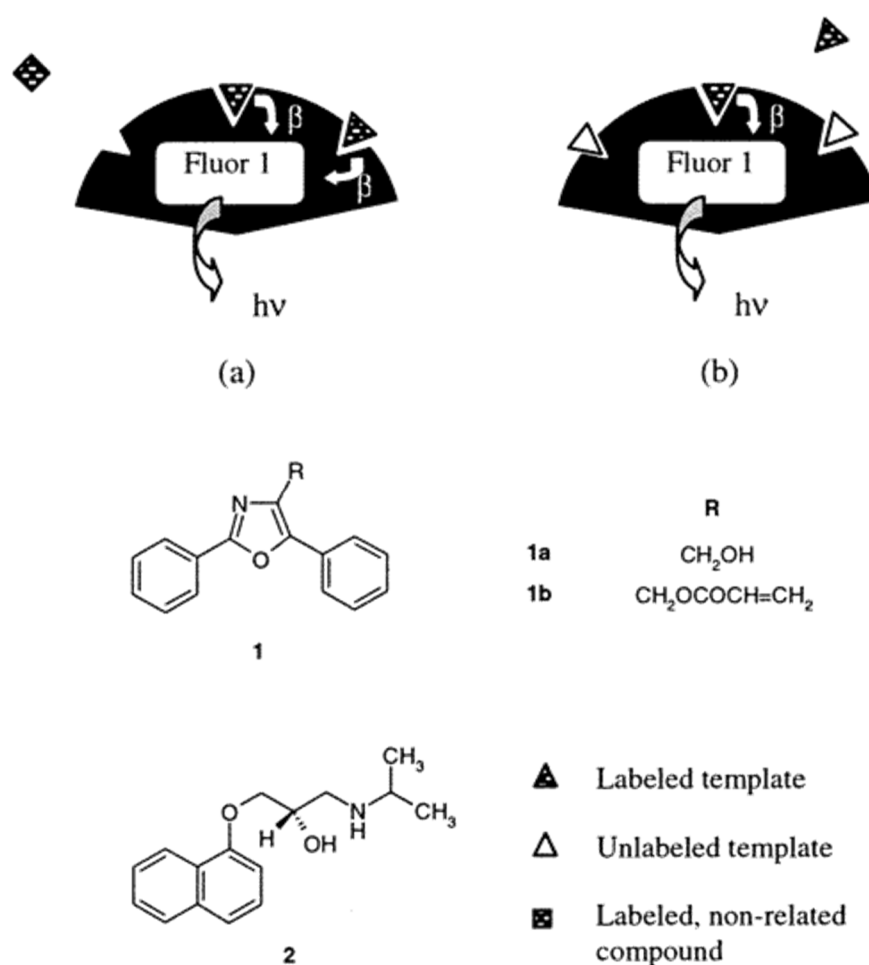


Figure 2. Schematic representation of chemical sensing with an imprinted polymer through proximity scintillation.²⁴ The polymerisable fluor (**1a**) is incorporated into imprinted particles with affinity for the template, naproxen (**2**). The fluor emits light in response to β -decay of tritium-labelled naproxen, but not other labelled analytes (**a**); competition between radiolabelled naproxen and free (unlabelled naproxen) (**b**) can be used to quantify the analyte without separation of the bound and free components. Reproduced from Ye et al.²³ with permission from the American Chemical Society.

1.3. Radio-labelled MIAs

A series of significant breakthroughs in MIP technology came as a result of novel synthetic methods to generate spherical, molecularly imprinted beads as an alternative to conventional MIP particles produced through bulk polymerisation followed by grinding into small particles. Various approaches were developed, such as dispersion polymerisation,²⁵ suspension polymerisation,²⁶⁻²⁸ activated swelling and thermal polymerisation,²⁹ precipitation polymerisation,³⁰⁻⁴⁶ distillation precipitation polymerisation,^{47, 48} core-shell polymerisation,⁴⁹⁻⁵⁵ surface grafting methods,⁵⁶⁻⁶⁰ Pickering emulsion polymerisation,⁶¹⁻⁶³ hierarchical imprinting in porous silica,^{64, 65} and mini-emulsion polymerisation,⁶⁶ allowing for a diverse number of strategies for generating regular sized beads with narrow size distributions for different applications. Some of these methods have been reviewed by Pérez-Moral and Mayes.⁶⁷ Numerous investigations were thus carried out in order to assess the potential advantages of these new MIP formats in MIAs, with most being initially tested through incorporation into radio-labelled MIAs.

Based on previous work on polymerisation precipitation, the group of Wei et al. reported an optimisation of the technique for the preparation of 17 β -estradiol imprinted nanospheres for use in radio-labelled MIAs.⁶⁸ This work focused on accurate control and optimisation of the governing parameters for precipitation polymerisation, taking into consideration the nature of the cross-linker, the monomer concentrations, and the polymerisation temperature, and their consequent effects on the imprinted nanospheres generated. From these investigations, 17 β -estradiol imprinted beads of 400 nm diameter were used in the development of a competitive binding assay, which showed a linear detection range from 0.01 to 1000 $\mu\text{g mL}^{-1}$ with significant stereoselectivity for 17 β -estradiol over its α -epimer.

Similar studies were performed by Ye et al., who successfully synthesised (*R,S*)-propranolol imprinted spherical nanoparticles of 130 nm with uniform size distribution by modifying precipitation polymerisation conditions.⁶⁹ Through varying the composition of the cross-linker it was found that the particle size could be reasonably controlled over the range 130 nm to 2.4 μm , whilst the favourable binding properties remained intact. This led to the development of a highly enantioselective competitive radioligand binding assay, where the small MIP nanoparticles (MIP NPs) exhibited 20 times affinity for (*S*)-propranolol over the (*R*)-enantiomer, demonstrating a six- to sevenfold increase over previously reported irregular particles.

Aside from precipitation polymerisation, Kempe and Kempe reported modifications on suspension polymerisation in mineral oil for the preparation of (*R,S*)-propranolol imprinted microspheres.⁷⁰ The one-step synthesis avoided the use of water and stabiliser/surfactant, which had been a criticism of other techniques because of

interference with hydrogen bonds effecting template–monomer complex formation during noncovalent imprinting. The size of beads synthesised was controllable over the range of 1–100 μm , which were obtained in almost quantitative yield, with higher binding capacities observed in comparison to MIP particles prepared through bulk polymerisation, likely due to better accessibility of binding sites in the spherical beads. The MIP microbeads were subsequently used for analysis of propranolol in human serum samples in a 96-well plate radio-labelled MIA, which was effective in determining propranolol concentration between 1 mM and 1 μM .

Following these optimisation studies, the use of radio-labels in MIAs saw a huge decline as fluorescence- and enzyme-labelling became more popular, for reasons previously discussed. A rare example saw their use in the evaluation of a MIP for the selective recognition of testosterone.⁷¹ Whilst previous efforts had been made to synthesise testosterone-templated polymers,^{72–76} these had failed to display impressive imprinting factors, the best reported being around 4, making them unsuitable for an application as an antibody mimic. This study aimed to improve on this, with the intention of optimising testosterone imprinted MIPs in an aqueous environment for use in a radiolabelled MIA. The imprinted polymers developed showed appreciable binding affinity with association constants of $K_a = 3.3 \times 10^7 \text{ M}^{-1}$, whilst the non-imprinted controls bound virtually no radiolabelled testosterone, leading to a high imprinting factor compared with those previously reported. When applied to a radio assay in an aqueous environment, the MIPs achieved an IC_{50} of 9 μM , making them less sensitive than commercial antibody kits; however, the selectivity exhibited was higher for the MIPs.

1.4. Fluorescence-based MIAs

With the decline in use of radio-labelled tracers, a consequent rise in fluorescent-labelled MIAs occurred. In a typical fluorescence-labelled MIA, the target analyte is used as the template during MIP generation, whilst a fluorescent probe with similar structure is employed in competition with free analyte for binding to the polymer during the assay. This allows for sensitive and quantitative analysis through detection of the fluorescence signal. Despite its advantages, fluorescently labelled MIAs are hindered somewhat by the necessity to modify the target analyte in cases where there is no inherent fluorescence, in order to detect a signal. This is usually achieved through the addition of a fluorescent tag/group, making the structure of the probe chemically different to the analyte. The fluorescent conjugate may therefore display different binding behaviour to the original analyte, which could impact on the sensitivity and selectivity of the assay. Nevertheless, impressive results have been achieved with this MIA format, with some recent developments, such as the incorporation of quantum dots, eliminating these problems entirely.

1.4.1. Heterogeneous fluorescent assays

Heterogeneous fluorescence-based assays are characterized by the physical separation of bound and unbound analyte prior to measuring the fluorescence intensity of the supernatant (or polymer) in order to perform a quantitative analysis.

Modification with pyrene or dansyl moieties led to the development of novel, highly fluorescent derivatives of the β -lactam antibiotics.⁷⁷ These compounds were ideal for optical sensing purposes and were, hence, employed in an imprinted-polymer based competitive assay for penicillin G (PenG).⁷⁸ Selection of the most appropriate probe was conducted using radio-labelled competitive assays, with pyrenemethylacetamido penicillanic acid showing the most promise from the candidate library. The resulting fluorescence assay exhibited a dynamic range of 3–890 μ M in 99:1 acetonitrile-water solution, with reasonable degrees of cross-reactivity (from 57% to 0%). When applied to the analysis of PenG in a commercial pharmaceutical formulation, recoveries from 92% to 103% were found. This assay was later adapted to an automated flow-injection MIA system, combining the simplicity of flow methods with the sensitivity and selectivity of the fluorescence detection.⁷⁹ The analyte and a fixed concentration of pyrenemethylacetamido penicillanic acid probe were injected into the MIP-packed reactor, where competition for the binding sites of the MIPs imprinted with PenG procaine salt occurred. Following application of a desorbing solution, the fluorescence of the labelled derivative eluted from the sorbent was measured and related to the analyte concentration in the sample. When applied to the direct analysis of PenG in spiked urine samples, mean recoveries of 92% were observed, over a dynamic range from 787 nM to 17.1 μ M. The total analysis time was 14 min per determination, with the MIP reactor capable of performing 150 cycles without significant loss of recognition. Furthermore, use of novel urea-based functional monomers in the MIP-synthesis facilitated compatibility of the system with aqueous samples—a first for automated MIAs.

Following the success of radio-labelled MIAs based on MIP micro- and nanoparticles, controlled radical polymerisation was explored as a method for the synthesis of surface-imprinted core-shell nanoparticles.⁸⁰ Surface reversible addition fragmentation chain transfer polymerisation was utilised on the surface of functionalised silica nanoparticles in the presence of 2,4-D as template. The nanoparticles afforded by this process were subsequently applied to fluorescent-labelled MIAs using 7-carboxy-4-methylcoumarin as fluorescent probe. Whilst the nanoparticles generated showed no advantages over conventional irregular particles with regards to cross-reactivity, this new technology demonstrated a robust and controllable synthesis with more freedom for monomer/solvent compositions.

Generally, the preparation of MIPs uses single-template imprinting; however, reports of MIPs containing multiple sites with the ability to recognize two or even three molecules are known.⁸¹⁻⁸³ In an attempt to prepare a receptor model for biological mixed neurotransmitter receptors, Suedee et al. synthesised a dual dopamine/serotonin-selective MIP by bulk polymerisation using methacrylic acid and acrylamide (AAm) as

functional monomers, together with *N,N*-methylene bisacrylamide (BIS) as cross-linker in the presence of both templates, dopamine and serotonin.⁸⁴ This dual-MIP was used in a competitive binding assay, where quantification was achieved by using the native templates as fluorescent probes. In this manner, the assay was used to attain the ligand binding activities of a series of ergot family alkaloids, in order to assess their ability to displace dopamine/serotonin from the MIP binding sites. Results were comparable to those obtained from a competitive immunoassay using receptors derived from rat hypothalamus, demonstrating binding affinities in the micromolar or submicromolar range and showing that MIPs can be capable of mimicking natural receptors in their interactions with drug targets.

1.4.2. Homogenous fluorescent assays

In contrast to heterogeneous assays, homogeneous assays allow direct analyte measurement without the need for a physical separation step; however, this does mean that a more elaborate method for recognizing bound analyte as opposed to unbound analyte is required.

With the intention of combining the principles of a homogenous MIA and the use of a fluorescent probe, Hunt et al. developed a fluorescence polarisation (FP) molecular imprinted sorbent assay for 2,4-D.⁸⁵ When the fluorescent probe, in this case 7-carboxy-4-methylcoumarin, binds to a MIP in solution, its tumbling rate falls, and consequently the measured fluorescence will be more isotropic than that of free probe, which tumbles faster. The FP hence increases with the percentage of probe bound, or decreases with the amount of competing analyte. In order to perform fluorescence measurements on a mixture of a fluorophore and polymer particles in solution, it was important that fluorescence could be distinguished from the scattering of excitation light by the polymer particles. This required the excitation and emission wavelengths to be well separated, and the polymer particles to be very small. Micrometer-sized particles as previously used were therefore too large, and consequently the paper demonstrated for the first time that MIP microgels of diameter less than 300 nm could indeed have affinities and selectivities similar to those of bulk polymers. The LOD of the assay was 10 μM for 2,4-D, while selectivity was shown for the template molecule over the related herbicides 3,4-dichlorophenoxy acid and 2,4-dichlorophenoxybutyric acid.

A similar MIA utilizing FP as an analytical technique was also developed for the direct detection of fluoroquinolone antibiotics in food and environmental samples.⁸⁶ As the fluoroquinolones of interest display inherent fluorescence, the need to integrate an additional probe into the system was not necessary, unlike in the previous example. Water-compatible MIP NPs were synthesised with enrofloxacin as the imprinting template; however, this also showed similar affinity towards ciprofloxacin and norfloxacin. The assay was successfully applied to determine fluoroquinolones in real samples without any prior concentration step by simply adding a known amount of MIP, with no interference from sample components observed. In tap water, the LOD for enrofloxacin was 0.1 nM using 5 $\mu\text{g mL}^{-1}$ of MIP, whilst in milk, enrofloxacin and

danofloxacin, whose maximum residue limits have been fixed at 0.28 μM and 0.08 μM , respectively, could be selectively measured and distinguished from other families of antibiotics.

Turner et al. incorporated *N*-2-propenyl-(5-dimethylamino)-1-naphthalene sulphonamide into imprinted polymer films as a fluorescent indicator for the detection of nitroaromatic compounds in the vapour phase.⁸⁷ Binding of the explosives was detected within a few minutes as a quenching of fluorescence. Enhancement of fluorescence upon binding template is less common, but examples exist. Ivanova-Mitseva et al. prepared nanoparticles by grafting to a dendrimer core simultaneously modified with dansyl amide groups and a dialkyldithiocarbamate ester (iniferter).⁸⁸ The nanoparticles produced showed a positive fluorescent response to the presence of the template (acetoguanamine) at nanomolar concentrations ($\text{LOD} = 3.0 \times 10^{-8} \text{ M}$), which was selective over close structural analogues. A similar “light-up” detection for amino acid derivatives has been demonstrated with a urea-based functional monomer designed to interact with the carboxylate anion on the template.⁸⁹ The polymer showed enantioselective binding of L-phenylalanine benzyl ester at micromolar concentrations.

An interesting development in homogeneous fluorescence MIAs came as a result of improvements in luminescent nanomaterials. Incorporation of these materials was first demonstrated by Zhao et al., who reported the rational and rapid fabrication of quantum dot (QD)-MIP fluorescent nanospheres capable of recognising diazinon in aqueous media.⁹⁰ Based on energy transfer from the excitation of ZnS:Mn^{2+} (donor) to the absorption of diazinon (acceptor), the fluorescence of the QDs-MIP NPs was greatly quenched as the template molecules rebound into the recognition cavities (Figure 3). The dramatic fluorescence quenching could be applied to the direct and selective fluorescence quantification of diazinon in aqueous media, with the developed assay displaying a

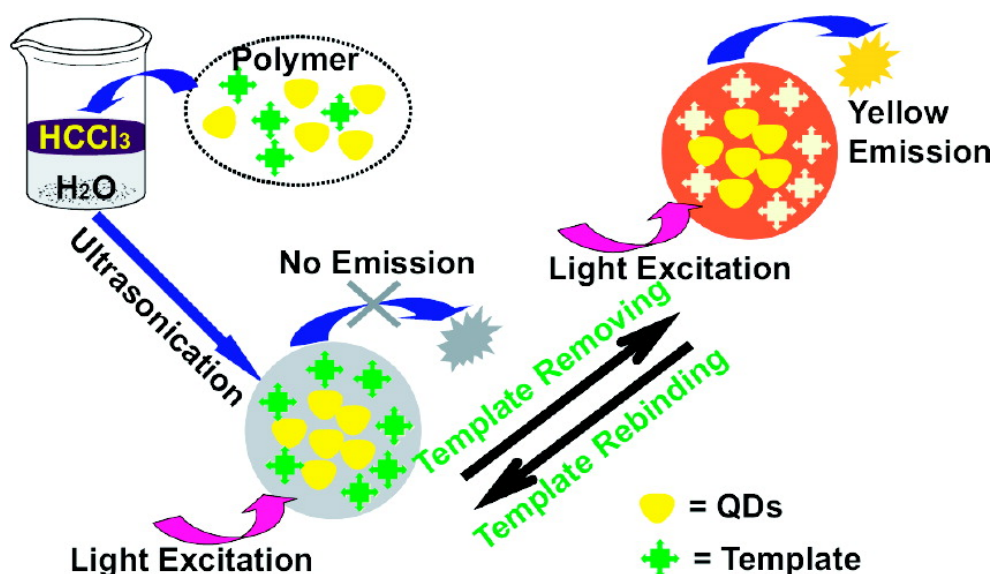


Figure 3. Scheme for the preparation of QD-based MIP nanospheres, and the fluorescence quenching effect following rebinding of template as a method of detection. Reproduced from Zhao et al.⁹⁰ with permission from the American Chemical Society.

linear relationship over the concentration range 50-600 ng mL⁻¹. As a proof of concept, the QDs-MIP NPs were applied to the analysis of diazinon in tap water samples spiked with 200 ng mL⁻¹ of the analyte, with excellent recoveries varying from 98.2% to 105.4%, demonstrating the applicability to detection in real environmental water samples without any pre-treatment.

Incorporation of QDs as a source of fluorescence signalling was also the method of choice adopted by Lee et al. during development of the first MIP sandwich assay.⁹¹ The sandwich fluoroimmunoassay was designed to detect and quantify digestive proteins in saliva, utilising quantum dots incorporated in protein imprinted poly(ethylene-co-vinyl alcohol) as a fluorescent signal (Figure 4). The same polymer was also used as an imprinted thin film to coat microplate wells as a replacement for primary antibodies in the sandwich assay system. The system relies on the random imprinting of different surface features of the target protein (epitopes) in the primary and secondary polymer components, similar to that obtained with polyclonal antibodies. When applied to measurements of saliva samples, the recovery accuracy attained by this method was ±20%-25%, whilst the linear range for amylase, lipase, and lysozyme stock solution were 0.1-10 ng mL⁻¹, with the LOD as low as 1 pg mL⁻¹. These results therefore represented the most sensitive detection yet achieved with MIPs.

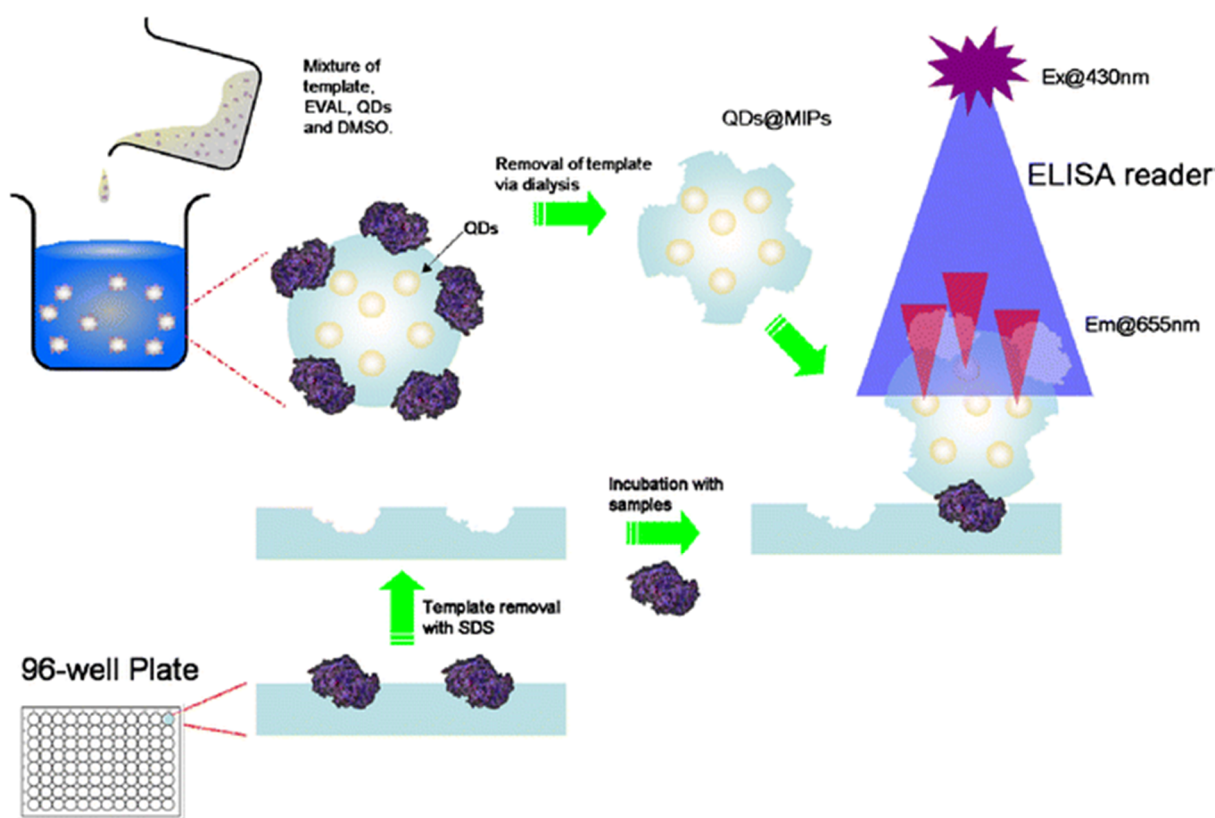


Figure 4. Recognition by template-imprinted poly(ethylene-co-vinyl alcohol)/quantum dots nanoparticles following binding to imprinted polymer coated 96-well microplates to form a sandwich-type assay for protein detection. Reproduced from Lee et al.⁹¹ with permission from Springer.

1.5. Enzyme-linked MIAs

The use of enzyme-labelling analytes was first implemented as early as 1968, and has since become the most popular method for labelling in immunoassays. This trend has translated over to MIAs also, as traditional problems of incompatibility with water and accessibility of binding sites with the use of enzymes with MIPs have been overcome. Enzyme-labels still suffer the same problems as fluorescent probes with regards to conjugation of the label to the analyte and the effect this consequently has on the recognition and binding of the labelled analogue; however, the commercial availability of many enzymes at low cost and general ease of conjugation offer significant advantages. Additionally, many enzyme labels catalyse simple colorimetric/fluorimetric reactions during their application, requiring detection devices no more complex or expensive than a multichannel colorimetric/fluorimetric reader.

The aforementioned difficulty of binding site availability has led to adoption of in situ polymerisation of imprinted films on the surface of 96-well plates as the most popular technique for development of biomimetic ELISA-like assays (Table 1). By utilizing a film format, a large surface area can be achieved, whilst control of the film thickness assists in access to binding sites. The method has been used extensively for a variety of templates, with the developed assays being applicable to determination of their respective analytes in environmental water samples,^{92, 93} soil,⁹² pork,⁹⁴ urine,^{94, 95} vegetables,⁹⁶ chick feed,⁹⁷ sea cucumber,⁹⁸ French fries, and crackers.⁹⁹

Recent work reported by Shi et al. describes the development of a MIP-based ELISA for simultaneous multi-pesticide analysis.¹⁰⁰ The chosen template, 4-(dimethoxyphosphorothioylamino)butanoic acid, had been shown to share a common structure and functional groups with organophosphorus (OP) pesticides, and so the intention was that this template could be used to produce a MIP with recognition for the OP class of compounds, rather than just the template. The imprinted film proved to be effective for selectively recognising trichlorfon and acephate, with an IC₅₀ of

Table 1. Recent examples of MIAs utilising enzyme-labels and in situ prepared imprinted films on the surface of 96-well μL plates.

Analyte	Range ($\mu\text{g L}^{-1}$)	IC ₅₀ ($\mu\text{g L}^{-1}$)	LOD ($\mu\text{g L}^{-1}$)	Ref.
Tribenuron-methyl	0.10–10,000	19.7 \pm 1.2	0.3	92
Estrone	0.50–50,000	200 \pm 40	8.0 \pm 0.2	93
Ractopamine	0.01–1000	15.8 \pm 3.2	0.01	94
Methimazole	0.60–60,000	70.0 \pm 4.0	0.9 \pm 0.04	95
Trichlorfon	3.20–50,000	6800 \pm 60	6.8 \pm 0.2	96
Olaquinox	17.0–50,000	700 \pm 60	17 \pm 1.6	97
Chloramphenicol	0.30–30,000	30.0 \pm 2.0	0.9 \pm 0.01	98
Acrylamide	16.0–50,000	8000 \pm 0.4	85 \pm 4.2	99

12.0 mg L⁻¹ and 30.0 mg L⁻¹ for each analyte, respectively. Overall, the assay showed linearity from 0.1 to 100,000 µg L⁻¹, making it suitable for the desired purpose of determining trace amounts of pesticides in food samples. When subjected to spiked asparagus and cucumber samples, recoveries from 72.1% to 92.0% for trichlorfon and 70.0% to 85.0% for acephate were achieved.

An interesting variation on surface-imprinting was performed in order to achieve the first 96-well microplate MIP ELISA for glycoprotein detection and quantification.¹⁰¹ In this work, a 96-well microplate was functionalised with a common boronic acid at the well surface, allowing a target glycoprotein to be immobilised by virtue of boronate affinity. Following this, a hydrophilic coating formed by in-water self-copolymerisation of aniline was deposited onto the well surface, affording a 3D cavity complementary to the molecular shape of the target following removal with acid (Figure 5). The group prepared α -fetoprotein (AFP)-imprinted microplates to develop a MIP-based sandwich ELISA, which showed good linearity over the range 0-50 ng mL⁻¹. When applied to a human serum sample, the AFP concentration was determined to be 12 ± 2.0 ng mL⁻¹, which was in good agreement with the value determined by radioimmunoassay (10 ng mL⁻¹), showing a promising prospect of the proposed method in clinical diagnostics.

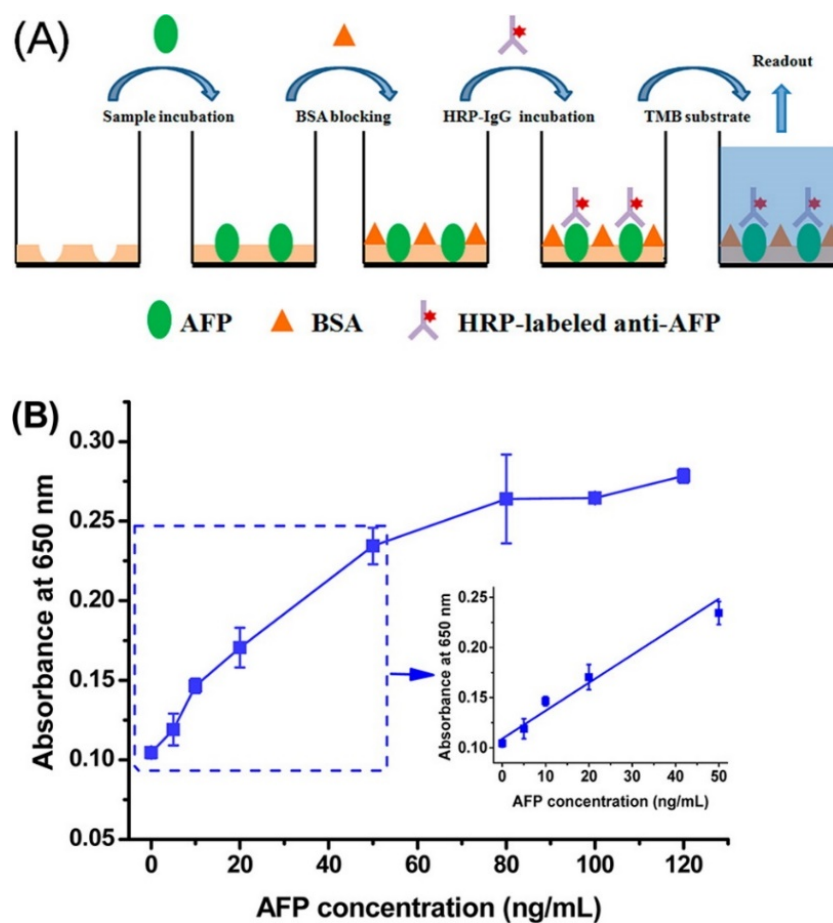


Figure 5. Sandwich ELISA for AFP following boronate affinity-based oriented surface imprinting. Reproduced from Bi et al.¹⁰¹ with permission from the American Chemical Society.

Although impressive results have been achieved using molecularly imprinted films, attempts to improve upon this method have been made. With regards to the films used in these assays, their resemblance to polyclonal antibodies gave rise to high levels of nonspecific binding, whilst their manufacture relied on manual, labour intensive methods of synthesis. The assays themselves utilised complex immobilisation protocols and lacked generality, requiring substantial modification to the analytical procedures traditionally used in ELISA. In an attempt to resolve some of these problems, Poma et al. developed a method for solid-phase synthesis of MIP NPs with pseudomonoclonal binding properties suitable for automation in a computer-controlled reactor.¹⁰² To demonstrate the potential of materials prepared in this manner, a novel assay for vancomycin directly replacing antibodies with MIP NPs in ELISA was proposed.¹⁰³ In order to utilise previously synthesised MIP NPs, a simple and straightforward technique for coating microplate wells was required. This was achieved through physical adsorption by allowing a solution of MIP NPs to evaporate to dryness within each of the microplate wells, removing the necessity for a complex immobilisation method or in situ formation of the imprinted material through polymerisation in the test wells. Following immobilisation, the MIP NPs could be used in competitive binding experiments between free and HRP-labelled vancomycin (Figure 6). The assay was capable of measuring vancomycin in buffer and in blood plasma within the range of 0.001-70 nM, a sensitivity three orders of magnitude better than a previously described ELISA based on antibodies. The generic nature of MIP NP preparation by solid-phase synthesis suggests that assays for many more analytes may also be created in this manner.

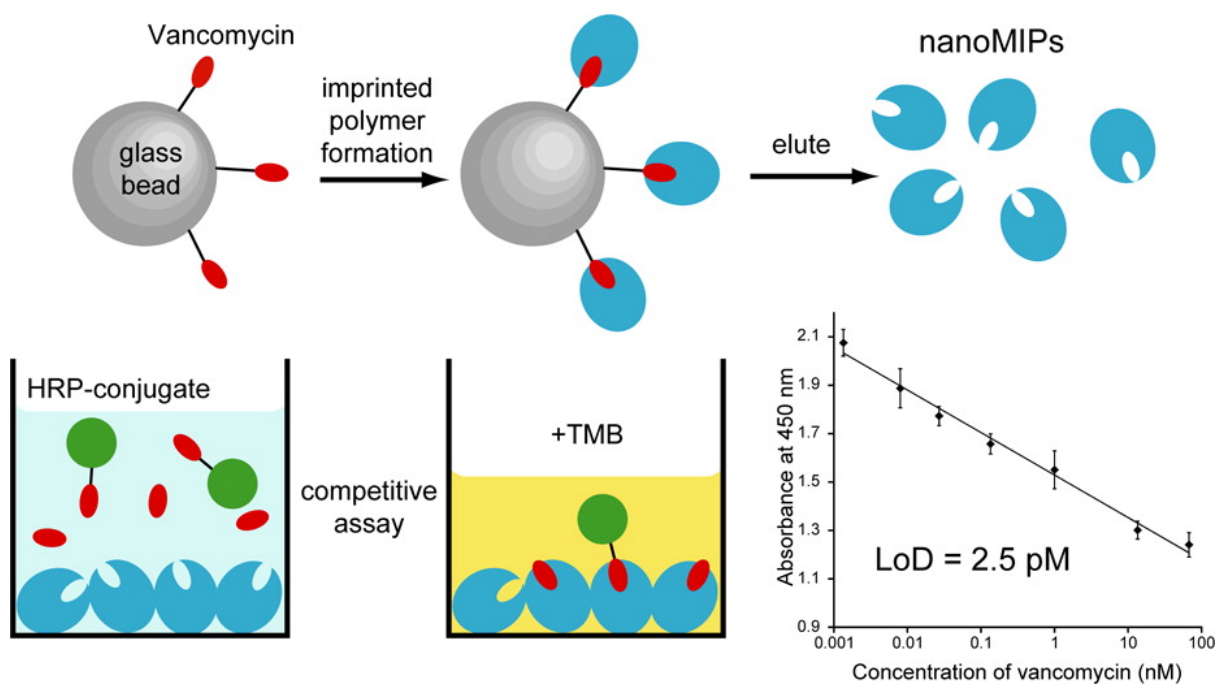


Figure 6. ELISA utilizing MIP NPs synthesised using a solid phase protocol. Reproduced from Chianella et al.¹⁰³ with permission from the American Chemical Society.

1.6. Other MIA formats

Although the majority of MIAs fall into the previously discussed categories, several novel assay types have been developed utilising the unique properties of MIPs.

Taking advantage of the swelling/deswelling behaviour of hydrogels, Hu et al. developed an ultrasensitive specific stimulant assay based on molecularly imprinted photonic hydrogels.¹⁰⁴ In this work, colloidal crystals and molecular imprinting were combined to prepare imprinted photonic polymers (IPP) with three-dimensional, highly-ordered, macroporous structures, which could be used to optically determine analytes by means of the shift of the Bragg diffraction attributable to a change of the periodic lattice spacing. The IPP hydrogels swell in response to chemical stimuli, giving rise to a visually perceptible colour change, which can easily be implemented into a rapid and sensitive assay (Figure 7). IPP-hydrogel films against theophylline and (1R,2S)-(-)-ephedrine both exhibited high sensitivity and selectivity, enabling the quantification of as low as 0.1 fM concentration of analyte even in a competitive urinous buffer.

Similar detection methods have been demonstrated in colloidal crystal and inverse opal configurations. Although many of these have been described as sensors, rather than assays, they are worthy of mention since they operate in the same manner. Analytes determined in this fashion include bisphenol A,^{105,106} OP compounds,¹⁰⁷ imidacloprid,¹⁰⁸ glucose,¹⁰⁹ amino acids,¹¹⁰ progesterone,¹¹¹ tetracycline,¹¹² and 17 β -estradiol.¹¹³

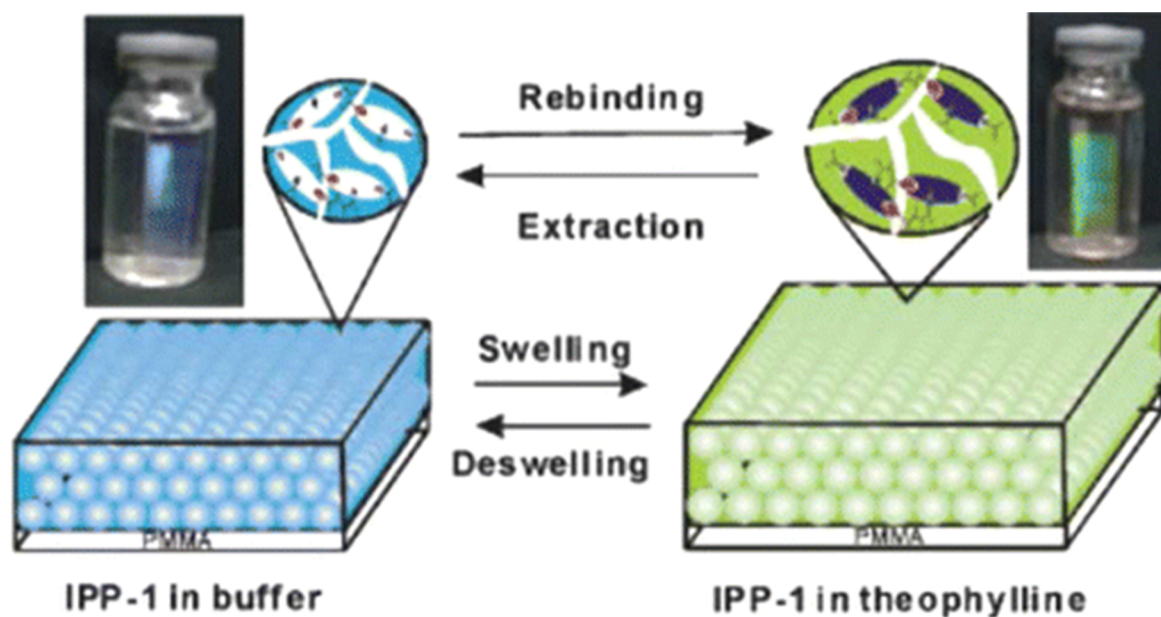


Figure 7. Schematic illustration of the created IPP structure and the colour change as a result of swelling/deswelling following rebinding or extraction of analyte. Reproduced from Hu et al.¹⁰⁴ with permission from John Wiley and Sons.

Volume changes have also been employed in the detection of proteins in hydrogels imprinted using novel functional monomers based on aptamers.¹¹⁴ In this work, the protein thrombin was used as the template with two distinct polymerisable aptamer sequences as functional monomers chosen to bind to different regions of the protein surface. After template removal the hydrogel could be used to detect protein at femtomolar concentrations through changes in the macroscopic dimensions (shrinkage) of the gel (Figure 8).

Similarly to fluorescence, chemiluminescence has also been employed as a signalling method for MIAs. An assay for dipyridamole has been developed utilizing light emitted from dipyridamole peroxyoxalate chemiluminescence as a means of detection.¹¹⁵ MIP microspheres of 0.7 μm diameter were prepared using precipitation polymerisation with methacrylic acid as functional monomer and trimethylolpropane trimethacrylate as cross-linker in the presence of dipyridamole, with poly(vinyl alcohol) utilised to immobilise the imprinted polymers to the walls of 96-microtiter well plates. Following sample incubation, the amount of polymer-bound dipyridamole was determined using a high-resolution charge coupled device camera to measure the chemiluminescence. Under optimal conditions, the relative chemiluminescence imaging intensity was proportional to dipyridamole concentration from 0.02 to 10 $\mu\text{g mL}^{-1}$, with the assay format able to perform 96 independent measurements simultaneously in 30 min.

A MIP-based lab-on-paper chemiluminescence device for the detection of dichlorvos (DDV) was reported by Liu et al., generating chemiluminescence signals following reaction of DDV, luminol, and H_2O_2 in alkaline medium, allowing for a powerful and sensitive tool for selective monitoring of DDV.¹¹⁶ The MIP layer was adsorbed onto the paper surface, whilst the depth was controlled at 600 μm by stacking glass slides with double-sided tape of 600 μm depth. When applied to vegetable samples, the device was effective from 3.0 ng mL^{-1} to 1.0 $\mu\text{g mL}^{-1}$ with a detection limit of 0.8 ng mL^{-1} .

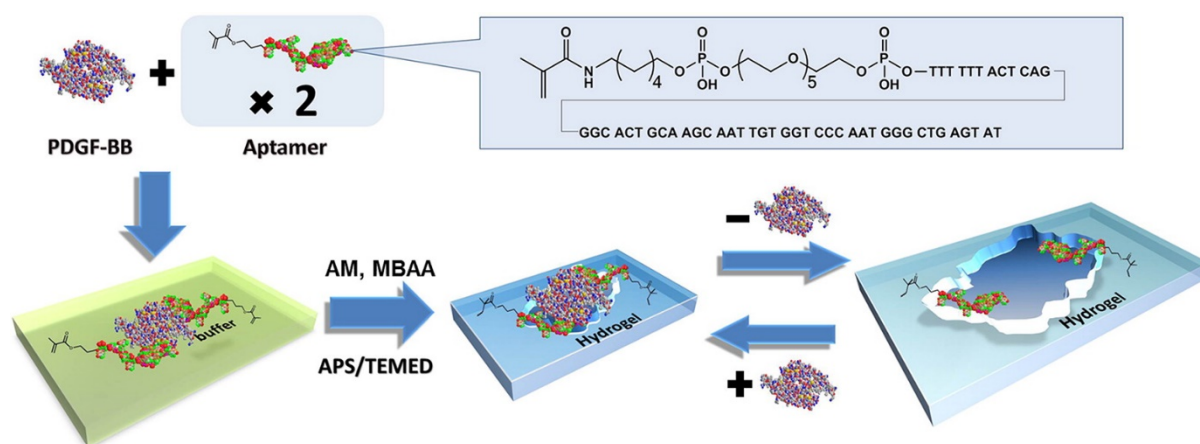


Figure 8. Aptamer-based hydrogels imprinted with thrombin that show macroscopic changes in dimension on binding the target protein down to femtomolar concentration.¹¹⁴ Reproduced from Bai et al. with permission from the American Chemical Society.

Whilst the work demonstrates the promise of chemiluminescence-based detection for paper microfluidic chips, the adaptability of this device to the analysis of other analytes could be limited, as they, like DDV, would be required to elicit a chemiluminescence signal following addition of luminol/H₂O₂.

Although the replacement of antibodies with synthetic mimics has been the focus of biomimetic ELISA-like assays, the added advantages (mainly storage/thermal stability and low cost) afforded by use of these materials is not effectively exploited if the assay system still requires the use of a biological reporter enzyme. In an attempt to rectify this, Shutov et al. reported the integration of catalytically active Fe₃O₄ with molecularly imprinted nanoparticles (MINs) as combined recognition and signalling functionalities in a core-shell nanoparticle format to develop the first ELISA-like assay to completely replace all biologics with synthetic analogues.¹¹⁷ The intrinsic peroxidase mimicking activity of Fe₃O₄ nanoparticles makes them attractive substitutes for enzymes in a variety of assays, with suitable catalytic activity over a broad range of temperatures, low cost/long shelf life, and ease of manufacture. A variation of the solid-phase imprinting protocol was utilised to produce the composite core-shell Fe₃O₄-MIN, using vancomycin as template (Figure 9). Subsequent magnetic separation ensured that only high-affinity nanoparticles containing the catalytic Fe₃O₄ core were recovered from the process.

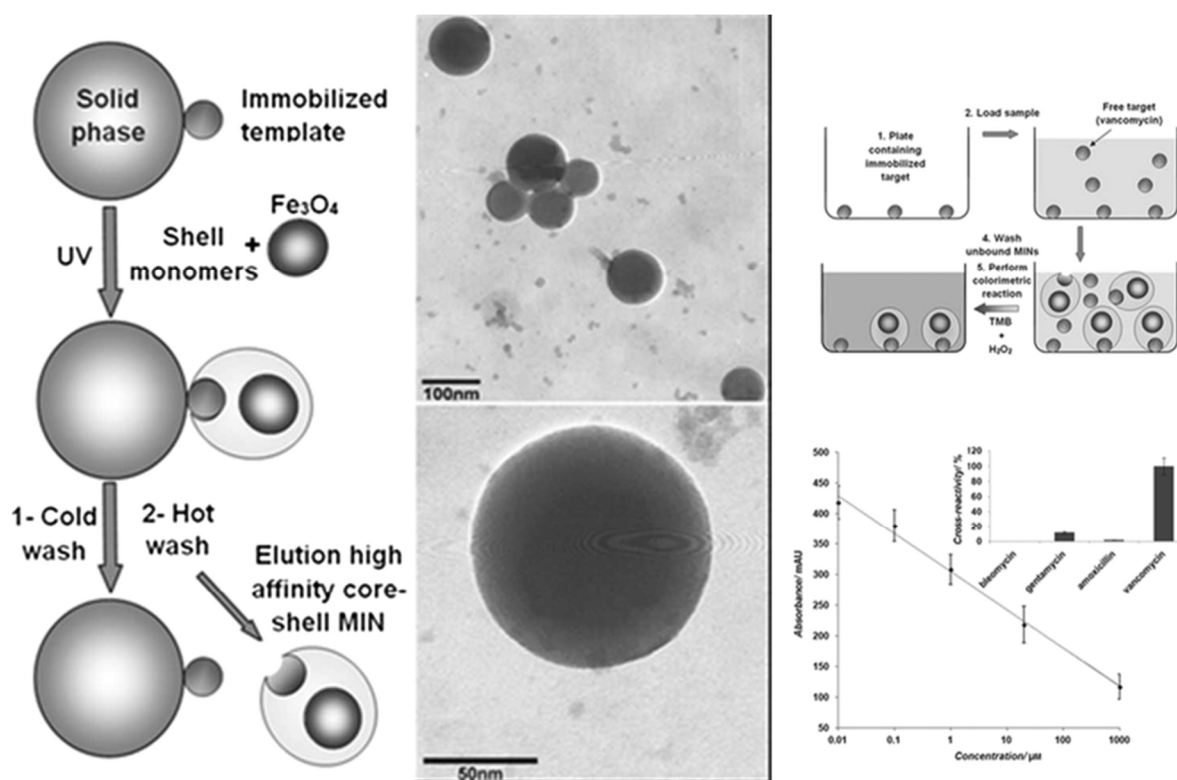


Figure 9. Schematic of the solid-phase synthesis protocol with addition of Fe₃O₄ for preparation of peroxidase-mimicking core-shell MIN (top left) and transmission electron microscopy (TEM) image of the obtained Fe₃O₄-MIN particles (top right). The assay format (bottom left) and calibration curve (bottom right) are also shown. Reproduced from Shutov et al.¹¹⁷ with permission from John Wiley and Sons.

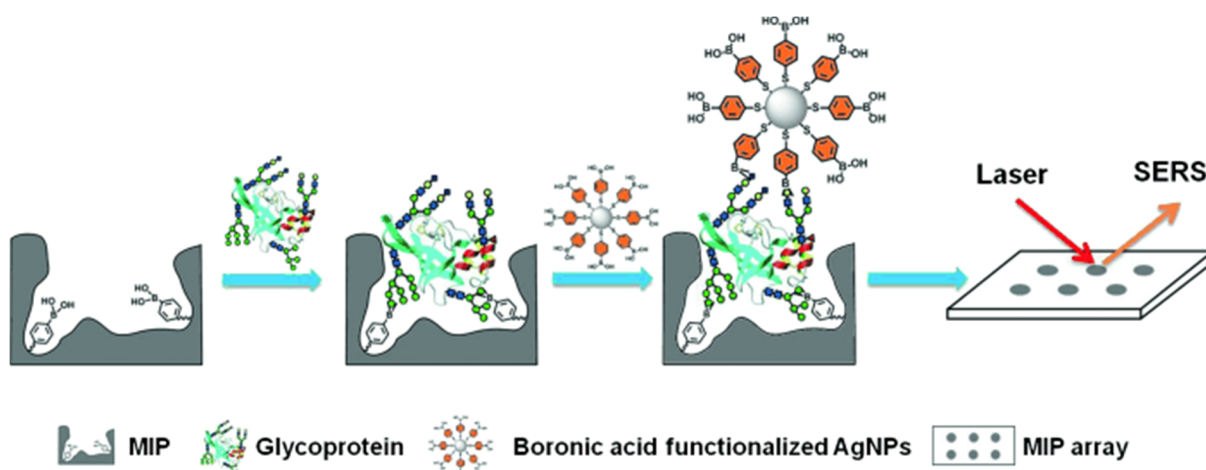


Figure 10. Schematic representation of the boronate-affinity sandwich assay of glycoproteins. Reproduced from Ye et al.¹¹⁸ with permission from John Wiley and Sons.

By immobilizing the template (vancomycin) to the surface of well plates, a competitive assay could be performed using the previously synthesised core-shell nanoparticles, with quantification made possible through the oxidation of 3,3',5,5'-tetramethylbenzidine to give a colorimetric response proportional to the quantity of Fe_3O_4 catalyst bound to the template. The developed assay was effective over the range of 10 nM to 1 mM, retaining applicability even in complex sample matrices such as porcine serum, although this did require use of a spacer between immobilized vancomycin and the well surface.

A number of sandwich-type assays have been developed, achieving impressive sensitivity often surpassing that of other previously mentioned methods. A new approach, termed the boronate-affinity sandwich assay, was applied for the specific and sensitive determination of trace glycoproteins in complex samples.¹¹⁸ The technique relies on the formation of sandwiches between boronate-affinity MIPs, target glycoproteins, and boronate-affinity surface-enhanced Raman scattering probes (Figure 10). In this way, the MIP ensures the specificity, whilst the surface-enhanced Raman scattering detection provides sensitivity. The feasibility of the boronate-affinity sandwich assay approach for real-world applications was demonstrated by an assay of the glycoprotein AFP in human serum. The MIP array exhibited a linear response toward AFP within the range of 1 ng mL^{-1} to $10 \text{ } \mu\text{g mL}^{-1}$, and was able to determine the analyte concentration in good agreement with results from other methods ($13.8 \pm 3.3 \text{ ng mL}^{-1}$ compared with $12.0 \pm 2.0 \text{ ng mL}^{-1}$).

A further novel sandwich-type immunoassay for simultaneous determination of AFP and carcinoembryonic antigen (CEA) using graphene–Au grafted recombinant apoferritin-encoded metallic labels loaded with Cd and Pb ions with dual-template magnetic MIPs (MMIPs) as capture probes was designed by Wang et al.¹¹⁹ After a sandwich-type immunoreaction, the labels were captured at the surface of MMIPs, allowing electrochemical stripping analysis of the metal components from the immunocomplex to provide a means of quantification based on the peak currents of Cd and Pb (Figure 11). Experimental results showed that the assay could simultaneously

detect AFP and CEA in a single run with a dynamic range of 0.001–5 ng mL⁻¹. The possibility to expand the number of analytes for simultaneous analysis by implementing more recombinant apoferritin nanoparticles (including Pb, Cd, Cu, and Zn) as distinguishable labels shows promising potential for this approach in clinical detection of multianalytes.

By taking advantage of the inherent chemical properties of chloramphenicol (CAP), a portable and antibody-free sandwich assay for determination of CAP in food based on a personal glucose meter was developed by Chen et al.¹²⁰ The assay utilised polydopamine molecularly imprinted film modified Fe₃O₄ nanoparticles and a β -cyclodextrin (β -CD)/invertase bioconjugate for recognition and subsequent glucose generation. A fragment imprinting technique was adopted for the synthesis of the polymer film, in which 2,2-dichloroacetamide was used as template. This enabled

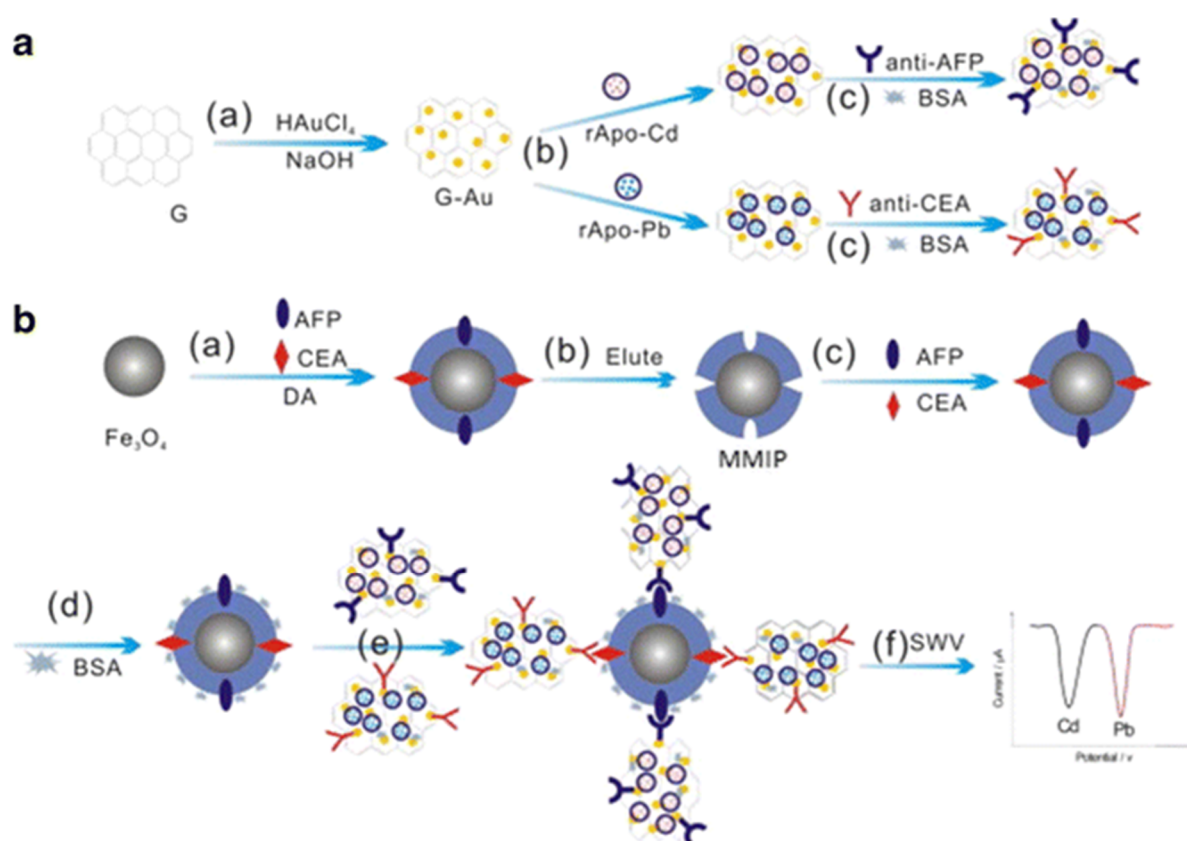


Figure 11. Schematic representation of simultaneous electrochemical immunoassay. (A) preparation of signal tags: (a) in situ reducing HAuCl₄ onto graphene to form graphene-Au; (b) immobilization of labels; (c) labelling with anti-AFP and anti-CEA and blocking of excess active sites with BSA (1.0 wt%). (B) synthesis of the capture probes and electrochemical detection: (a) polymerisation of DA to form a PDA coating on Fe₃O₄ in the presence of template proteins; (b) Eluting with SDS to remove embedded template proteins and obtain MMIP; (c) recognition with target analytes (AFP and CEA); (d) blocking with BSA; (e) antigen-antibody specific reaction with above signal tags; (f) magnetic separation and electrochemical detecting with SWV. Reproduced from Wang et al.¹¹⁹ with permission from Elsevier.

affinity for a section of CAP resembling the used template, without interfering with the nitrophenol fragment in CAP. β -CD is known to combine with nitrophenol to form a host-guest complex by means of the hydrophobic cavity, and so this exposed region following MIP binding could be utilised for attachment of a β -CD-based signal tag to form a sandwich-type complex for CAP detection. Invertase was selected for conjugation to β -CD, where it could facilitate the generation of glucose from sucrose to elicit a measurable response using a personal glucose meter (Figure 12). Using this method, the concentration of CAP was found to be proportional to the amount of glucose formed, which could qualitatively assess the CAP with a dynamic range of $0.5\text{-}50\text{ ng mL}^{-1}$ and a detection limit of 0.16 ng mL^{-1} . Although an elegant strategy, there is great dependence on the structure of the analyte for this method to be applicable because of the need for a nitrophenol moiety to facilitate β -CD complexation, and so the number of substrates able to be analysed in this manner is limited.

Binding of analytes to the specific recognition sites of imprinted polymers results in a change in the heat-transfer resistance of the materials, which can be used as a sensing or assay technique for their detection. The method (heat-transfer method) has been used as a means of quantifying a range of analytes, including l-nicotine, histamine, and serotonin^{121, 122} and mammalian cells, including cancer cells.¹²²⁻¹²⁵ The method is sensitive, does not require labels, and is compatible with biological entities.

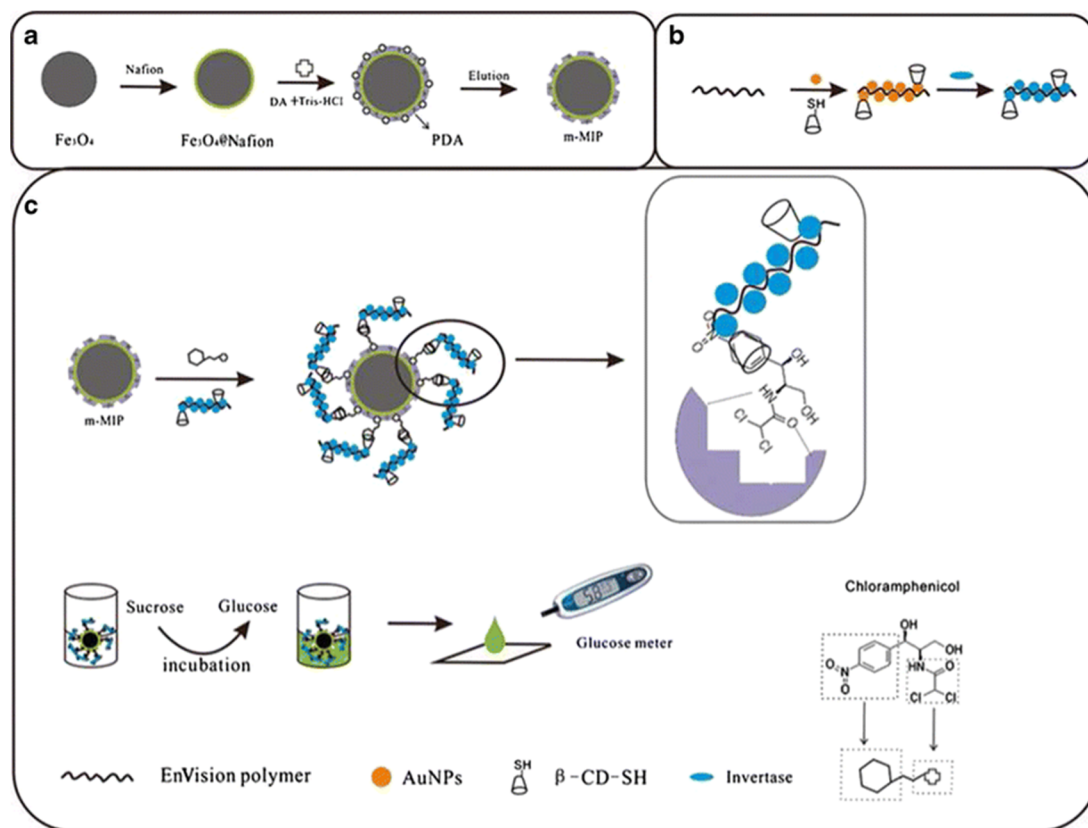


Figure 12. a) Preparation of MMIPs. b) EnVision reagent-Au- β -CD/invertase signal tag preparation. c) Scheme for the sandwich assay. Reproduced from Chen et al.¹²⁰ with permission from Elsevier.

1.7. MIAs targeting peptides and proteins

The molecular imprinting technology is not, however, without its limitations. Following an empirical statistical analysis of all research articles within the field, the general preference was for low molecular weight, hydrophobic, chemically inert templates with low polar surface areas.¹²⁶ In biological systems, molecular recognition occurs in aqueous media, with large macromolecules such as proteins the targets of binding. These are in stark contrast, and not without reason; difficulties regarding the imprinting of water-soluble biological macromolecules emerge due to their large size and structural complexity leading to steric and conformational issues, as well as the aqueous environment having a dramatic effect on the interactions required for binding.^{127, 128}

Many biomarkers for disease diagnosis and monitoring are peptides and proteins. Reports of protein imprinting in the literature have greatly increased in recent years; however, as mentioned, proteins are difficult templates to work with and not all reports provide strong evidence for imprinting. Kryscio et al. have shown that the structure of proteins typically employed as templates are adversely affected by exposure to monomers and cross-linkers commonly used in imprinting.^{129, 130} Verheyen and co-workers have also highlighted the problems of nonspecific interactions with polymers carrying charged monomers, which can overwhelm specific binding to MIPs.¹³¹ They argue that high binding affinity for proteins can only arise with a combination of hydrogen-bonding, electrostatic, and hydrophobic interactions in the correct balance. These and other issues have been raised in other reviews,^{132, 133} which recommend that surface imprinting approaches be employed with whole protein templates to avoid entrapment and poor binding kinetics. They also point out that epitope imprinting¹³⁴ avoids many of the pitfalls associated with imprinting macromolecules, as long as the nonspecific binding issue is addressed.

As a result of these problems, examples of MIAs for peptides and proteins are very few, despite their importance as targets. The work of the Liu group, mentioned previously, is one such example. In a series of papers, the authors describe assays targeting glycoproteins, utilising boronate affinity-based oriented surface imprinting.^{101, 118, 135-137} Whilst impressive results have been achieved, this approach relies on immobilisation of a template glycoprotein on a boronic-acid-functionalised surface through boronate affinity interaction, and thus is limited to this subset of proteins. A further example of a protein imprinted MIA is that of Xu et al.¹³⁸ In this work, a sandwich fluorescence immunoassay to detect trypsin was developed using a fluorescently labelled water-soluble core-shell MIP. The format utilised immobilisation of *p*-aminobenzamidine, a competitive inhibitor of trypsin, to capture the template in an oriented position and preserve its native conformation, prior to binding of the fluorescent MIP for quantification (Figure 13). The assay showed little to no cross-

reactivity with other serine proteases and unrelated proteins, and achieved a limit of quantification of 50 pM in non-diluted human serum. Whilst again impressive, there is a dependence on the template-inhibitor binding which limits the scope of this assay format, much like the previous example.

As the only cases to be found in the literature, there is clearly still work to be done in the development of peptide and protein MIAs. Whilst the assays reported by Liu employ surface imprinting, MIPs grafted to the surface of microplate wells hold promise but are unlikely to be adopted by industry because of manufacturing difficulties. The alternative strategy proposed for imprinting of proteins, epitope imprinting, is yet to be utilised in the context of generating MIPs with recognition for proteins to be applied in an MIA.

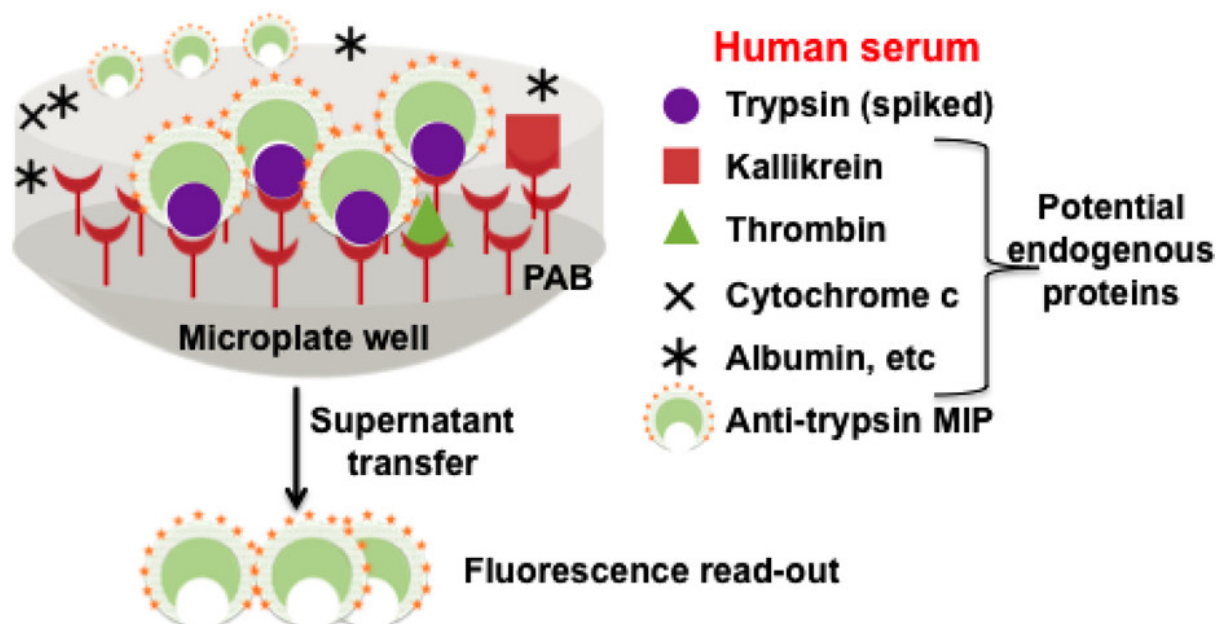


Figure 13. Illustration of fluorescent antitrypsin MIP as a synthetic antibody for detecting serum trypsin.¹³⁸ Reproduced from Xu et al. with permission from the American Chemical Society.

1.8. Prospects for diagnostic applications

During the last decade, significant progress has been made with regards to MIAs. Many of the problems that inhibited the growth of the area have been resolved following improvements in synthetic methods and a greater understanding of the molecular imprinting process, with fluorescent and enzyme-linked MIAs now commonplace. Recent years have seen a move away from traditional “bulk” MIP synthesis in favour of particle-based syntheses; in particular, MIP NPs hold great promise as they are more easily incorporated into existing assays formats.

The motivation for developing assays employing MIPs in place of antibodies has been the advantages that these materials would bring to the field. Generally, MIP development is shorter and less expensive than antibody development, targets do not require conjugation to immunogenic proteins, experimental animals are not involved in the process, and MIPs do not require cold storage and cold-chain logistics. Barriers to adoption of these new technologies may be uncertainty over security of supply and the perception that changes need to be made in manufacturing practices and plant in order to make the switch from antibodies to MIPs. This need not be the case, however, as several groups have demonstrated assays with MIP NPs that have been used as direct replacements for antibodies in a number of assay formats.

The lack of generality amongst assay formats and development is a further discouraging factor against the adoption of MIAs over conventional immunoassays. Whilst many elegant methods for specific templates have been devised, a simple, universal format applicable to any analyte of interest would be a far more attractive prospect. Of particular interest are homogeneous assays that do not require separation steps, since they simplify analysis and reduce the possibility of errors in measurement. If these conditions could be met, as well as maintaining the sensitivity and specificity which has already been demonstrated, then there should be little argument against the adoption of MIAs by the diagnostic industry.

1.9. Aims of the project

The work presented in this thesis aims to address the challenges regarding the imprinting of biological macromolecules, and overcome the barriers opposing the adoption of MIAs—namely the lack of a universal assay format. In doing so, the intention is to develop a reliable and rapid strategy to streamline the process of MIP optimisation, and production of a functional assay for any target of interest.

A combination of solid-phase and epitope imprinting will be utilised in the development of a novel assay-like format for rapid optimisation and testing of polymerisation mixtures, to afford MIPs with monoclonal-like binding to a target protein without the need for large-scale syntheses and time-consuming binding analysis.

The MIPs generated in this manner will then be applied to a number of assay formats, to be directly compared for their accuracy, sensitivity, selectivity, and ease of development, with the intention of designing the simplest generic biologic-free homogenous assay which is unrestricted by the analyte one wishes to detect.

The potential application of these techniques will then be demonstrated using a model protein, acetylcholinesterase (AChE). MIPs are to be prepared to map the topography of the surface of the protein and to identify peptide sequences which may be useful for MIP NP preparation using an epitope approach. The identified epitopes will then be synthesised and used as templates for polymerisation mixture optimisation and MIP generation. Changes in structure and enzymatic activity of AChE as a result of epitope-imprinted MIP binding will be explored, before their final application in the detection of AChE in the preferred assay format, utilising the different epitopes identified.

In this way, the aim is to demonstrate a process which can be used to identify binding sites on a protein, generate high affinity recognition materials for these sites through a rapid optimisation process, and then use these in a generic assay format for detection of the original protein of interest.

CHAPTER 2: MOLECULAR IMPRINTING OF PEPTIDES AND PROTEINS

The defining property underpinning the success or failure of molecular recognition is the strength of the complementary interactions between the functionalities presented by the analyte and receptor. In the case of a MIP, these functionalities are introduced through the monomers which the polymer is composed of, the selection of which is therefore crucial to maximising the ability of a polymer to bind the desired template. The optimisation of monomer compositions is however a very time consuming process, with lab-based approaches focusing on combinatorial synthesis and screening.^{139, 140} This has led to monomer selection often being made on the basis of previous experience or chemical intuition, with very little optimisation performed.

With vast quantities of functional monomers either commercially available or readily synthesised, narrowing the selection to those most optimal for a particular target is a daunting task. The advent of *in silico* tools to aid in this process is therefore welcomed, and coupled with a rapid lab-based screen has potential to produce far superior MIPs to those synthesised using typical compositions without investing a large amount of time.

By selecting and varying the composition of monomers in this way and directly observing the effect this has on the polymer's affinity for the template, it should become clear which interactions are essential to the recognition of peptides and proteins in aqueous media, and aid in our understanding and design of MIPs for such templates.

Aims of this chapter

- Design of a screening procedure for optimisation of polymer compositions.
- Confirm the relationship between optimisation procedure, MIP affinity, and yield.
- Compare compositions optimised in this manner to those typically used.

2.1. Introduction

Much of the early work in the field of molecular imprinting has been focused on small molecules. Small molecule imprinting, whilst challenging in its own right, is now quite well understood, and design of receptors for these templates is rather routine. Due to their small size, limited functionalities will be available to exploit in order to generate strong binding affinities. Whilst this may at first appear a problem, it instead simplifies the issue of monomer selection, as polymer compositions can be rationally designed through chemical intuition by selecting monomers which will have strong complementary interactions with the small number of interaction sites. In this way recognition can be achieved through fewer, stronger interactions, which is beneficial in regards to reducing cross-selectivity, as the functionalities unique to the template compared to its analogues can be focused upon specifically.

Unfortunately, moving to larger templates complicates the process of polymer design. Due to the sensitive structural nature of biomacromolecules imprinting needs to be performed in an aqueous environment, which immediately limits the number of monomers significantly compared to those available for organic polymerisation against small molecules. A more important consequence of this solvent requirement however is the impact on available interactions—hydrogen bonding has a large contribution to the affinity of MIPs in organic aprotic solvents, however the effect of these interactions is largely diminished in an aqueous system.¹⁴¹ In an aqueous environment there is therefore more reliance upon ionic and hydrophobic interactions to facilitate recognition, however charge and hydrophobicity will vary strongly across different regions of a protein's surface and similar sites are more likely to be present in other templates, leading to increased non-specific binding and cross-reactivity.

Encouragingly, despite these challenges, the number of papers related to protein imprinting have begun to increase, with over 11% of the publications from the MIP community in 2018 targeting protein templates. Of the work published in the last year, however, over a third of the templates can be considered model proteins (albumin, haemoglobin, lysozyme), which have contributed to the majority of the literature on protein imprinting since 1985.¹³¹ The continued extensive use of these model proteins suggests that molecular imprinting of proteins is still in development, and research in the area is still focused on proof of concept studies using well-defined proteins with known polymer compositions for successful MIP generation. Multiple reviews of the field have been critical of work in the area, concluding that evidence of molecular imprinting is not convincing in numerous publications, and that the persistent challenges of macromolecular imprinting still make it unclear whether a high selectivity for similar proteins can be achieved.^{131, 142} The selection of functional monomers used is rarely commented upon, with little optimisation of polymer compositions appearing to be

performed—considering the known difficulties with protein imprinting, it is unusual that this factor is not explored further. This may be due to the lack of an established method for optimisation of monomer composition for proteins; to date there are no examples of a screening procedure or combinatorial library against a protein template in order to assess the influence of specific monomers on the resulting polymers affinity and selectivity.

Peptides occupy an interesting middle ground between small molecules and proteins. Akin to small molecules, they possess a more rigid structure, unlikely to take on any secondary conformation. Whilst it is therefore possible to perform peptide imprinting in organic solvents in the same way as for a small molecule, for practical applications it is most beneficial to achieve recognition in an aqueous environment. Representing a simpler system than a protein, optimisation of polymer composition against peptides may help bridge the gap between small molecule and protein imprinting. In a study designed to generate MIPs against a 26 residue peptide, melittin, Hoshino et al. synthesised a small combinatorial library of polymers by varying the relative concentrations of a selection of monomers.¹⁴³ The selected monomers consisted of six acrylamide derivatives: the bulk of each polymer consisted of *N*-isopropylacrylamide (NIPAm) as backbone monomer in combination with AAm, acrylic acid (AAc), *N*-(3-aminopropyl)methacrylamide hydrochloride (APMA), and *N*-*tert*-butylacrylamide (TBAAm), as hydrogen bonding, negative-charged, positive-charged, and hydrophobic functional monomers, as well as BIS (2 mol%) as a cross-linker (Figure 14). Of the 13 polymers synthesised, only two compositions showed appreciable affinity towards the target when analysed via quartz crystal microbalance (QCM), demonstrating the importance of optimising monomer composition to achieve successful imprinting. The work has since received over 250 citations, with the polymerisation mixture widely used for a variety of templates in aqueous environments. Interestingly, in contradiction to the original paper, the strict requirement for optimisation of molar ratios for successful imprinting does not appear to be discussed in the publications which have followed.

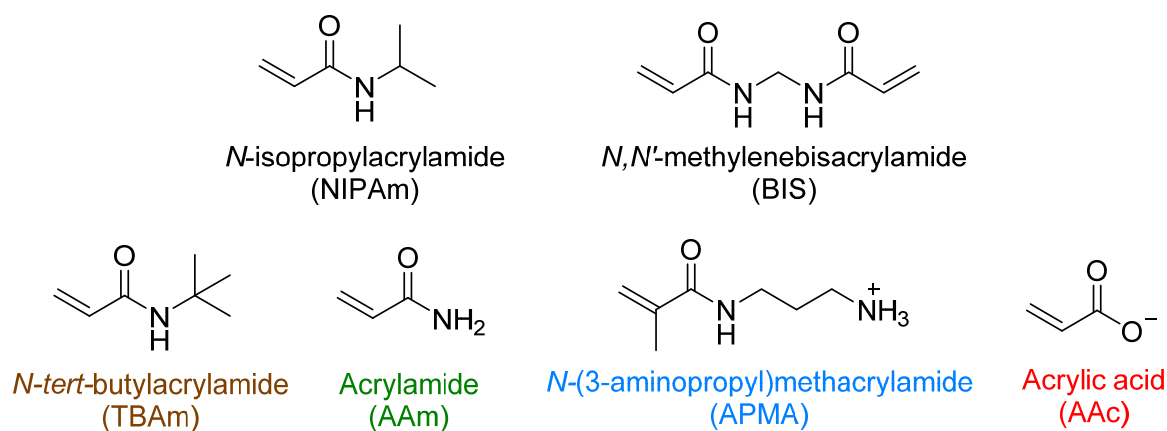


Figure 14. Monomers used by Hoshino et al. in combinatorial library preparation. Hydrophobic, hydrogen bonding and positive/negative charged functional monomers are indicated in brown, green, blue/red.

This is likely due to the time-consuming and labour-intensive nature of synthesising a combinatorial library such as that in the original study. The fact this monomer composition has been successfully applied without optimisation in numerous other works suggests that the monomers employed are versatile and capable of recognition in an aqueous environment for a variety of protein/peptide templates. This selection of monomers therefore provides a good starting point for achieving recognition in an aqueous environment. It would however be desirable to have a high-throughput screen in order to optimise the polymer composition if, such as in the case of melittin, the “standard” composition does not lead to appreciable affinity. As the aim of this work is to develop a universal strategy for protein/peptide detection, such a screening process is necessary for more challenging templates, as detection cannot be achieved without a well performing receptor.

Inspired by solid-phase peptide synthesis and affinity separation columns, Piletsky et al. proposed and designed a novel strategy for solid-phase MIP synthesis (Figure 15).¹⁰² The approach has a number of advantages over traditional polymer synthesis methods: the use of an immobilised template eliminates contamination of the product with template; MIPs are collected through an affinity separation system, resulting in more uniform binding properties; and the process is scalable without detriment to the quality of polymers produced. Imprinting in this way presents an ideal method for performing small-scale syntheses for testing polymerisation mixtures, as information regarding the MIPs affinity can be assessed as part of the elution process, without a need for time consuming analysis such as QCM or surface plasmon resonance (SPR).

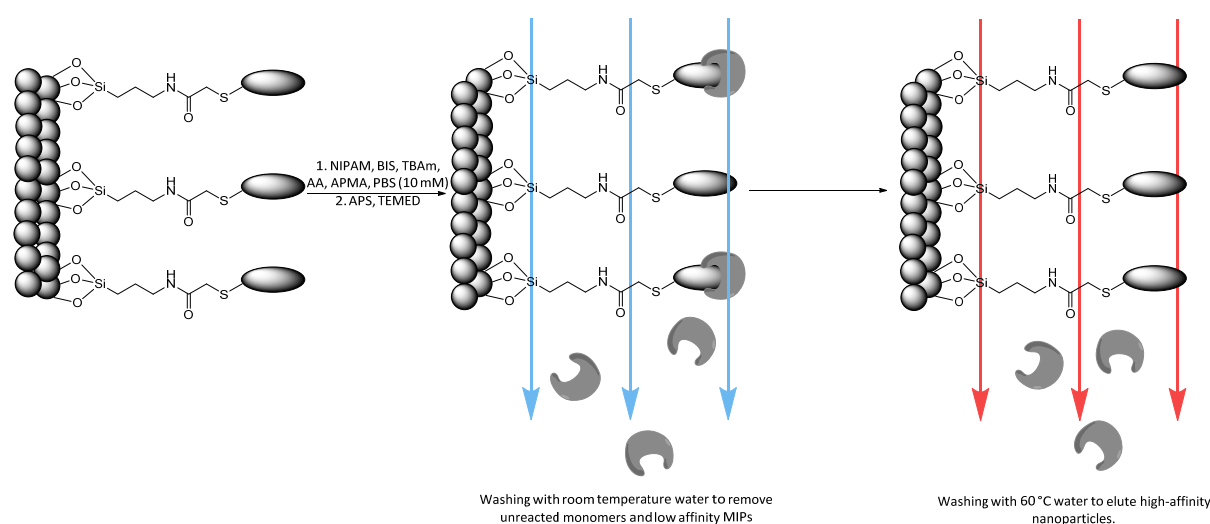


Figure 15. Schematic representation of solid-phase imprinting with affinity-based separation of polymers.

2.2. Small scale synthesis screening strategy

To facilitate rapid synthesis and screening of a combinatorial library of polymers the solid-phase synthesis method was scaled down to just 50 mg of template-immobilised solid phase, allowing a single well of a 96-well microplate to function as an individual reaction vessel. In this way, 32 different polymer compositions can be simultaneously produced and tested in triplicate. Utilising filtration microplates allows the elution and washing steps to be performed in a similar manner to the large scale synthesis, whilst incorporation of a fluorescent monomer makes it possible to follow the quantity of polymer eluted from the solid phase under different washing conditions.

The monomer mixture recommended by Canfarotta et al. for the solid-phase synthesis of MIPs against peptides and proteins has been adapted from that used by Hoshino et al.¹⁴⁴ Whilst any combination of monomers could be tested using the proposed method, the recurrence and recommendation of these same monomers led to their selection in this initial proof-of-concept study, with the functional monomer composition ratios altered to probe their importance to the polymer's affinity for the template (Table 2).

Table 2. Functional monomer composition ratios. Mol% made up to 100% with NIPAm.

Entry	Functional Monomer Composition Ratio (mol%)		
	TBAm	AAc	APMA
1	40	0	5
2	40	10	5
3	40	15	5
4	40	5	0
5	40	5	10
6	40	5	15
7	0	5	5
8	55	5	5
9	65	5	5
10	40	5	5

2.3. Polymer composition for imprinting of peptides

Three peptides were investigated using the proposed screening method (Figure 16). Two of the selected peptides have identical sequences differing only through their phosphorylation state; the parallel structures were chosen as a way to assess the selectivity introduced through different polymer compositions for chemically similar structures. The third peptide was chosen to be distinctly different to the others, to observe how much influence the amino acid sequence would have on the optimal polymer composition.

Peptide-immobilised solid phase was prepared in bulk before dividing into 50 mg aliquots for direct addition to each microplate well. Briefly, this involved activation of silica beads through boiling in sodium hydroxide, prior to silanisation to afford free amine groups on the surface for functionalisation. Succinimidyl iodoacetate (SIA) was subsequently used to couple the free amines to the terminal cysteines of the peptides, achieving site-specific immobilisation of each peptide in a fixed orientation (Figure 17).

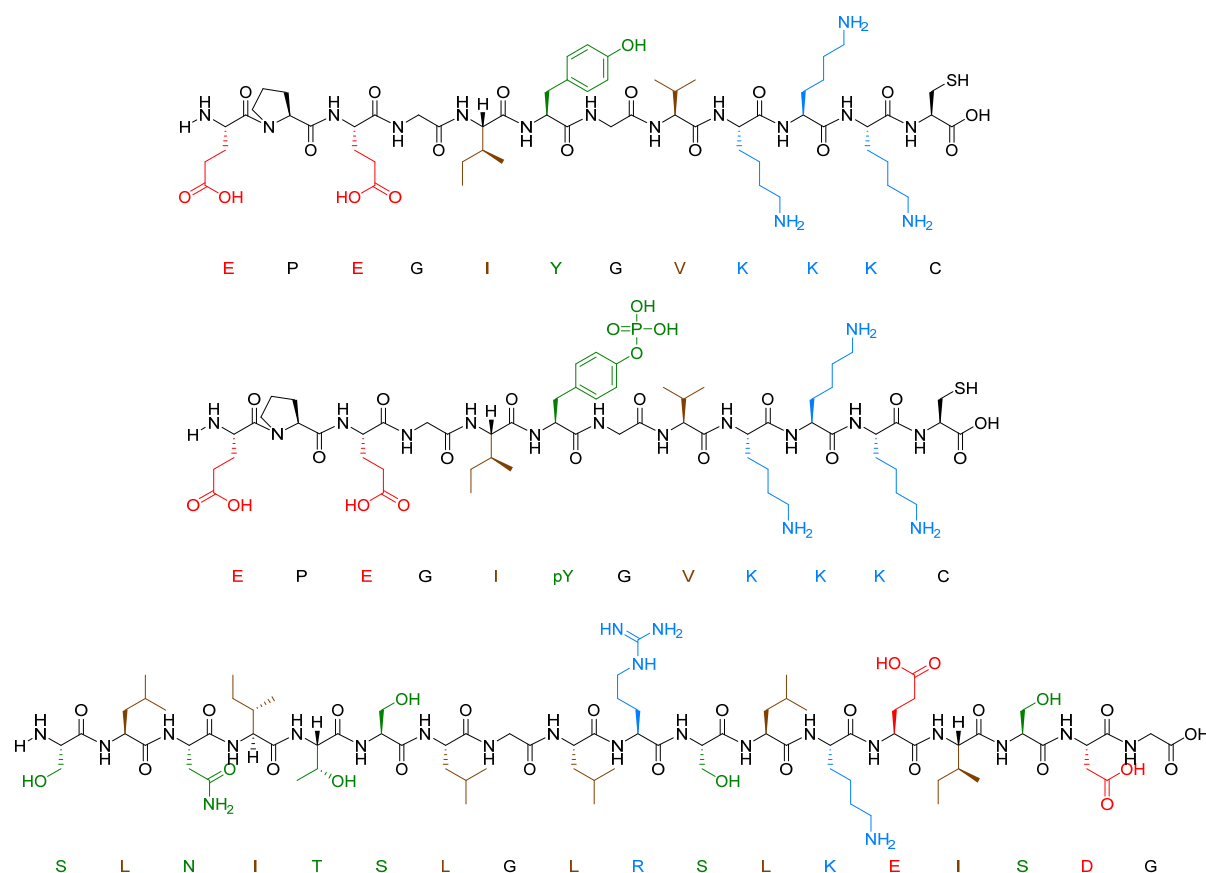


Figure 16. Peptide templates employed for composition screening. Acidic (red), basic (blue), polar (green) and hydrophobic (brown) residues are all highlighted.

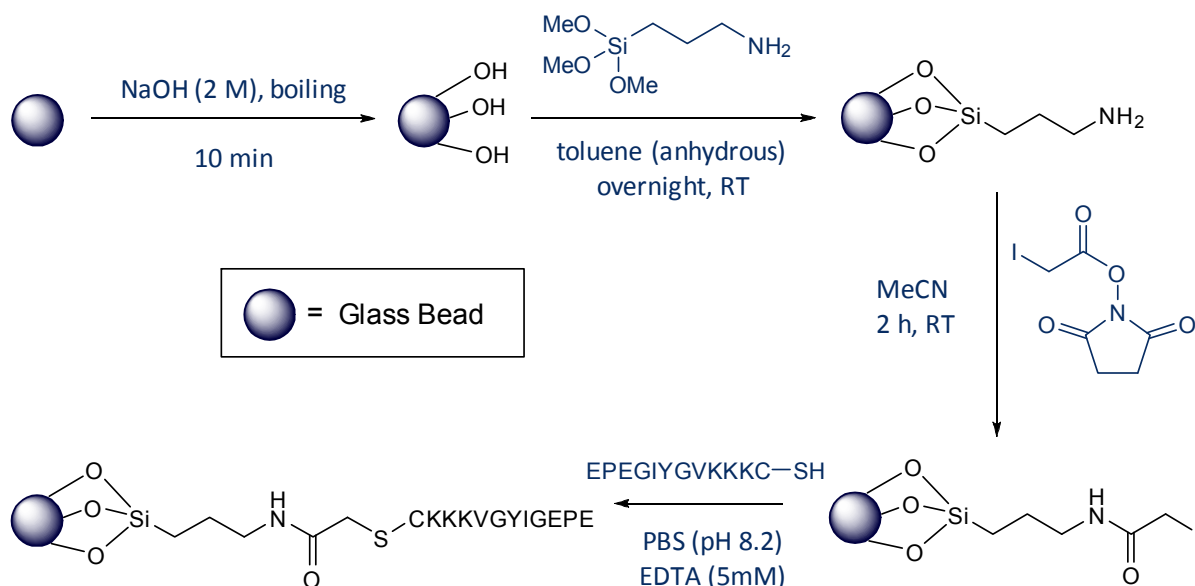


Figure 17. Immobilisation of peptide template for solid-phase imprinting performed using protocol optimised by Canfarotta et al.¹⁴⁴

Having loaded peptide-immobilised solid phase into the wells of a filtration microplate, the prepared monomer solutions were added and polymerisation initiated chemically through addition of ammonium persulfate (APS) and *N,N,N',N'*-tetramethylethylenediamine (TEMED). After an hour the unreacted monomer and low affinity polymer were removed by vacuum filtration, and the solid phase washed with 10 volumes of cold water (no appreciable drop in fluorescence was observed with additional washes), before measuring the fluorescence. A further 10 washes with 60 °C water were then performed, to emulate the elution step of the large scale synthesis (Figure 18).

A large amount of information can be acquired from this data. Firstly, from looking at what remains on the solid-phase after the cold washes alone, it can be concluded that regardless of polymer composition, what is referred to as “high affinity” MIPs by Canfarotta et al. remains on the solid-phase for collection. This is in contrast to the work carried out by Hoshino et al., in which very few polymer compositions demonstrated appreciable affinity. This can be rationalised by comparing the two synthetic methods; in Hoshino’s experiments MIPs were prepared by precipitation polymerisation with no affinity separation step. A sample of MIPs produced in this way will therefore demonstrate a wide distribution of affinities for the template, with the response observed by a method such as QCM representing the average affinity of all polymers in the sample. It has been noted that a large proportion of polymer produced in this way does not contribute to specific binding,¹⁴⁴ and therefore the response observed by QCM may appear to show little affinity, regardless of the presence of a small proportion of high affinity MIPs. In solid-phase synthesis however MIPs with low affinity are discarded—whilst this results in lower polymer yield, the nanoparticles produced will have a narrower and higher affinity distribution.

There are also clear trends which can be identified from the data collected after washing of the solid phase. It appears that for each peptide, the exclusion of AAC is beneficial. Whilst it is not immediately obvious why its inclusion would be detrimental to the polymer, there are no residues in the EPE- peptides which can accommodate a positive charge and form a strong electrostatic interaction with AAC. There is therefore no reason based on chemical intuition to include this monomer for this template. It should be noted that the lysine residues of the linker could form such a complementary interaction with AAC, however due to being so close to the solid phase these residues are assumed to not be involved in polymer formation for steric reasons. It is interesting that for SLN-, which has positively charged lysine and arginine residues, the same trend was observed. The benefit of completely removing AAC was not as pronounced as for the

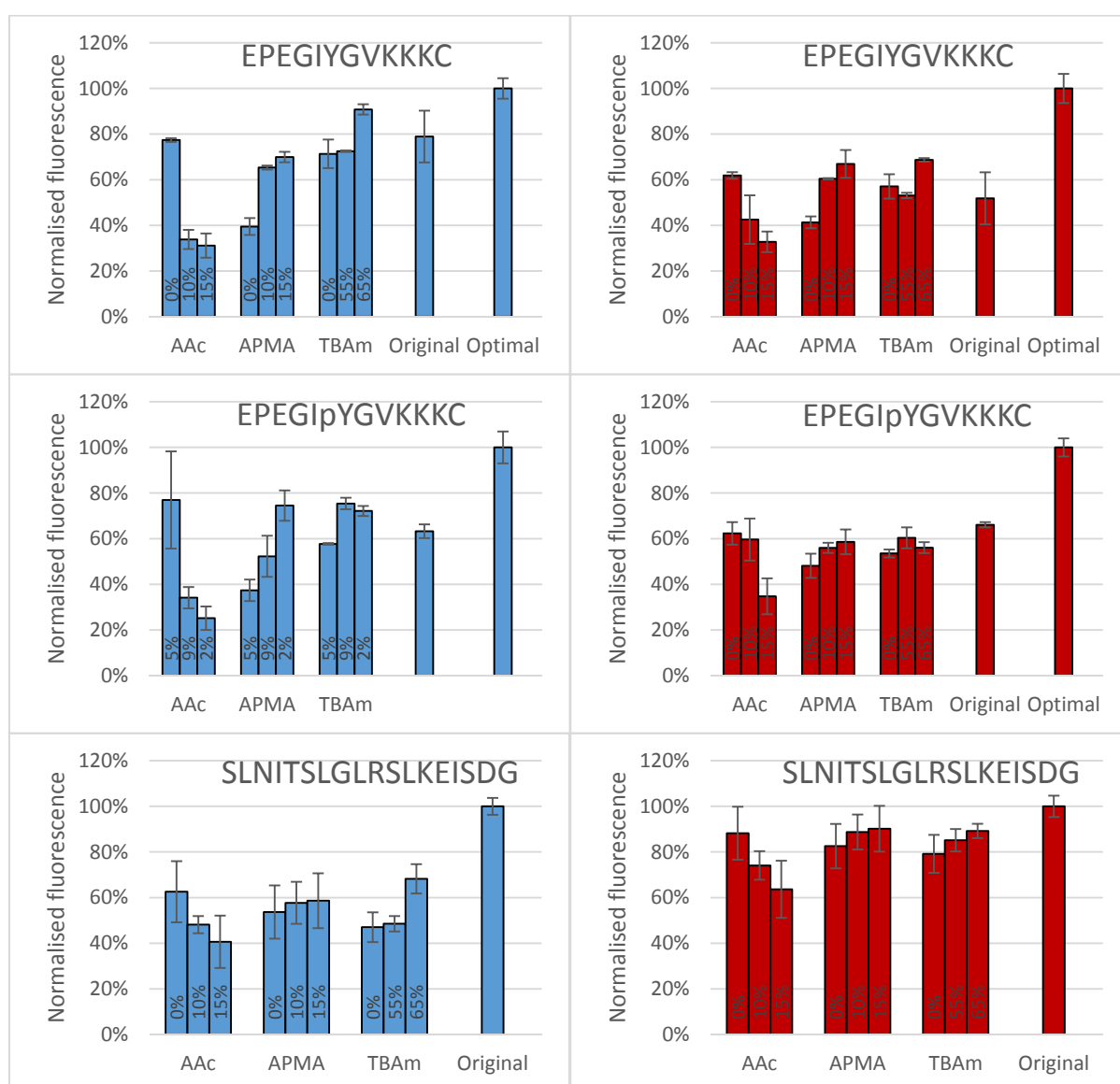


Figure 18. Normalised fluorescence of each polymer composition against all three peptides following washing with 10 volumes of room temperature (blue) and 60 °C (red) water.

other peptides however (43% increase in signal from removal of AAc for EPE- vs 15% for SLN-). This suggests that in general for peptides it is not beneficial to include AAc, however with an increased number of basic residues it may become advantageous.

For APMA and TBAm the opposite trend is observed for all three peptides, where increasing the concentration of these functional monomers results in a greater retention of polymer. All three peptides contain negatively charged glutamic acid residues, and so increasing concentration of APMA being favourable is logical. The benefit is most drastic in the phosphopeptide, indicating that the introduction of additional negative charge through the phosphate group compared to the non-phosphorylated peptide could be taken advantage of to introduce selectivity, through increasing the concentration of APMA in the polymer composition. Again, all three peptides contain hydrophobic residues, and so TBAm being beneficial is of no surprise.

Following analysis of these results, an optimal polymerisation mixture was prepared for the EPE- peptides, using the monomer ratios which gave the highest signal (0% AAc and 15% APMA and TBAm). When tested, this optimal composition led to the highest retention of MIP on the solid-phase, indicating that a greater yield of high affinity MIP was achieved. The same was not done for SLN- however, as the original monomer ratio (Table 2, Entry 10) already gave a higher signal than any of the other compositions tested.

The fluorescence after the cold washes is a result of the “high affinity” MIPs which still remain on the solid phase. The difference between these results and those after the 60 °C washes is therefore an indication of the yield of MIP that would normally be collected as product in the large scale synthesis. The first point of interest from the results presented in Figure 18 is that MIPs are still bound to the solid phase following the high temperature elution procedure. This suggests that MIPs with even higher affinities still remain to be eluted if even harsher conditions are employed to disrupt their interactions with the immobilised template. From looking at the change in ratios of peak heights before and after 60 °C elutions, it is possible to qualitatively assess the yield of high affinity nanoparticles collected for different compositions under these elution conditions. This is most clear for EPE-; prior to high temperature elution the ratio of original to optimal compositions is 0.79, however afterwards the ratio is 0.52—this indicates that if as part of the large scale synthesis only this elution step is performed a higher yield will be obtained using the original polymer composition as opposed to the optimal, regardless of the fact that there is still more MIP on the solid phase when using the optimal composition.

The results of this screening led to a reassessment of the original aims. The intention of developing a screening method was to optimise functional monomer composition ratios in a time-efficient manner, in order to generate MIPs with appreciable affinity for the template of interest. The data collected indicates that this has been achieved with this protocol—the optimal composition following screening with a small set of monomers produced MIPs with greater retention for the solid phase. However, the data also highlighted that an increase in affinity can actually lead to a decrease in yield if the

MIP produced can no longer be removed from the solid phase. This leads to the question of whether it is necessary to optimise the polymer composition at all, as it has been observed that using the solid phase synthesis with the original monomer composition yields MIP for all three of the peptides tested.

The overall aim of this work is to develop a generic assay format for peptides and proteins utilising MIPs as a receptor. It would therefore be advantageous if a single, generic polymerisation mixture could successfully be used for MIP generation, as this would remove the step of receptor optimisation from the assay development. Antibodies typically used in assay development will have affinities in the low micromolar to nanomolar range; as long as the affinity distribution of MIPs collected during the 60 °C elutions falls within this range they can be considered adequate receptors to transfer into assay development, without modifying the polymer composition.

MIPs were therefore synthesised against a number of peptides using the solid phase protocol, all with the original polymer composition. The affinity of these MIPs was then confirmed using SPR, to ensure that the MIPs collected using high temperature elution consistently demonstrated nanomolar binding.

A total of six peptides were tested in this manner: of these, all peptides imprinted using the solid phase protocol and the original polymer composition produced MIPs

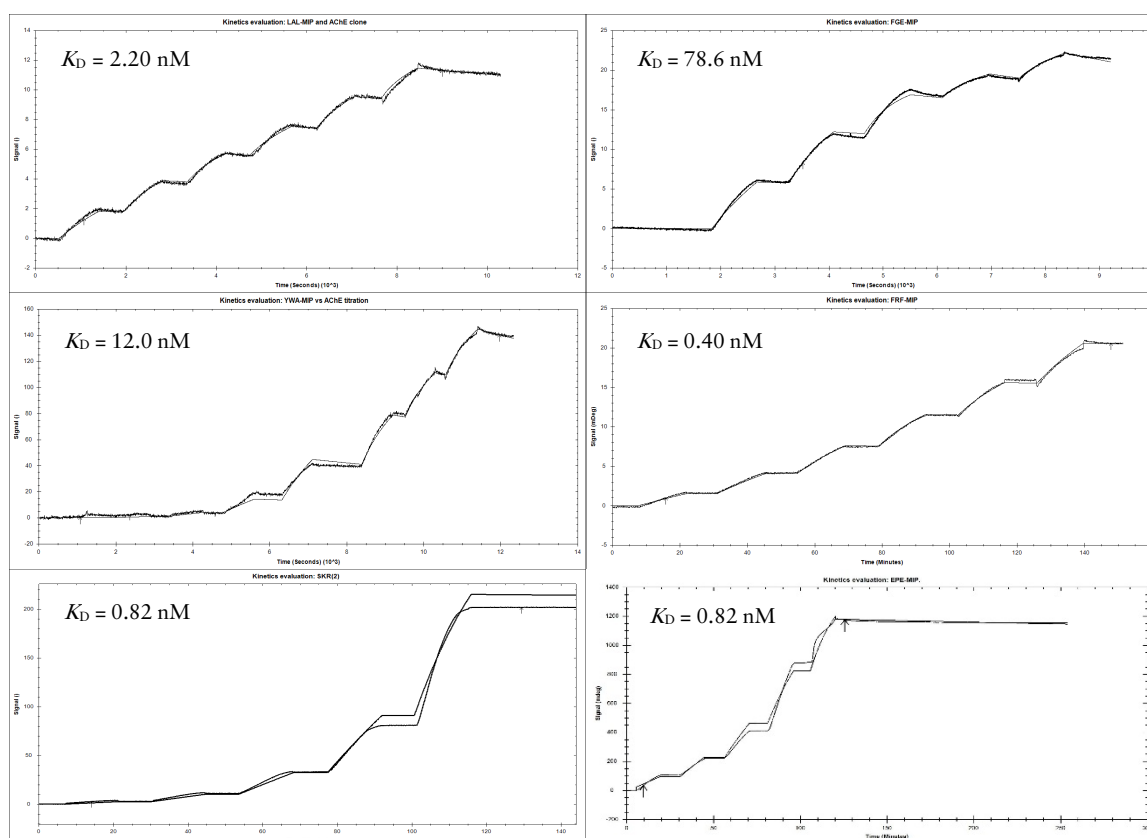


Figure 19. SPR sensorgrams obtained with a MP-SPR Navi 220A NAALI (BioNavis). Sensorgrams show response in degrees as a function of time, following sequential injections of increasing concentrations of analyte.

demonstrating nanomolar affinity when analysed by SPR (Figure 19). It was therefore concluded that for generation of MIPs for recognition of peptides, affinities appropriate for use in assay development could be achieved without the need for optimisation of polymer composition. For this reason the screening strategy was not developed any further as part of this work, however the results collected are encouraging and the strategy may well be worth pursuing if a given application demands MIPs with greater affinity—as an example, the application of MIPs for extraction of an analyte from a mixture would benefit from having as high an affinity as possible. Whilst all peptides tested demonstrated nanomolar affinities without optimisation, it should be noted that this is still too small a sample to say with confidence that a single polymer composition will work for all templates, and so there is still value in having this optimisation protocol should the standard composition fail for a more challenging analyte.

2.4. Polymer composition for imprinting of proteins

Three proteins; amylase, albumin, and trypsin were investigated in the same manner as the aforementioned peptides (Figure 20). The most immediate observation from this data is how little influence the polymer composition has on the MIPs retention compared to the experiments conducted against peptides. For all of the compositions tested, the difference in response was no greater than 20%. This is not particularly surprising; when imprinting such a large template with an abundance of interaction sites available for monomers to pre-assemble themselves around, it would be very unlikely that the inclusion/omission of a particular monomer would result in an inability to generate a high affinity interaction with any of these points of interaction. This leads to the same conclusion as for peptides: that optimisation of the polymer composition is an unnecessary step for the synthesis of nanoparticles with appreciable affinity.

This conclusion obviously does not help regarding the issue of poor selectivity of protein-imprinted MIPs however, but does provide useful information for how to attempt resolving this problem. The results highlight that trying to optimise polymer composition against a particular protein is futile, if the monomer composition ratios are changed, then monomers will likely arrange themselves around different interaction sites on the protein's surface—this being the reason for no appreciable change regarding affinity being observed in these experiments. Whilst the affinity-based elution in the solid phase synthesis will ensure a narrow affinity distribution, because imprinting is taking place against multiple sites across the protein, a broad selectivity distribution will still be present. This result therefore supports the epitope imprinting strategy for generation of protein-selective MIPs as this introduces a far narrower selectivity distribution, reducing the likelihood that a sample of MIPs will have affinity for a protein other than that containing the epitope imprinted against. This is by no means a complete answer for the problem of cross-selectivity, as non-specific binding will occur simply through interactions of the polymer's surface functionalities with that of a protein, regardless of

the imprinted cavity of the MIP and which surface epitope has been imprinted against; however the affinity of these non-specific interactions should be considerably weaker than those of the imprinted cavity for its template.

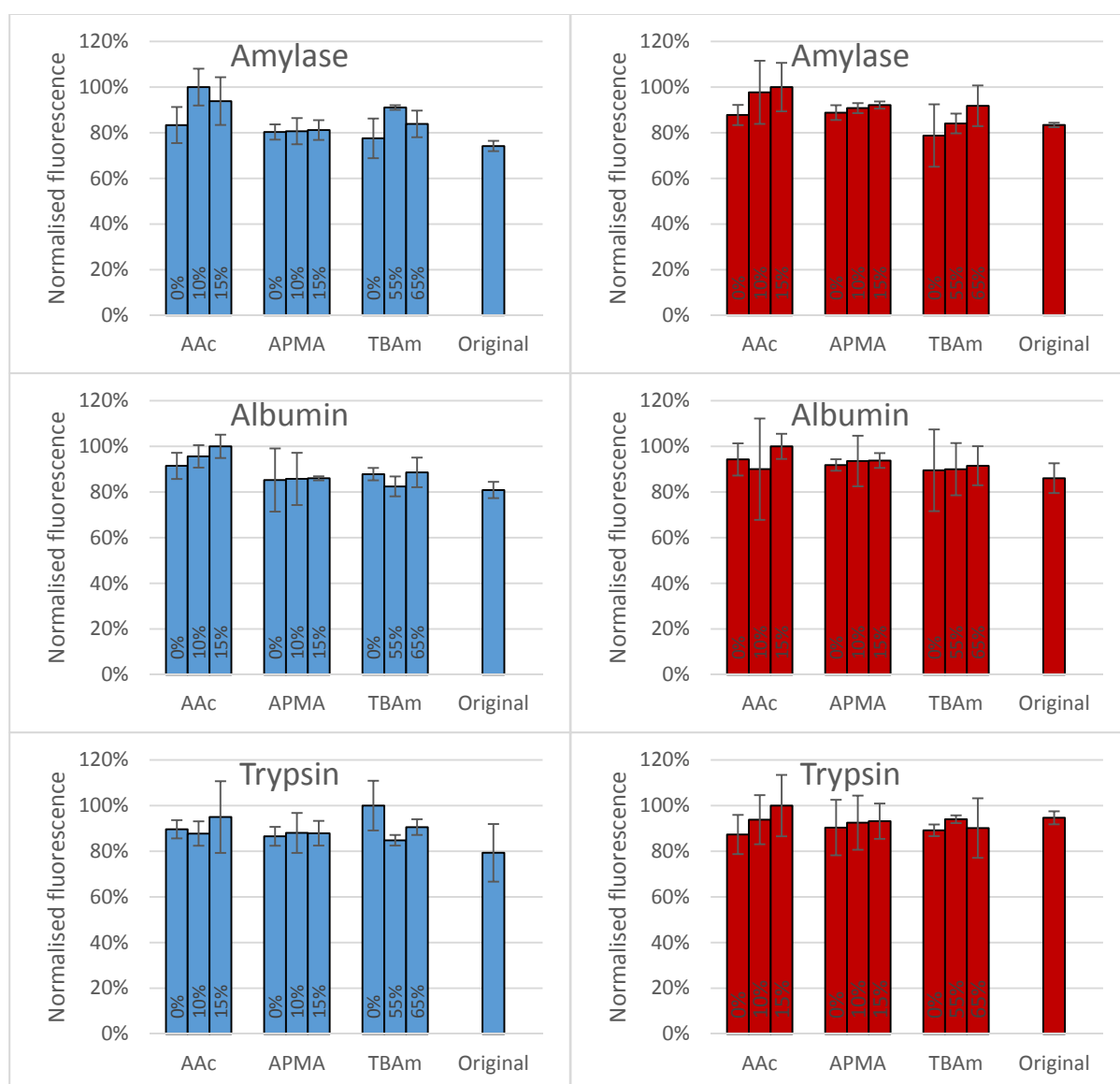


Figure 20. Normalised fluorescence of each polymer composition against all three proteins following washing with 10 volumes of room temperature (blue) and 60 °C (red) water.

2.5. Conclusions

A screening procedure for optimisation of polymer compositions was designed utilising a 96-well filtration microplate, solid-phase synthesis with affinity separation, and a fluorescent reporter monomer. This allowed the simultaneous evaluation of 32 different monomer compositions in triplicate, generating information regarding affinity and selectivity introduced through a variety of monomers. Three peptides and three proteins were assessed using this method against a library of 10 functional monomer composition ratios. Modification of monomer ratios had an observable impact on the resulting MIPs affinity for peptide-immobilised solid phase, however very little influence was observed for protein-imprinted MIPs. Optimal monomer compositions were selected from the screening results and demonstrated greater retention for the solid phase, however this increase in affinity led to a decrease in yield using the normal elution protocol, as MIP could no longer be easily removed from the immobilised template. Whilst harsher elution conditions could be explored in order to collect the remaining MIPs with higher affinity, this was deemed unnecessary, as the affinity distribution of MIPs produced for six different peptides and collected with 60°C water were confirmed using SPR to exhibit nanomolar dissociation constants, which is adequate for application to binding assays. Although not observed as part of this study, in the event that MIPs synthesised using the solid-phase protocol do not demonstrate appreciable binding, the developed screening method will provide a useful tool for optimising compositions for enhanced affinity.

CHAPTER 3: DEVELOPMENT OF A GENERIC HOMOGENOUS ASSAY FORMAT

The most important components of any assay are the receptor and the signal. Having developed a method to optimise the receptor in the previous chapter, the focus of this chapter is on optimisation of the signal generated through binding. The most commonly employed signalling methods, as described in detail in chapter 1, are colorimetric and fluorimetric. The problem with these methods are that the physical separation of bound and unbound analyte prior to measuring the signal intensity is normally required in order to perform a quantitative analysis (known as a heterogeneous assay). Methods which avoid this separation step (homogeneous assays) have been devised, however this is usually done with a single analyte in mind and is not applicable to other targets.

FP is a commonly used technique suitable as a detection method in homogenous assays. Whilst previous examples of MIAs utilising this detection method have used the inherent fluorescence of the analyte of interest, conjugation of a polarisable fluorophore allows even non-fluorescent targets to be detectable. This technology has therefore been explored in this work as a potential generic assay format.

A novel assay relying upon microplates modified with magnetic inserts, template functionalised iron-oxide nanoparticles, and fluorescent MIPs has also been developed as an alternative. Both methods can therefore be directly compared for their suitability to high-throughput screening applications and evaluated in relation to the currently dominant assay format for diagnostic screening, ELISA.

Aims of this chapter

- Assess the suitability of FP as a MIA format.
- Explore the use of mNPs in a novel assay format.
- Compare the accuracy, sensitivity, dynamic range, run time, ease of measurement, and ease of development of each format.

3.1. Introduction

ELISA is an analytical quantification technique which dominates diagnostic and drug screening platforms. It utilises the high affinity and selectivity of antibody-antigen interactions to capture analytes of interest, and the development of a visible signal through conjugated enzyme activity. The technique is very well established, with over 140,000 publications on the topic in the Web of Science Core Collection as of July 2018. Likewise, antibodies are currently the gold standard of affinity reagents, with an estimated \$1.6 billion spent worldwide on these reagents in 2011.¹⁴⁵ Whilst there may appear little reason to pursue alternative diagnostic tools to compete with such a highly adopted product, there is growing concern surrounding the quality of antibodies,^{145, 146} as well as niche, but very significant, applications where the use of antibodies is not possible. There are also notable drawbacks of the ELISA method, which whilst currently accepted, do leave room for improvement.

Improvements however will not be enough to persuade current researchers and companies to abandon such a tried and tested technique. An MIA developed in 2013 demonstrated that antibodies could be directly replaced by MIPs requiring no further modification to the ELISA protocol, with the MIPs outperforming their biological counterpart with sensitivity 3 orders of magnitude better¹⁰³—however the widespread adoption of MIPs has still not been forthcoming, 5 years later. Groff et al. outlined multiple paths to assist researchers in the transition from animal-derived antibodies to modern affinity reagents, noting that whilst the advantages are clear, financial incentives need to be in place to support this transition.¹⁴⁷ For industry in particular, an estimated cost of \$2-10 million would be associated with proving the equivalence of an alternative affinity reagent to a mAb, demonstrating that even a small procedural change such as that described in the MIA above can lead to significant costs for companies.¹⁴⁸

In order to catalyse the establishment of MIPs as a commercial diagnostic product, a more effective strategy than trying to compete with antibodies would therefore be to exploit the areas where antibodies have failed. By focusing efforts on analytes of high significance which are non-immunogenic or unsuitable antigens, such as small molecules, toxic compounds, and immunosuppressants, it will be possible to demonstrate the potential of MIAs in a platform where there is no satisfactory alternative. Taking advantage of the gaps in antibodies applicability will allow the strengths of MIPs as affinity reagents to be showcased; coupling this with a more desirable assay format than ELISA—one which is homogenous, generic, and quick to develop—should assist in highlighting the benefits of moving from an antibody-based ELISA to a MIA and assist MIP technology to establish a foothold in the diagnostic affinity reagents market.

Phosphopeptides are one such desirable target where antibodies have fallen short. Phosphorylation is one of the most common post-translational modifications, affecting

essentially every basic cellular function; such as cell growth, proliferation, differentiation, apoptosis, and signal transduction.¹⁴⁹ This process is catalysed by protein kinases, which facilitate the transfer of a phosphate group to specific amino acids; most commonly Ser, Thr and Tyr residues. It is estimated that approximately one-third of all proteins in a eukaryotic cell are phosphorylated at any one time.¹⁵⁰ With such a high proportion of phosphorylation events, disruptions in signalling pathways regulated by kinases and phosphatases can provide key biomarkers for a wide variety of diseases, including cancer,¹⁵¹⁻¹⁵³ diabetes,¹⁵⁴ neurodegenerative,¹⁵⁵⁻¹⁵⁷ cardiovascular,^{158, 159} and inflammatory diseases.^{160, 161}

Analysis of phosphorylation events is not straightforward however. The stoichiometry of phosphorylation from a stimulus is relatively small, with many of the signalling molecules present at a low abundance within cells. This makes enrichment a prerequisite to analysis typically performed by mass spectrometry (MS) methods.¹⁵⁰ Phosphospecific antibodies are routinely used to immunoprecipitate specific proteins, however this is only considered successful for enrichment of tyrosine-phosphorylated proteins.¹⁶² Enrichment of tyrosine-phosphopeptides results in insufficient amounts for analysis,¹⁶³ whilst antiphosphoserine and antiphosphothreonine antibodies are not routinely used due to their poor selectivity.¹⁶⁴ The application of MIPs to overcome these problems is not a novel idea. Enrichment of phosphotyrosine peptides has been achieved, with subsequent analysis indicating superior performance of MIPs when compared to three commercially available antiphosphotyrosine antibodies.¹⁶⁵⁻¹⁶⁷ Phosphohistidine¹⁶⁸ and phosphoserine¹⁶⁹ have also successfully been imprinted. There is therefore a clear advantage to the use of MIPs for the detection of phosphopeptides, where antibodies do not adequately perform. Current applications of MIPs for detection of phosphorylated biomarkers have focused on enrichment with analysis carried out using MS methods, however a more high-throughput format would be more desirable. Phosphopeptides are therefore an ideal analyte for development of a high-impact, high-throughput MIA, where antibodies are unable to compete.

Whilst identifying analytes where antibodies are currently unavailable is rather trivial, identifying significant weaknesses and areas to improve in the ELISA protocol is more challenging. The generic nature of ELISA, allowing the same protocol to be carried out regardless of template, is a huge strength. Whilst there are drawbacks, such as the heterogeneous nature of the procedure requiring multiple separation and incubation steps, these issues have been overcome through the application of robotics and automation, allowing high-throughput analysis regardless of the multi-step protocol. Most screening laboratories will already have invested significant money into these facilities, and so there is no real incentive to change assay format. Regardless of this, a mix and read homogenous assay format would still present a significant reduction in screening time, which on a large scale would be notably advantageous. With the intention of trying to showcase a technology, it is worth the investment to improve on every aspect of the current format, and so exploring homogenous assays compatible with MIPs is worthwhile.

From surveying the literature, the most common homogenous assays are FP, FRET, and fluorescence quenching/enhancement. Of these, polarisation appears the most promising candidate for developing a generic protocol. FRET relies on multiple fluorophores, as well as a distance dependant signal, which may be compromised in larger molecules where the fluorophore is conjugated far from the binding site. Fluorescence quenching/enhancement with MIPs has been employed in specific circumstances where the fluorescent properties of a reporter monomer are modified in response to binding, or the analyte of interest itself is inherently fluorescent and affected through interactions with the MIP. FP however relies solely on the conjugation of a single polarisable fluorophore to the analyte of interest. Whilst this could be considered a drawback, as conjugation of a fluorophore may interfere with the ability of a MIP to recognise the native analyte, this does not pose a limitation in the context of an MIA, as the same conjugation strategy adopted for solid-phase immobilisation during MIP generation can be employed for fluorophore conjugation, removing the possibility of the fluorophore interfering with rebinding.

FP assays are a competition based detection consisting of sample analyte, a fluorescently-labelled tracer, and a binder with affinity for both. Under controlled temperature and viscosity the fluorescent polarisation is directly dependent on the effective molecular size of the fluorophore. Small molecules with fast Brownian motion will therefore have a low polarisation, whilst larger molecules will have a higher FP value. This effect is also observed through complexation, so whilst a small molecule will be depolarised, the polarisation will increase through association with a binder, due to the increase in effective molecular size (Figure 21). In the absence of analyte in the sample, the tracer will therefore be bound and a high FP will be observed; in the presence of analyte this will compete with the tracer therefore increasing the concentration of unbound tracer, leading to a decrease in polarisation.¹⁷⁰

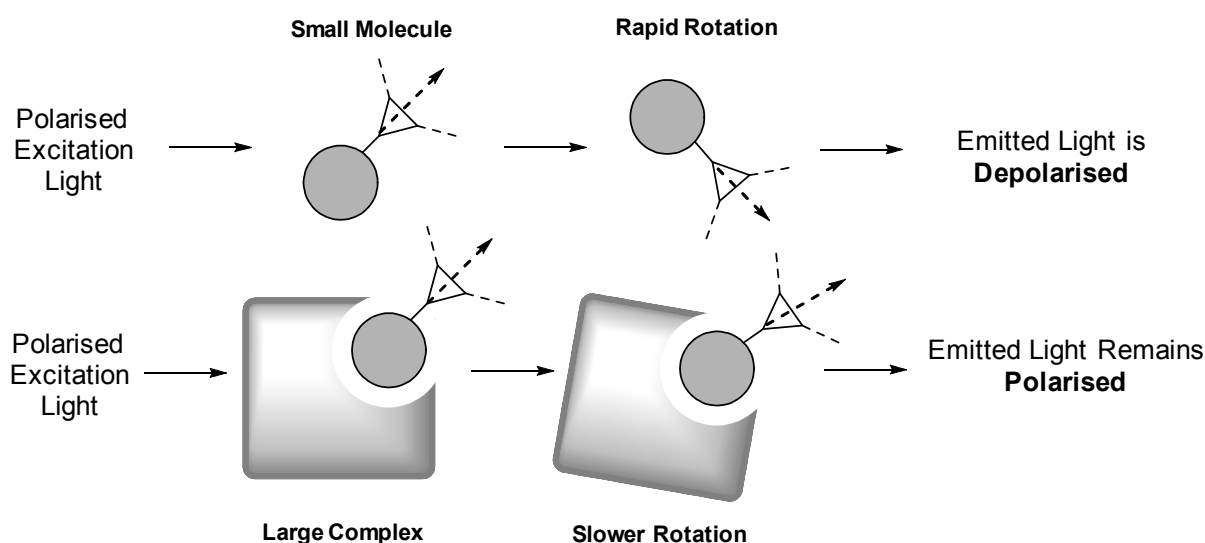


Figure 21. Relationship between FP and effective molecular size.

An alternative novel assay format has also been devised for exploration as part of this work, with the same advantages as FP in mind. The assay utilises microplates modified with magnetic inserts, which are able to remove iron oxide nanoparticles from the sample solution. Through conjugation of the analyte of interest to the magnetic nanoparticles (mNPs) (again, using the same immobilisation chemistry as used in MIP generation so as not to interfere with binding), the MIP is able to be pulled out of solution based on its affinity for the analyte. By incorporating a fluorescent monomer into the polymer's composition, the removal of MIP from solution can be followed, and a concentration-dependent response obtained, as increasing concentration of free analyte would increase the amount of MIP which remained in solution (Figure 22). In this way a homogenous assay can be achieved, which should be compatible with any analyte which can be immobilised for imprinting and conjugation.

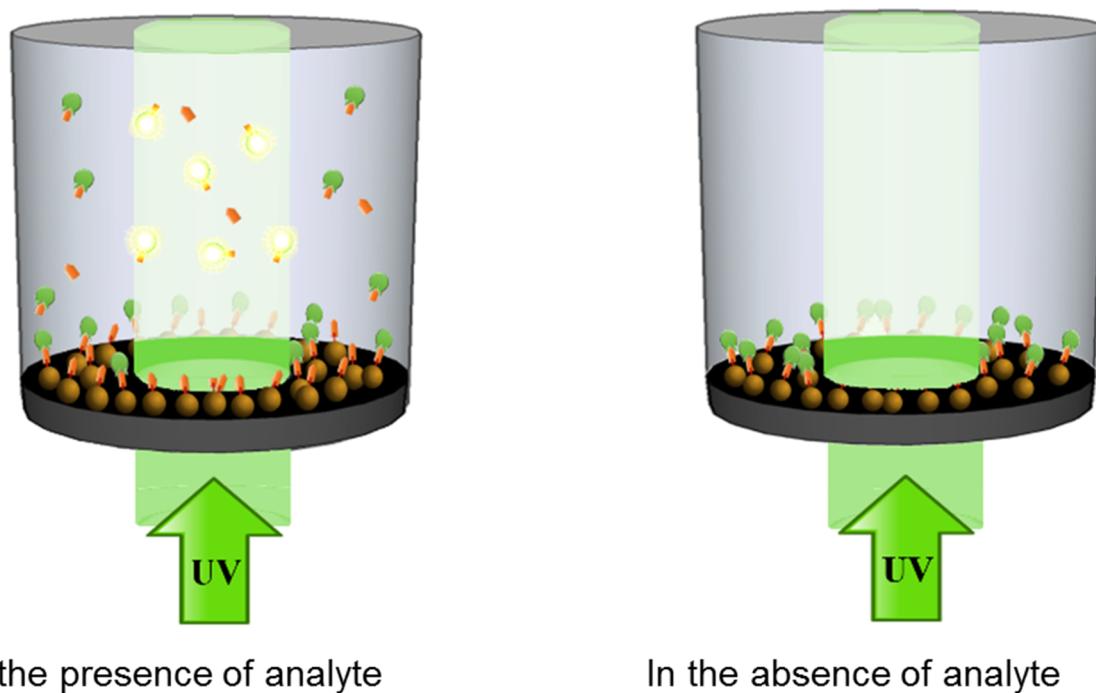


Figure 22. Principle of magnetic template based assay.

3.2. Fluorescence polarisation molecularly imprinted assay

As template for this work, an 8-amino acid peptide sequence containing a phosphotyrosine residue was selected, having been identified as a potential biomarker by a collaborating oncology group (Figure 23a). The peptide was modified through the addition of a 3 amino acid lysine linker, and terminal cysteine. This was done with the intention of achieving site-specific immobilisation and conjugation through selective reaction with the cysteine thiol group, to ensure that all templates were available in the same orientation for imprinting, and that the site of fluorophore conjugation would not interfere with binding. MIPs were prepared as described in the previous chapter using the monomer composition described by Canfarotta et al, as this had already been shown to produce MIPs with acceptable yields and affinity for initial tests. Cy3B was selected as fluorophore for peptide labelling due to having particularly well suited properties for FP; a short fluorescence lifetime (2.8 ns) and high fluorescence intensity allow a larger polarisation range than conventional fluorophores.¹⁷¹ Additionally, the maleimide functionality allowed for specific conjugation to the cysteine-thiol through control of buffer pH, and thus was ideal for the selected template. Coupling was achieved using a protocol adapted from Amersham¹⁷² (Figure 23b), followed by purification by high-performance liquid-chromatography and matrix-assisted laser desorption/ionisation-MS analysis.

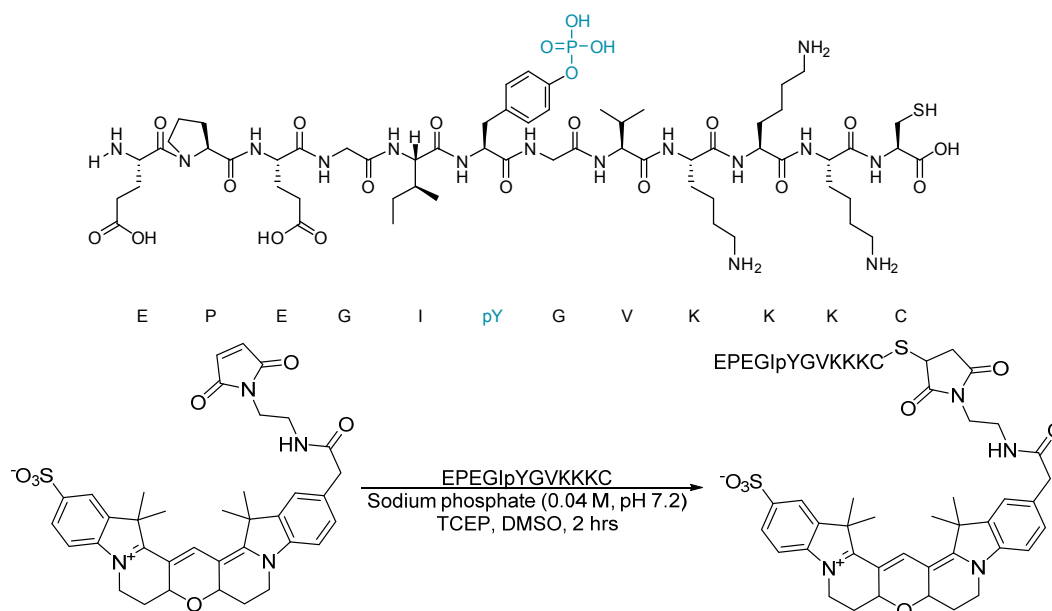


Figure 23. a) 8-amino acid phosphopeptide template selected for assay development, with triple lysine linker and terminal cysteine for selective immobilisation. b) Reaction conditions for conjugation of Cy3B to phosphopeptide.

The emission and excitation spectra of the resulting conjugate were subsequently acquired to evaluate the integrity of the dye and aid in microplate reader filter selection (Figure 24). By integrating the area under the curve covered by the filters available Em560/40 and Ex620/10 were deemed optimal, and verified experimentally by comparing the signal to noise with other filter combinations. The interaction between MIPs and phosphopeptide-Cy3B was then evaluated by titration of MIP ($15.6 - 250 \mu\text{g mL}^{-1}$) against a fixed concentration of label (4.50 nM) (Figure 25). The millipolarisation units (mP) increased proportionally to MIP concentration, indicating that the rotation of the transition dipole moment of phosphopeptide-Cy3b was being restricted through complexation with MIPs. Whilst the curve did not reach saturation even with $250 \mu\text{g mL}^{-1}$ of MIP, a 120 mP change in polarisation was observed with errors of less than 5%, corresponding to a Z-factor of 0.71.

Having established conditions allowing an observable change in polarisation, the competitive binding nature of phosphopeptide and label was investigated in order to relate the concentration of free phosphopeptide in solution to the polarisation of the label. MIP ($100 \mu\text{g mL}^{-1}$) was therefore added to solutions consisting of both phosphopeptide-Cy3B (1.13 nM) and phosphopeptide ($5.86 \text{ pM} - 6.00 \text{ nM}$) (Figure 26). Polarisation decreased with increasing concentrations of phosphopeptide, indicating that phosphopeptide was competitively binding to MIP and increasing the amount of

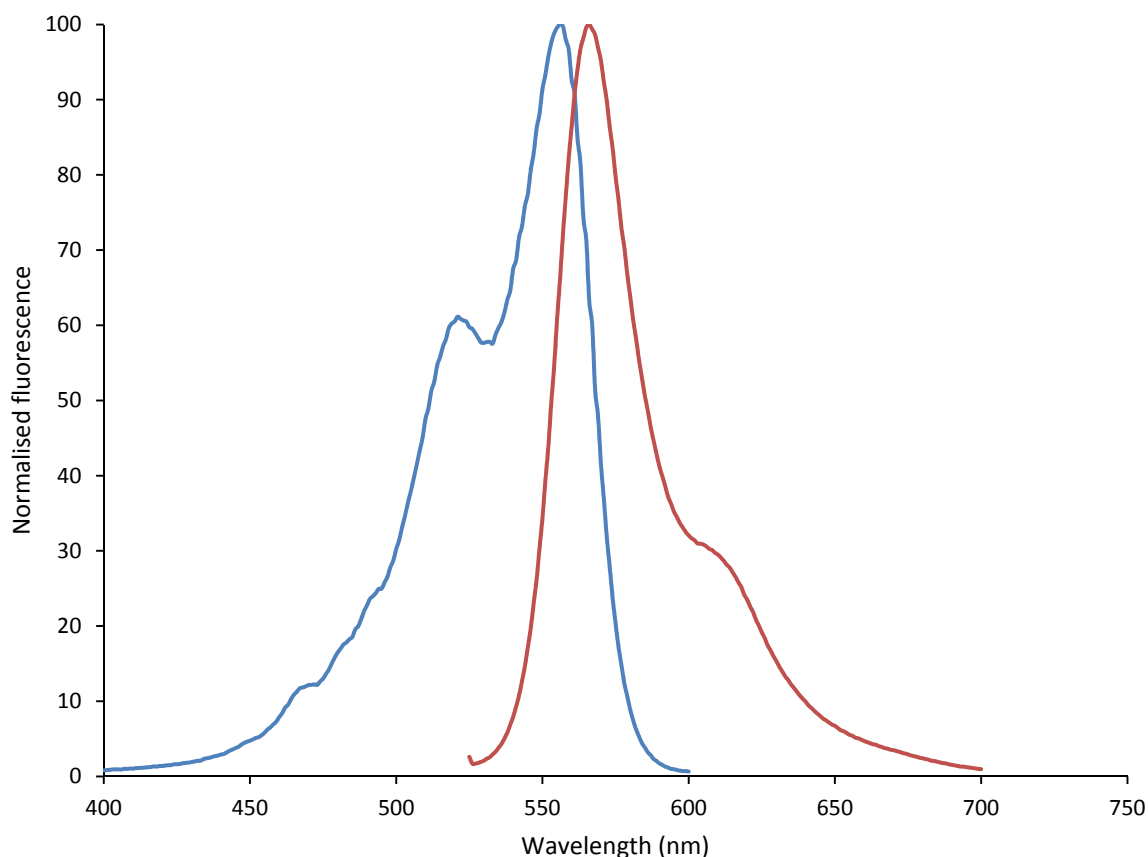


Figure 24. Emission and excitation spectra of phosphopeptide-Cy3B conjugate.

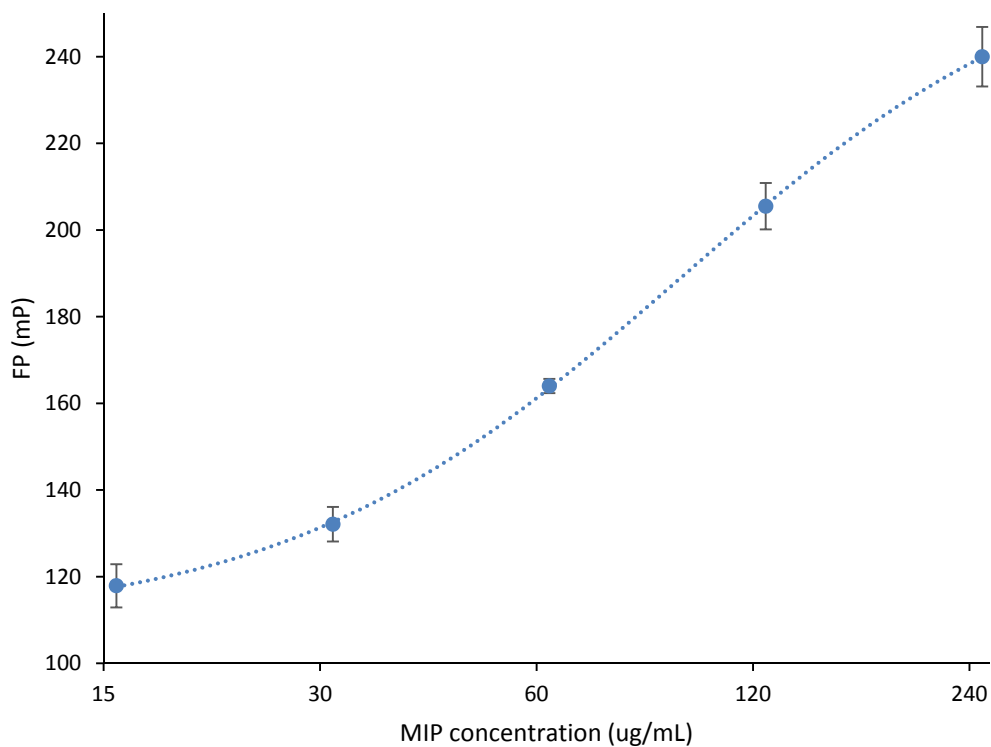


Figure 25. FP behaviour of phosphopeptide-Cy3B with titration of MIPs.

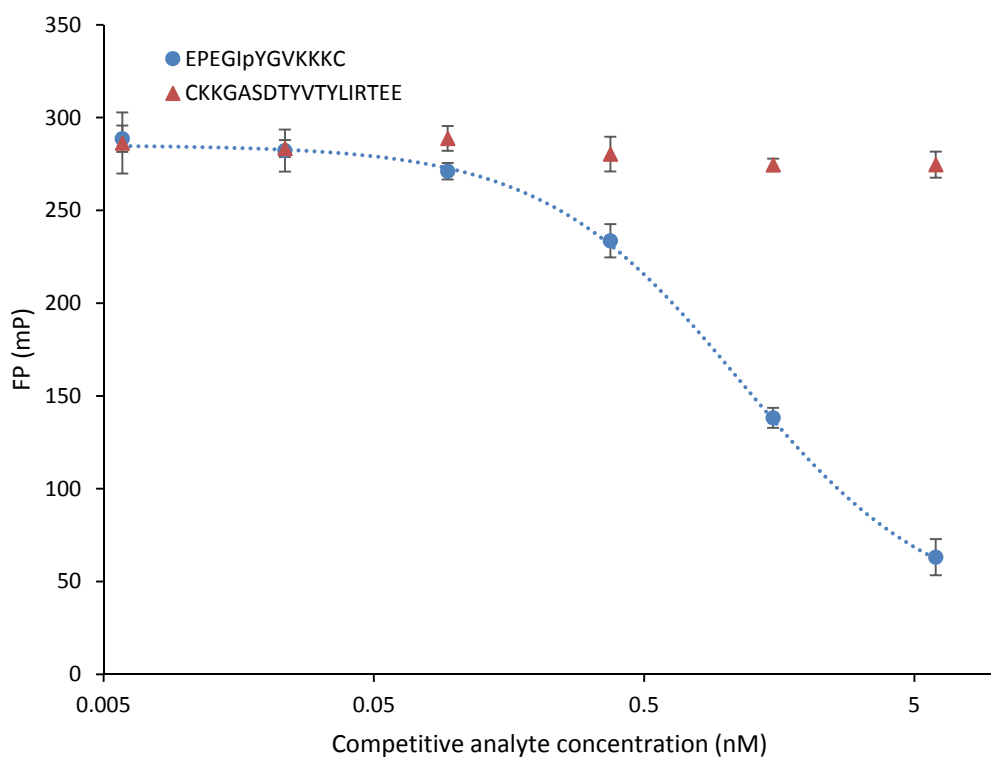


Figure 26. Fluorescence polarisation molecularly imprinted assay (FPMIA) of phosphopeptide using MIPs ($100 \mu\text{g mL}^{-1}$) and phosphopeptide-Cy3B (1.13 nM).

free label in solution, which was consequently able to rotate more rapidly resulting in the decrease in polarisation observed. The large difference of 225 mP and average error of less than 5% resulted in a Z' of 0.80, over an assay window of 3 orders of magnitude and a LOD of roughly 50 pM. In addition, negligible change in polarisation was observed with addition of a similarly sized peptide (CKKGASDTYVITYLIRTEE), indicating no competitive binding was experienced with this control peptide.

Whilst only a single analyte has been used for development of a FPMIA in this work, due to the only requirement for detection being conjugation of a dye to the analyte of interest, this method can be considered generic and applicable to any template. There is a potential limitation related to the size of analyte, as a larger template such as a protein would be more polarised in its unbound form, reducing the observable change in signal; however, this study demonstrates that polarisation is at least suitable for peptides and small molecules. With the wide variety of polarisable dyes available, it should also be possible to develop a multiplexed assay based on this format for simultaneous detection of multiple analytes in a single sample, if desired. As dye conjugation is a requirement for signal generation, the assay format is well paired with MIPs synthesised through the solid-phase protocol, as the same functionality of the template used for immobilisation can be used for labelling. Once MIP and labelled analyte have been synthesised, optimisation of the assay itself is relatively straightforward; in this work all that was required was selection of an appropriate filter set to provide an adequate signal, and investigations into optimal concentrations of MIP, label, and free analyte. Whilst further improvements could be made through optimisation of buffer, surfactants, and incubation times, this was deemed unnecessary, as the Z -factor of 0.80 already indicated an excellent assay. Once ideal conditions have been determined, a 96-well plate will take less than half an hour to prepare standards for manually, and a matter of minutes to analyse due to the ability to simply mix and read. These results demonstrated that a sensitive and selective assay could be developed using FP as a generic detection method.

3.3. Molecularly imprinted magnetic nanoparticle assay

As template for this work, an 8-amino acid peptide sequence was selected (Figure 27). As with the previous peptide template, a linker and terminal cysteine were included for conjugation. MIPs were again prepared against the template as described previously, and affinity confirmed by SPR (Figure 19). In addition to the typically selected monomers, *N*-fluoresceinylacrylamide was also included in the monomer composition, as it was essential for the assay format for a reporter monomer to be present within the MIP itself. The emission and excitation spectra were acquired to evaluate the successful fluorophore incorporation and aid in microplate reader filter selection (Figure 28). By integrating the area under the curve covered by the filters available Em490/20 and Ex535/20 were deemed optimal, and verified experimentally by comparing the signal to noise with other filter combinations.

The final component required for the assay were the template-functionalised mNPs, prepared using a protocol adapted from Hermanson.¹⁷³ This involved sonication of iron oxide nanoparticles in a silane solution in order to afford exposed amines on the nanoparticles surface, before SIA coupling of the peptide in the same manner as that performed on glass microspheres.

In the FPMIA experiments the concentration of label was chosen as the K_d determined from SPR studies. Due to the labelled template in this case being the mNP conjugate, and the number of template molecules available on the surface of a single nanoparticle being unknown, selection of working assay concentrations was more difficult. Appropriate label concentration was therefore explored by varying the concentration of mNP against a fixed concentration of MIP (Figure 29). As expected, increasing mNP concentration led to a decrease in the remaining fluorescence, as more fluorescent MIP became bound and therefore removed from the solution. At mNP concentrations greater

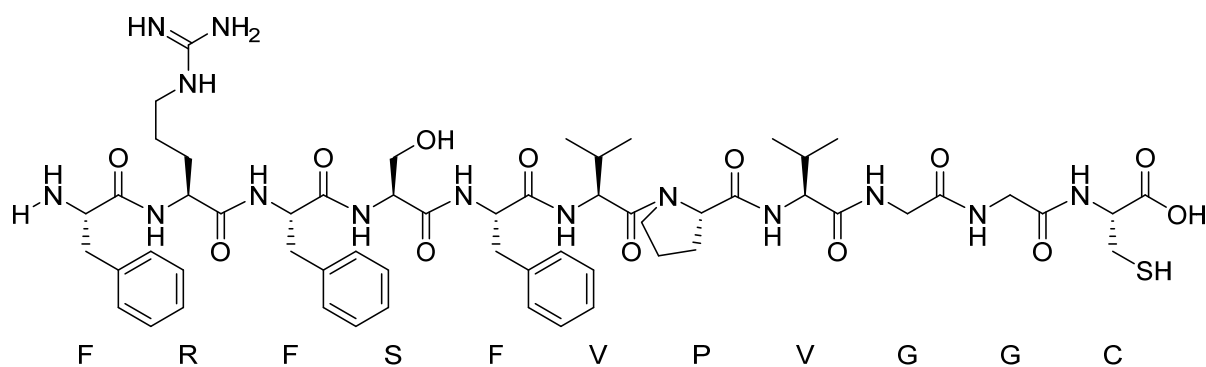


Figure 27. 8-amino acid peptide template selected for assay development, with double glycine linker and terminal cysteine for selective immobilisation.

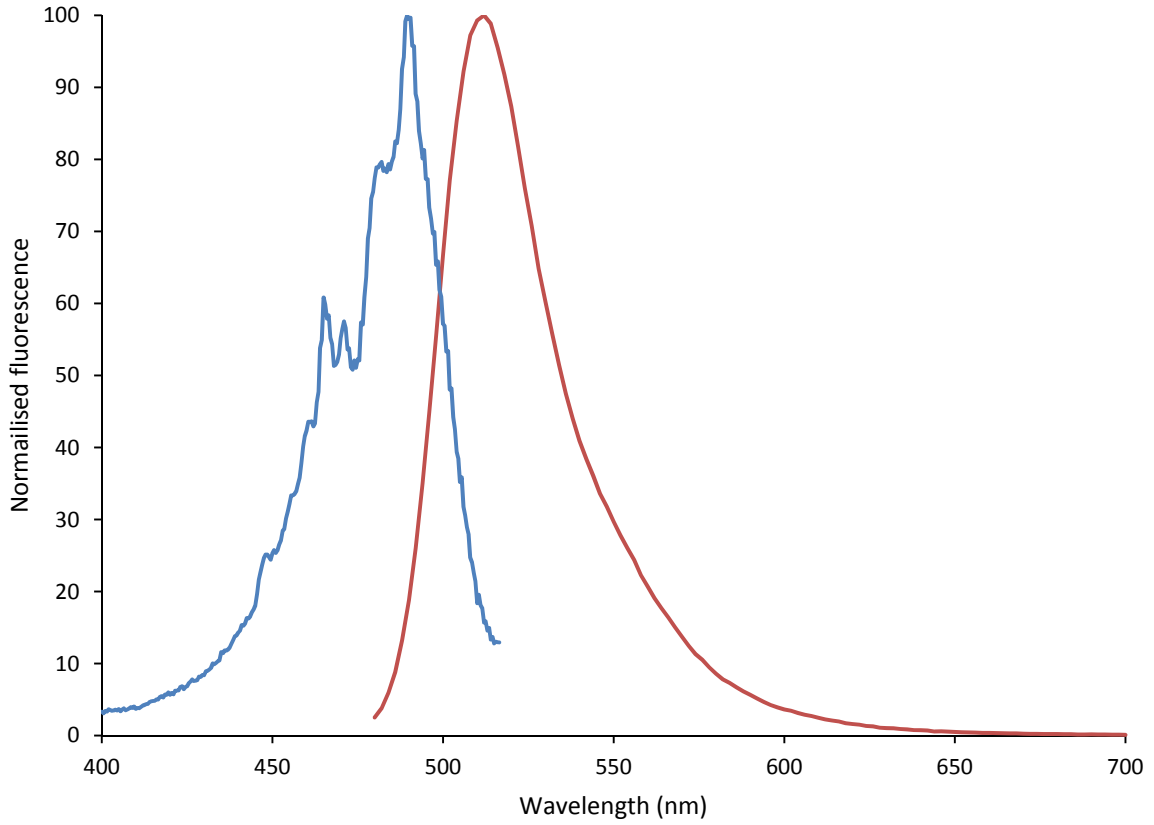


Figure 28. Emission and excitation spectra of fluorescent MIPs.

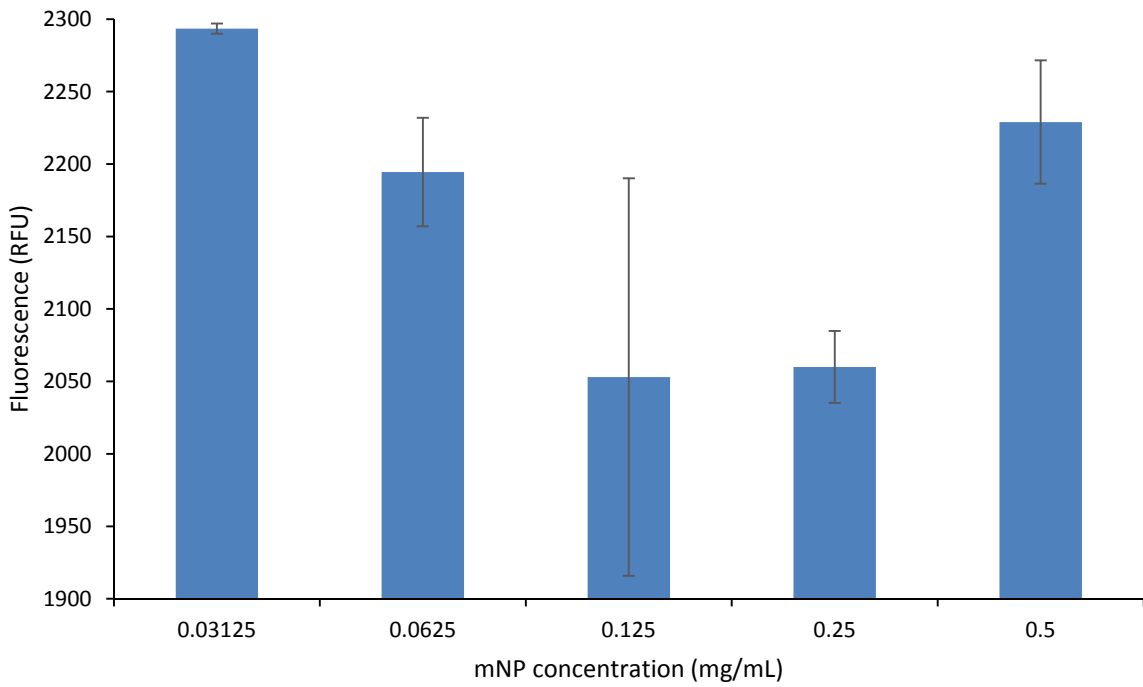


Figure 29. Fluorescence of supernatant following incubation of MIPs (2 mg mL⁻¹) with varying concentrations of mNP.

than 0.125 mg mL^{-1} an increase in fluorescence was observed; however, this was rationalised as a result of mNP aggregation decreasing the effective surface area, and consequently less template being available for binding (at these concentrations the solution was visibly cloudy and mNP would sediment over time). A mNP concentration of 0.125 mg mL^{-1} was therefore deemed optimal, and MIP titrated against this to determine the amount which could be removed from the solution by this concentration of mNP (Figure 30). The percentage bound increased with increasing MIP concentration, indicating that saturation of binding sites on the mNP was not an issue. Whilst a greater quantity of MIP could potentially have been bound to the mNPs, at 2 mg mL^{-1} the MIP solution was already very cloudy in appearance, with higher concentrations leading to aggregation and sedimentation of the polymer nanoparticles.

It was desirable to run the molecularly imprinted magnetic nanoparticle assay (MINA) in a competitive format in order to compare directly to the FPMIA experiments. This was attempted using a fixed concentration of mNP (0.125 mg mL^{-1}) and MIP (0.15 mg mL^{-1}). The concentration of MIP was selected to be as close as possible to 50% bound in the absence of free analyte, with a signal intensity high enough to still achieve an acceptable signal to noise and standard deviation. Unfortunately, a concentration dependent response was not observed when free analyte was titrated under these conditions. It is unclear why this was the case, however colleagues performing similar research had experienced greater success employing MINA in a displacement assay format,¹⁷⁴ and so this was explored as an alternative.

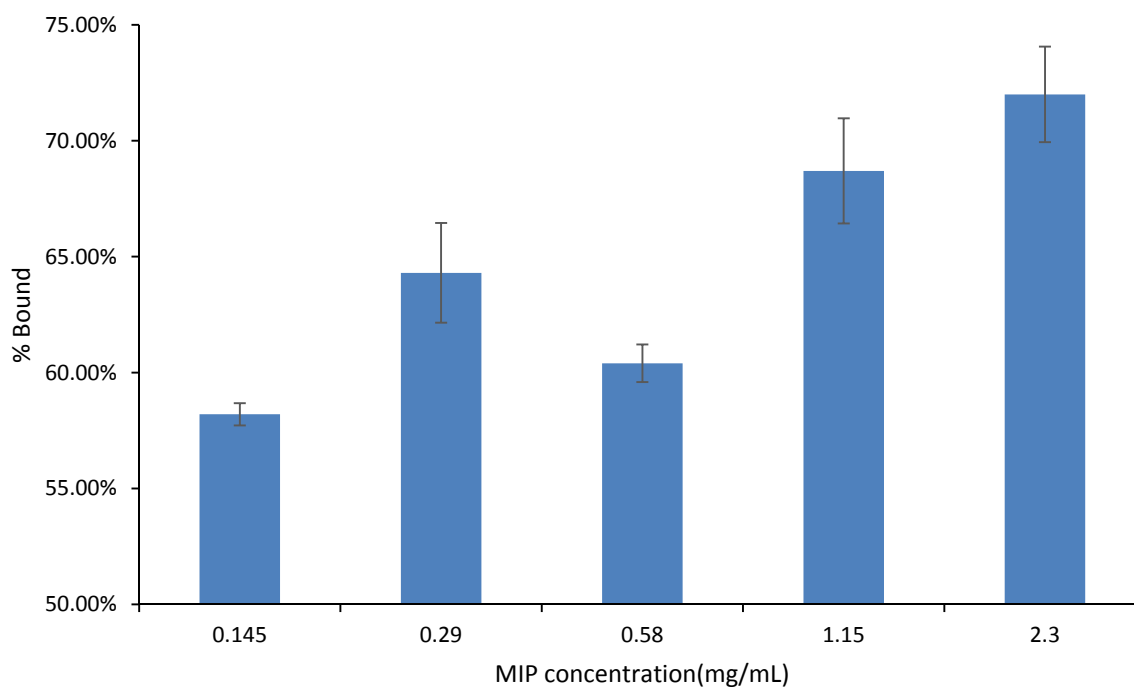


Figure 30. Percentage of MIP bound by mNP (0.125 mg mL^{-1}) as a function of MIP concentration.

The experiments thus far had been performed in phosphate buffer (pH 7.6), optimised as part of a solvent screen designed to obtain the highest percentage of MIPs bound to the mNPs. These conditions were ideal for loading the MIP onto the mNPs, however the rate of displacement was too slow to be useful as part of an assay. A further solvent screen was therefore performed to find conditions less favourable for binding to encourage displacement, but not so unfavourable as to prevent rebinding to analyte (Figure 31). The screen was performed by first loading MIPs onto mNPs in phosphate buffer, before exchanging the buffer system and monitoring the increase in fluorescence of the solution over time. Positive and negative controls consisting of buffer with a high concentration of analyte (1 mM) and buffer alone, respectively, were used to assess the effect of the solvent change on both displacement and rebinding of free analyte. Relatively little displacement was observed for acetate or tris-maleate buffer.

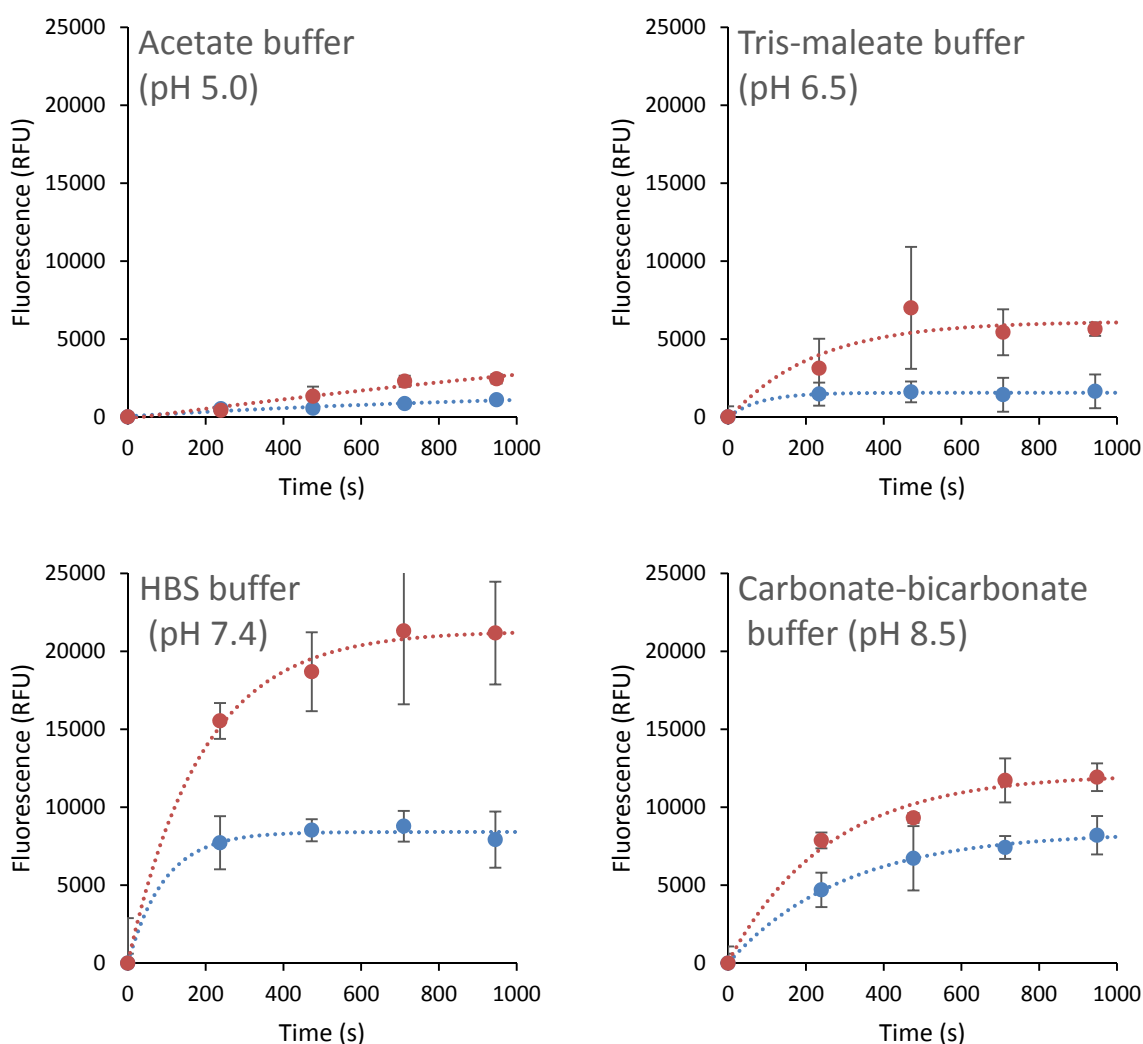


Figure 31. Displacement of fluorescent MIPs in different buffer solutions. Positive controls (red) are in the presence of peptide (1 mM), whilst negative controls (blue) are simply buffer.

Appreciable displacement was present in the carbonate-bicarbonate system, however the difference between positive and negative controls was small, indicating that MIPs were being displaced but not rebinding to free analyte. Of the buffers tested HBS was the most encouraging, displaying not only the largest increase in fluorescent signal but also the biggest difference between the positive and negative controls, and was therefore chosen for testing against multiple concentrations (Figure 32).

The assay was conducted over 5 orders of magnitude and displayed a good concentration dependent response, achieving a Z' of 0.85. It should be noted that this Z' could be slightly misleading—due to the nature of Z-factor calculation only the highest and lowest concentrations tested are considered, whilst clearly in this case the standard deviations of measurements taken at 0.1 and 1 μM are far larger. Recalculating taking 0.1 μM as the lowest concentration results in a Z' of 0.51 however, which is still considered an excellent assay. The greatest drawback of the current assay is the high concentration of free analyte required to displace MIP from the mNP. In this example significant displacement occurred at 1 μM , with the point of inflection at 11 μM . The necessary working range of the assay ultimately depends upon the final application and analyte one wishes to detect; however, it is commonly desirable to quantify analyte in the nanomolar concentration range. A lower working range could be achieved by decreasing the amount of mNP used and thus shifting the binding equilibrium to be more favourable towards the free analyte; however, this would also lead to a reduction

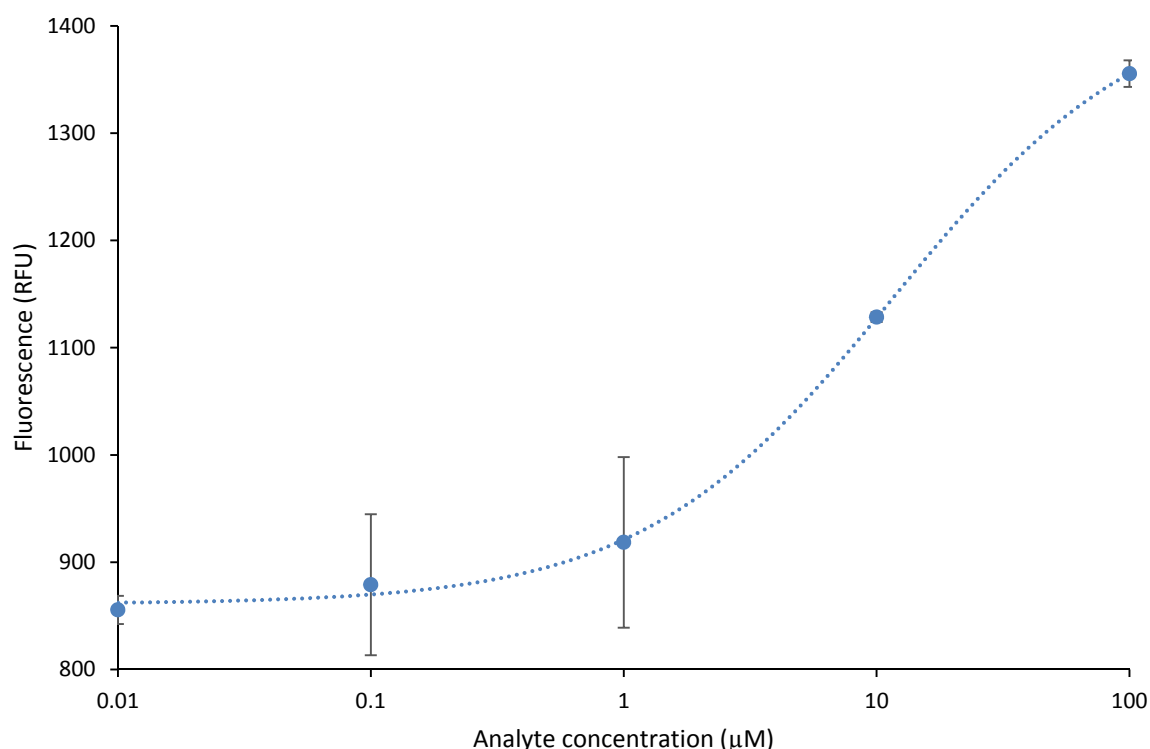


Figure 32. Displacement MINA fit to a 4 parameter logistic regression. $R^2 = 0.9993$, $Z' = 0.85$.

in the amount of fluorescently labelled MIP (as this is pre-loaded onto the mNP). Reducing the concentration of MIP consequently reduces the signal intensity, resulting in a poorer signal to noise ratio and compromising the assay's accuracy. The limiting factor to lowering the LOD is therefore the fluorophore used, *N*-fluoresceinyl-acrylamide. By incorporating a brighter dye with greater extinction coefficient and quantum yield into the polymer, less MIP will be required to generate a detectable signal and therefore these limits can be easily overcome.

3.4. Conclusions

Two assays for the detection of peptides have been developed to assess the suitability of the proposed formats as alternatives to ELISA. FPMIA and MINA were chosen for the advantages these platforms present over ELISA: they are homogenous, involve no biological components, and require very little practical expertise to perform. What separates the assays developed in this work from MIAs previously devised is the universal nature of detection. Whilst only a single template has been tested for each assay format, there is no reason why a measurable signal cannot be acquired for any template of interest in either format, permitted functionality is available for conjugation with a polarisable fluorophore or mNP.

The developed FPMIA was capable of quantitatively detecting an 8-amino acid phosphopeptide over 3 orders of magnitude, with negligible cross-selectivity when tested with a control peptide of similar size. A Z' of 0.80 and LOD of 50 pM was achieved with very little optimisation of conditions necessary, resulting in a remarkably small time investment to go from template identification to functioning assay. The rapid development and run time is the greatest strength of this format. The ability to simply mix and read means the format is suitable for high-throughput screening, and when coupled with the short generation time of MIPs screening of a compound library for a novel target could be completed weeks to months in advance of an equivalent immunoassay screen. Reduction of time of this magnitude in the early stages of drug development would be considerably advantageous in an industrial environment where patenting a lead compound before a competitor is crucial.

MINA is an emerging format, and as a consequence the development of this assay was not as straightforward as the FPMIA. Running the assay in a competitive format was unsuccessful; however, better results were achieved by employing displacement, with a Z' for the final assay of 0.85. The necessity to optimise buffers for both binding of the MIPs to mNPs and subsequent displacement, as well as concentrations of each of the assay components meant that development time was longer than that of FPMIA. The assay range and LOD were also higher than desired; however, this should be straightforward to address by incorporating a brighter dye into the polymer. Advantages of this assay format are more related to the manufacture than the assay itself. It has been shown that mNPs can be employed as solid phase for the synthesis of MIPs, with far

greater yield obtained as a consequence of the larger surface area.¹⁷⁵ The mNPs used for MIP synthesis can subsequently be used for MINA, therefore removing the need to prepare further template conjugate. The format is also well-suited for commercialisation—mNPs can be pre-loaded with MIP, dispensed into microplate wells with magnetic inserts and all solvent removed. These microplates can therefore be transported and stored dry, and analysis performed by simply adding the sample solution to the microplate and measuring the fluorescence.

There is clearly potential for both assay formats, however MINA does require further development to compete with commercial platforms. In its current state FPMIA is an attractive alternative to ELISA, and delivers on the original aim to provide a generic, homogenous MIA.

CHAPTER 4: APPLICATION TO A MODEL SYSTEM - ACETYLCHOLINESTERASE

Imprinting of peptides has been achieved in a similar manner as for small molecules; however, proteins present additional problems due to being macromolecules. As observed in chapter 2, modifying the polymer composition does very little for protein imprinting, as there is an abundance of interaction sites available on a protein's surface. Imprinting against a whole protein also produces polyclonal-like MIPs, with a single synthesis generating MIPs against many different binding epitopes. These two issues contribute to the relatively poor selectivity of protein-imprinted MIPs. Epitope imprinting addresses these problems, enabling the generation of monoclonal-like MIPs with specificity for a single binding site. Identification of imprintable epitopes can be performed experimentally through whole-protein imprinting; these sequences can then be synthesised and used as templates.

Whilst selection of an assay format for peptides in the previous chapter was rather trivial, for proteins this again has more complications. As previously mentioned, FPMIA may be less suitable due to the large size of a protein resulting in a higher unbound polarisation. MINA has therefore been explored against AChE as template protein, selected both for assay development and potential therapeutic interest. Generation of MIPs against multiple binding sites presents an opportunity to attempt a sandwich MINA for a more selective and sensitive protein assay than otherwise possible. The intention is therefore to demonstrate an entire process from target protein to functional assay, utilising the knowledge gained from work in previous chapters.

Aims of this chapter

- Identify imprintable surface epitopes of AChE.
- Synthesise MIPs with site-specific recognition to each identified epitope.
- Assess changes in structure and enzymatic activity upon binding.
- Apply MIPs in sandwich-MINA for quantification of AChE.

4.1. Introduction

AChE is a serine hydrolase that causes the termination of neuronal transmission at the cholinergic synapse by hydrolysing its natural substrate—acetylcholine—into choline and acetate ions.^{176, 177} Inhibitors of AChE act on two target sites on the enzyme, the active site (tacrine) and the peripheral site (fasciculins). The active site of AChE that contains the Glu/His/Ser catalytic triad is located at the center of the subunit at the end of a deep and narrow gorge.¹⁷⁸ Inhibitors directed to the active site prevent the binding of a substrate molecule, or its hydrolysis, either by occupying the site with a high affinity or by forming a covalent bond with the catalytic serine. The peripheral anionic site (PAS) is located at the entrance of the catalytic gorge approximately 20 Å distant from the active site itself. It binds acetylcholine as the first step in the catalytic pathway and allosterically modulates catalysis as well as binding specific inhibitory compounds.¹⁷⁹ It has been proposed that interaction of inhibitors with the PAS induces a movement of the Ω loop (67–95), allosterically modifying the orientation of a tryptophan residue, Trp-84, which serves as the choline binding site.¹⁸⁰

Dementia is a brain disorder that seriously affects a person's life and ability to carry out normal daily activities. Among older people, Alzheimer's disease (AD) is the most common form of dementia; characterized by memory loss, weakening intellectual abilities and severe behavioural abnormalities. AD is a complex disease that can be caused by both genetic and environmental factors, with approximately 6% of the population over the age of 65 years sufferers of the disorder, with incidence increasing with age.^{181, 182} Increasing life expectancy and an ageing population have led to projections of a 57% rise in the number of people with dementia by 2040.¹⁸³ The current estimated annual costs of dementia are \$26bn, with the average lifetime cost per patient in developed countries being as high as \$174,000—coupled with the projected increase in incidence, there is cause for concern regarding a substantial economic burden on health services.¹⁸⁴

AD is characterised by a loss of neurons and synapses in the cerebral cortex and subcortical regions, caused by a protein misfolding and accumulation of amyloid beta plaques in the brain.¹⁸⁵ Despite significant scientific progress, the causal treatment targeting the underlying beta-amyloid pathology remains unavailable. The moderate success in causal treatment of AD has been achieved using immunotherapy against beta-amyloid¹⁸⁶, however initial trials were halted due to side effects such as subacute aseptic meningoencephalitis and brain haemorrhages.^{187, 188} Currently most AD patients rely on symptomatic treatments with drugs that have no direct effect on the beta-amyloid deposition, and which can only temporarily slow disease progression. Treatment of AD with AChE inhibitors relies on the replenishment of acetylcholine, a memory-related neurotransmitter that decreases as a result of neurodegeneration.¹⁸⁹⁻¹⁹¹ The most efficient

symptomatic drugs for AD include acetylcholine esterase inhibitors such as tacrine, donepezil, rivastigmine and galantamine, as well as NMDA antagonists such as memantine.¹⁹²⁻¹⁹⁴ It is worth noting that drugs currently used for treating AD are marginally efficacious and have undesirable side-effects. For instance, tacrine, the oldest approved drug for the treatment of AD, has a short half-life and off-target effects such as hepatotoxicity.¹⁹⁵ 10-20% of users also suffer from common side effects such as nausea and vomiting.¹⁹⁶ In addition, a number of potential AChE inhibitors suffer from poor solubility in water. Thus, there is a large unmet need for better and safer drugs.

Whilst mild inhibition of AChE is desirable in the treatment of AD, potent inhibition of AChE can have detrimental effects on the neuromuscular system. This is exploited in OP pesticides, where irreversible inhibition of AChE leads to excessive cholinergic neurotransmission, resulting in paralysis of neuromuscular function and a cholinergic crisis. The excess acetylcholine leads to hyper stimulation of muscle and secretory glands, as well as altered central nervous system and cardiac activity, resulting in cardiovascular and respiratory compromise and ultimately death.¹⁹⁷ OPs function through a different mechanism to the previously mentioned drugs. Whilst mild inhibition is achieved through competitive occupation of- or restricting access to the active site, OP compounds induce acute toxic effects through formation of a stable phosphoserine ester bond with the catalytic serine within the active site. This then undergoes an “aging” process, with the modification considered irreversible following the cleavage of a phosphoester bond, rendering the enzyme unable to carry out further hydrolysis.¹⁹⁸

Unfortunately, OP pesticide ingestion is a common occurrence in agricultural areas,^{199, 200} whilst OP nerve agents still remain a threat in chemical terrorism, the most recent of which include the Novichok poisonings in Salisbury, UK.²⁰¹⁻²⁰⁵ Development of new therapeutics for OP intoxication is focused on oxime-based reactivators, however these are OP specific and not a broad-spectrum treatment,²⁰⁶ and are not able to cross the blood-brain barrier and reactivate phosphorylated AChE in the brain and central nervous system, rendering them ineffective for protection against seizures, irreversible brain damage and long-term sequelae of nerve agent poisoning.²⁰⁷ Computational modelling supports the hypothesis that allosteric AChE activators could provide a novel therapeutic route for treating OP intoxication.²⁰⁸ Because positive allosteric modulators do not interact directly with the active site but instead alter the shape or dynamics of that site, using allosteric therapeutics may provide broad-spectrum efficacy against OP inhibitors without regard to inhibitor structure. Two positive allosteric modulators have been developed which increased enzyme activity threefold, however failed to upshift the IC_{50} of a variety of OPs.²⁰⁹

There is therefore potential for both novel inhibitors and allosteric activators of AChE to improve upon the current, lacking therapeutics. Typically, small organic molecules have been utilised for both inhibition and activation; however, the use of these molecules for AChE presents special problems since the active site is located in a 20 Å deep cavity. Aliphatic molecules would be expected to bind well in the cavity due to hydrophobic

interactions, but their limited solubility raises concerns. The promising alternative to small molecules are monoclonal antibodies (mAbs). Various polyclonal and monoclonal antibodies have been shown to inhibit AChE by binding to modulatory sites on the enzyme surface.^{210, 211} Molecular characterization of mAbs shows they inhibit AChE by targeting the PAS and backdoor region, identified using complementary binding, inhibition, and mutagenesis approaches. All mAbs bound AChE with high affinity and were strong inhibitors with an apparent K_i value less than 0.1 nM, and maximal demonstrated inhibition of 84-96%.²¹² Curiously, these antibodies did not compete with one another or with other small organic anticholinesterase agents for binding to AChE. This lack of competition indicates they target different epitopes; at the entrance of the active site gorge, and at the backdoor region distant from the gorge entrance. This supports allosteric modulation of AChE, which in contrast to small molecules does not require direct interaction with the active site, and may alter the enzyme by blocking the back door or by inducing a conformational distortion within the active site.

Also very exciting was the observation that mAbs directed against fetal bovine serum AChE were able to inhibit the formation of amyloid fibrils.²¹³ This effect is not actually related to inhibition of the enzyme's catalytic properties but rather to the poorly understood ability of the brain AChE PAS to promote assembly of amyloid- β -peptides into Alzheimer's fibrils, acting as a heterogeneous nucleator.²¹⁴ Similar effects were also observed for small molecular weight AChE inhibitors that bind simultaneously to two sites such as the PAS and the catalytic anionic subsite.^{215, 216} The AChE motif within the PAS responsible for inducing the formation of amyloid fibrils has been identified as the surface loop 274-308.²¹⁷ Bourne et al. observed an association of the 275-308 loop with a small omega loop between residues 252-272 on an adjacent catalytic subunit, which bears a significant structural resemblance to both the amyloid β -peptide and the prion proteins, suggesting common mechanisms of aggregation.²¹⁸ Overall the PAS serves as a matrix of overlapping binding sites for low and high molecular weight binders due to the conformational flexibility of this region as a result of the surface loops.²¹⁹

The ability of mAbs to contribute to both symptomatic and causal treatment of AD is certainly worth investigating in future studies, as well as potential for allosteric activation in OP treatment. There are therefore three distinct mechanisms through which AChE activity can be influenced to achieve a beneficial effect. The use of mAbs in practical AChE treatment is however constrained by several important factors: high production costs, problems in manufacture, and societal issues involving use of animals; bio-distribution of mAbs, which is far more complicated than for the vast majority of small-molecule drugs—because of their large polar nature, the diffusion of mAbs across the vascular endothelium and specifically across the blood-brain barrier is negligible and requires special transporters²²⁰; immunogenicity—practically all therapeutic mAbs in current clinical practice exhibit at least some immunogenicity, which can affect the safety, efficacy, pharmacokinetics, and pharmacodynamics of therapeutic mAbs; and the inability to use oral delivery.

Nanoparticles provide an alternative to mAbs, able to retain their selective binding properties responsible for mAbs therapeutic value, with potential to avoid some of the aforementioned problems. With size of 50-100 nm, nanoparticles are considered one of the most promising drug delivery systems for targeting inaccessible regions of brain.²²¹ Nanoparticles can pass the blood-brain barrier by opening tight junctions between endothelial cells,²²² by transcytosis,²²³ or by endocytosis,²²⁴ and can be used not only as vehicles to deliver a drug but also as therapeutic agents capable of mimicking enzyme inhibitory functions of antibodies.^{225, 226} The particularly interesting class of therapeutic nanoparticles are MIP NPs.²²⁷ Specific inhibition of enzymes such as trypsin, thrombin and catalase by MIP NPs is well documented.²²⁸⁻²³² It is known that MIP NPs can function *in vivo* without triggering immune response,²³³ can penetrate through cell membranes by endocytosis,²³⁴ and can survive and deliver their drug cargo in the stomach.²³⁵ These features indicate strong potential for developing MIP NPs with the ability to reach the location of action (brain) after oral or percutaneous administration.

The aim when designing MIPs is to mimic the specificity of natural antibodies. The most advanced approach in preparation of MIPs for proteins is the epitope approach.¹³⁴ In this method a peptide with the same sequence as one of the target protein epitopes is used as a surrogate template for the whole protein. This approach is analogous to protein recognition by antibodies, where an epitope of the immunogenic protein is the site of antibody binding. The binding of antigens to antibodies is well understood, and the nature of that interaction (including the important aspects that must be considered when attempting to design such interactions) is as relevant to MIPs as it is to the natural molecules. The simplest way to decide if a protein fragment will make a good epitope for MIP design is to look at its position within the tertiary structure of the protein in the Protein Databank.²³⁶ There are many algorithms which have been written to predict antigenic regions and epitopes of proteins²³⁷, although unfortunately their prediction power is far from optimal, with the rate of hits for predicted epitopes of human AChE (hAChE) by such software reaching around 30%.²³⁸ It is also possible to consider imprinting known epitopes for AChE. There are approximately 65 known hAChE epitopes recorded in the Immune Epitope Database and Analysis Resource, however very few of the relevant antibodies are able to modulate AChE.

An experimental approach for using molecular imprinting to identify peptide sequences on the surface of proteins with potential antigenic properties has recently been described.²³⁹ This method involves synthesis of MIP NPs in the presence of whole protein, partial proteolysis of the protein bound to polymer, and subsequent sequencing of released peptides that were bound to the polymer (Figure 33). The important concept behind this principle relies on the assumption that MIPs synthesised in the presence of protein protect from proteolysis peptide sequences involved in MIP formation that are retained within the specific imprints. This approach provides the possibility of identifying regions of the protein surface which have not been demonstrated to be antigenic *in vivo*, but which may offer improved affinity or alternative modulatory mechanisms for therapeutic applications. As a target for this research *Electrophorus*

electricus AChE (EeAChE) was selected, which is available in suitable quantity and molecular homogeneity for structural and functional studies. Cross-immunoreactions of antigens and antibodies have shown that anti-human brain AChE antiserum exhibited strong cross-immunoreactivity between AChEs from different species.^{238, 240, 241}

It is therefore intended to achieve site-specific binding to different areas of the enzyme surface through an epitope imprinting approach, in order to both allosterically enhance and reduce substrate hydrolysis dependent upon the MIP administered and its target epitope. The developed materials could consequently be established as new therapeutic strategies for AD and OP intoxication, overcoming shortfalls of currently employed treatments for both. The identification and generation of MIPs against multiple binding sites is anticipated to allow the development of not only a mNP assay such as that of the previous chapter, but also a sandwich assay, utilising both magnetic and fluorescent MIPs. This will remove the requirement to immobilise protein on mNPs, which could be undesirable in circumstances where template protein is expensive or in limited availability; as well as improving the selectivity for the imprinted protein, as signal will only be generated upon two independent binding events to the same target.

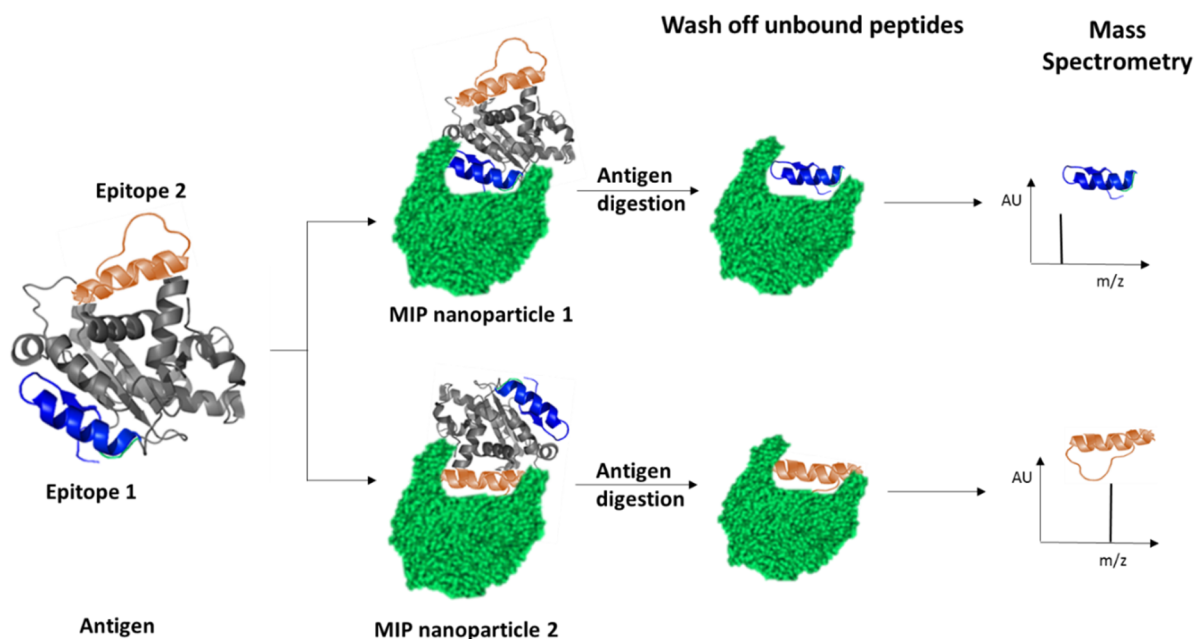


Figure 33. Schematic description of the process for using molecular imprinting and MS in identification of peptide sequences exposed on protein surfaces.

4.2. Identification of EeAChE epitopes for synthesis of MIP NPs

In the first instance MIPs were prepared to map the topography of the surface of the EeAChE and to identify peptide sequences which may be useful for MIP NP preparation using an epitope approach. The MIP synthesis, enzyme proteolysis and peptide sequencing were performed as described earlier.²³⁹ The composition of MIP was identical to the composition used previously in protein imprinting.²⁴² Table 3 shows the peptide sequences identified using molecular imprinting and MS that are the most prevalent ($\geq 40\%$ peak intensity) in the I-TASSER model.²⁴³ Four of the sequences identified match those found in literature,^{198, 238, 244, 245} however, three peptide sequences have not been previously identified as epitopes for acetylcholine esterase.

Only four of the EeAChE sequences: 200-217 LALQWVQDNIHFFGGNPK, 218-243 QVTIFGESAGAASVGMHLLSPDSRPK, 313-320 FRFSFVPV and 526-532 YWANFAR have matches with hAChE and for this reason represent potential therapeutic interest. Interestingly, parts of these sequences are known epitopes for anti-AChE antibodies. The following sequences: 209-215 (hAChE) LALQWVQ, 231-247 (hAChE) FGESAGAASVGMHLLSP, 326-333 (hAChE) FRFSFVPV, and 526-532 (hAChE) YWANFAR were identical for both EeAChE and hAChE.

The AChE's catalytic function is highly dependent on conformational integrity of the active site gorge and PAS area, where the adhesion site is located. In hAChE, 209-215 LALQWVQ is observed as part of an alpha helix (see Figure 34). 231-247 FGESAGAASVGMHLLSP is also contained within an alpha helix, which is the known binding site for huprine and galantamine; it would therefore be expected that MIP NPs with affinity to this region would exhibit inhibitory properties for AChE. 326-333 FRFSFVPV is part of a coil containing aromatic residues which line the surface of the active site gorge.

Table 3. Peptide sequences that are the most prevalent ($\geq 40\%$ peak intensity) in the I-TASSER model found using molecular imprinting and MS and their correlation with known epitopes.

Position ²⁴⁶⁻²⁴⁹	Sequence identified in MI work	Sequence of known epitope
200 – 217	LALQWVQDNIHFFGGNPK	LLDQRLALQW ²³⁸
218 – 243	QVTIFGESAGAASVGMHLLSPDSRPK	TLFGESAGAA ¹⁹⁸ KTVTIFGESAGGASVGMHILSPGSR ^{244, 245}
313 – 320	FRFSFVPV	VFRFSFVPV ²³⁸
375 – 382	EDFLQGK	
526 – 532	YWANFAR	YWANFAR ²³⁸
533 – 547	TGNPNINVDGSIDSR	
549 – 559	RWPVFTSTEK	

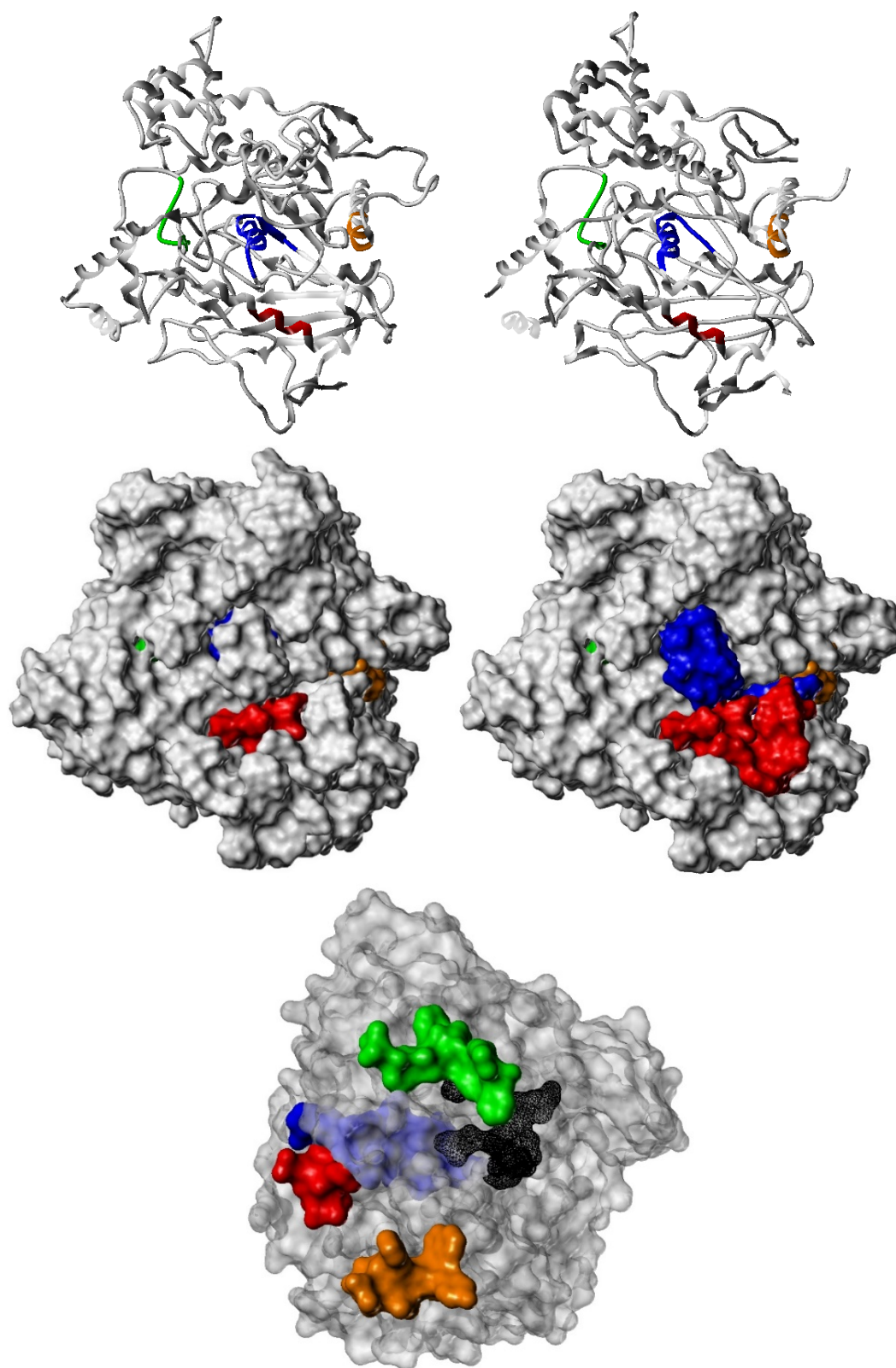


Figure 34. Four epitope sequences; LALQWVQ (red), FGESAGAASVGMHLLSP (blue), FRFSFVPV (green), and YWANFAR (orange). Top: epitope locations in EeAChE (left) in the I-TASSER model and hAChE (right) using PDB ID: 4EY4 (www.rcsb.org).²⁴⁶ Middle: locations of known epitope sequences (left) and those identified via imprinting (right). Bottom: Location of epitopes relative to the active site (black).

Phe330 is a particularly interesting residue since it is known that its benzene ring undergoes a significant conformational change to make an aromatic-aromatic interaction with the bound ligand.²⁵⁰ Hence it is also anticipated that MIP binding in this area will interfere with AChE catalytic function. The final epitope, 526-532 YWANFAR, is located within a beta strand. Two peptide sequences: 209-215 LALQWVQ and 526-532 YWANFAR do not belong to known targets of inhibitory actions for AChE. None of the sequences identified in this work are related to important sites for AChE inhibitors such as the PAS (residues 251–264, 270–279 and F330) or main chain nitrogens of G118, G119, A201 and H440 which form the oxyanion hole.²⁵¹ From these observations it is possible to assume that at least two peptide sequences identified from the epitope mapping work should generate MIPs with inhibitory properties for both EeAChE and hAChE. This is expected through two possible mechanisms; steric occlusion of substrate entry into the active site gorge, and/or an allosteric effect on the active site influencing substrate catalysis.

4.3. Synthesis and characterisation of MIP NPs

The corresponding peptides, including a linker consisting of two glycine residues and a terminal cysteine for covalent immobilisation to glass and gold surfaces, were first synthesised for use as templates. A solid-phase approach described by Canfarotta et al.¹⁴⁴ was adapted for MIP NP synthesis, where the terminal cysteine was utilised for immobilisation onto the surface of amine derivatised glass beads through SIA coupling. The polymer composition used was unaltered from the aforementioned publication. The selected monomers have previously been optimised for imprinting of peptides and have successfully been used in a number of studies since, with interactions being attributed to a combination of multiple weak electrostatic and hydrophobic interactions.¹⁴³ The concentration of nanoparticles was determined by weighing a lyophilised aliquot of stock solution, with a typical synthesis yielding 0.7 mg mL⁻¹ of MIP. The nanoparticle's sizes were measured using dynamic light scattering (DLS) and TEM, ranging from 20 to 180 nm (Figure 35).

Table 4. Characterisation of MIP NPs, and relation between affinity and MS peak intensity during identification of epitopes.

Epitope imprinted	K_D (nM)	MS intensity (native)	MS intensity (denatured)
YWANFAR	12.0	45%	45%
FGESAGAASVGMHLLSP	78.6	86%	10%
FRFSFVPV	0.40	10%	100%
LALQWVQ	2.20	100%	100%

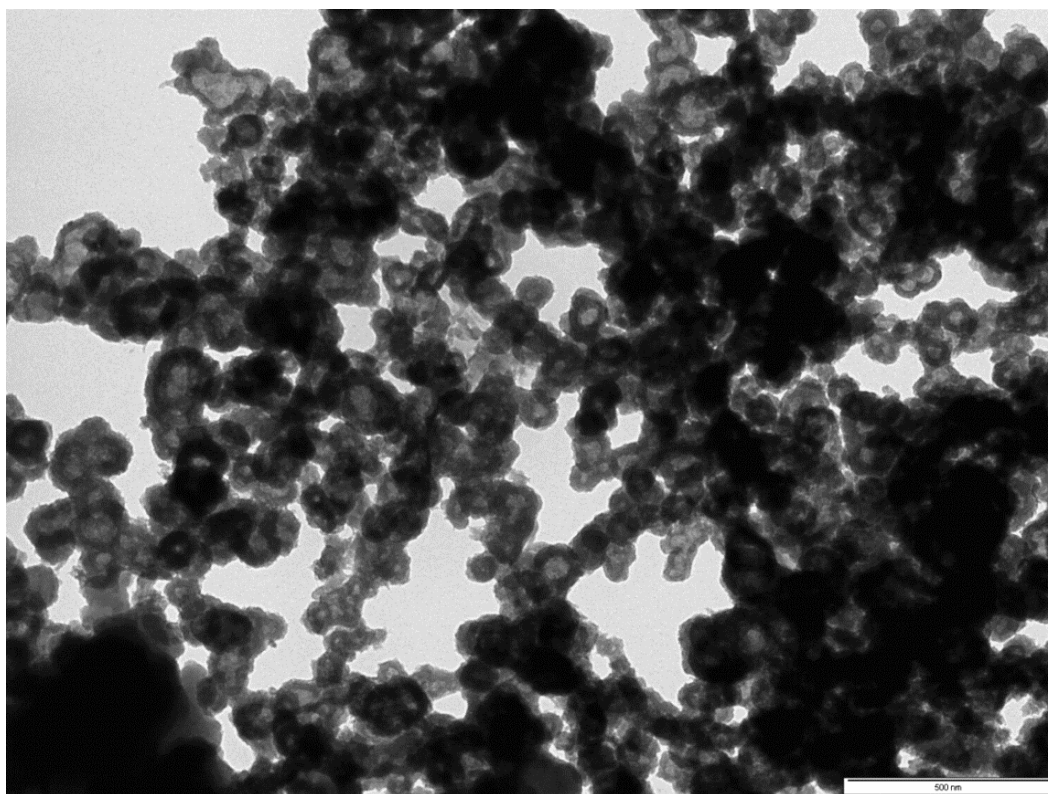


Figure 35. TEM image of MIP NPs specific for YWANFAR (scale bar 500 nm).

The affinity of MIPs imprinted against each epitope of AChE was assessed using an SPR instrument (MP-SPR Navi 220A NAALI). For these experiments, MIPs were covalently immobilised on the sensor surface and a kinetic titration performed, increasing concentration of protein with each injection. All MIPs exhibited excellent affinity for AChE, with K_D values in the low nanomolar range (Table 4, Figure 36).

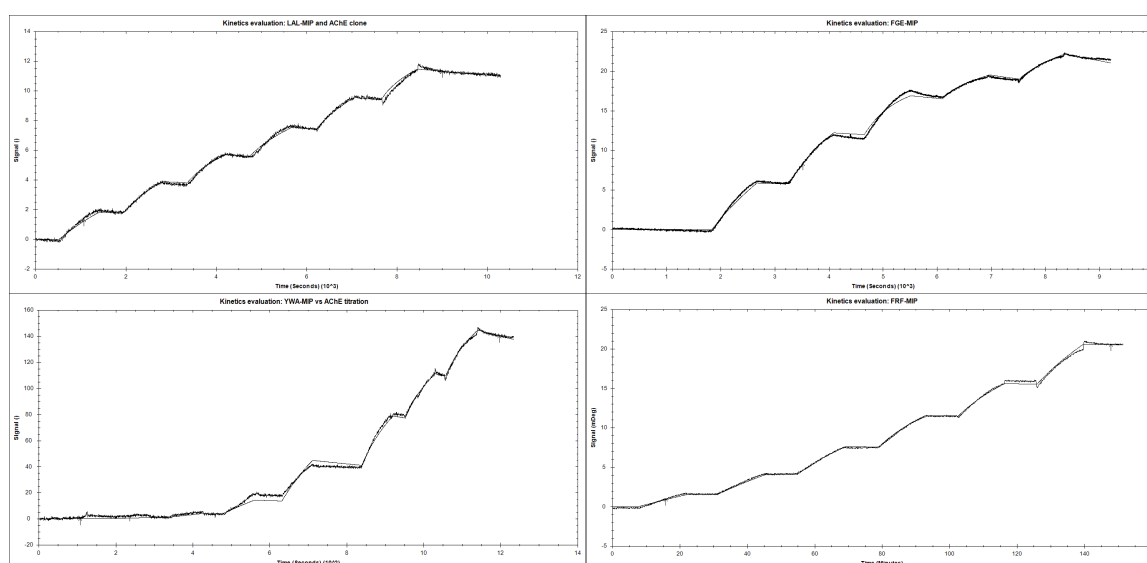


Figure 36. Sensorgrams showing response in degrees as a function of time, following sequential injections of increasing concentrations of analyte.

It is interesting to observe that whilst FRFSFVPV was difficult to imprint in the native protein—as is evident from the MS peak intensities—MIPs imprinted against this epitope exhibited the strongest binding to the native protein. Looking at the location of this epitope (Figure 34), very little of the sequence is exposed on the surface, which could suggest that a conformational change is occurring to expose this binding site. This suggestion of conformational changes to accommodate MIP binding bodes well for modulation of the enzyme’s activity, as AChE’s catalytic function is highly dependent on conformational integrity of the active site gorge and PAS area.

4.4. Modulation of enzyme activity

Having established that the epitope imprinted MIPs showed a strong affinity for AChE, the effect of this interaction on the enzyme activity could be explored. The Ellman method was utilised for this analysis, which uses 5,5'-dithio-bis-(2-nitrobenzoic acid) to quantify the thiocholine produced from the hydrolysis of acetylthiocholine by AChE.²⁵² MIPs imprinted against all four epitopes were pre-incubated with AChE for 15 minutes, before simultaneous addition of 5,5'-dithio-bis-(2-nitrobenzoic acid) and acetylthiocholine to initiate the reaction. Tacrine—a known AChE inhibitor—was employed as a control, as well as observing the enzyme catalysed hydrolysis without any added modulator (Figure 37).

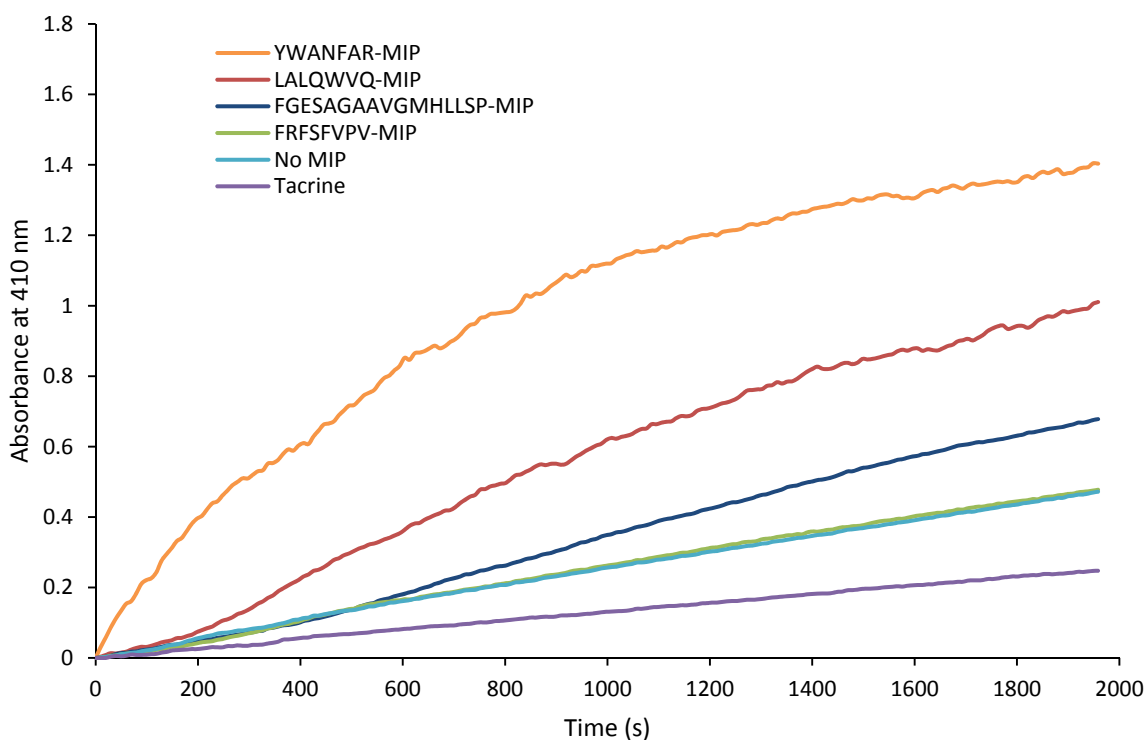


Figure 37. Hydrolysis of ATCh by AChE in the presence of AChE epitope imprinted MIPs.

The results of this experiment clearly indicate an activating effect as a result of MIP binding. This effect was greatest for YWANFAR-MIPs, where the rate of hydrolysis was increased 10-fold. Interestingly, MIPs against this epitope were observed to have the weakest affinity to AChE, indicating that the activating effect is not reliant upon the strength of the interaction, but is likely due to the binding site specificity introduced through epitope imprinting. Whilst Ellman's assay is a fast and cheap method to measure cholinesterase activity, there are limitations.²⁵³ Due to the uncommon nature of allosteric activation, the improved enzyme activity was further verified by directly measuring the substrate conversion in a kinetic MS assay (Figure 38).

The FRFSFVPV-MIP used in this experiment was the least active in the Ellman assay; however, it was still observed to almost double the rate in the MS assay. Discrepancies between the rates of reaction can be explained by the differing concentrations of enzyme, substrate and MIP employed in the different assay formats, even so the trend was the same and confirms that the MIPs enhance the enzyme's activity. This effect was investigated further through varying the concentration of enzyme to ascertain the extent to which MIPs could influence the reaction kinetics (Figure 39).

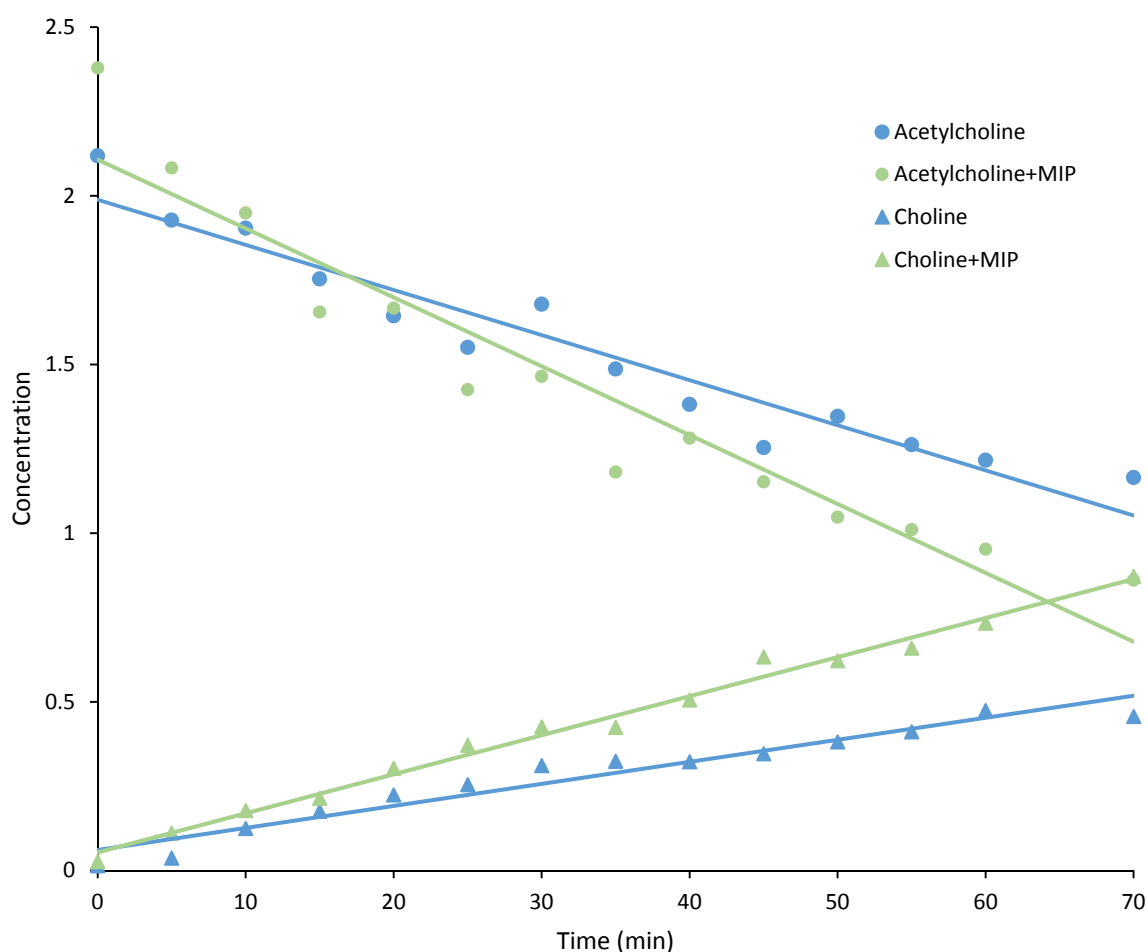
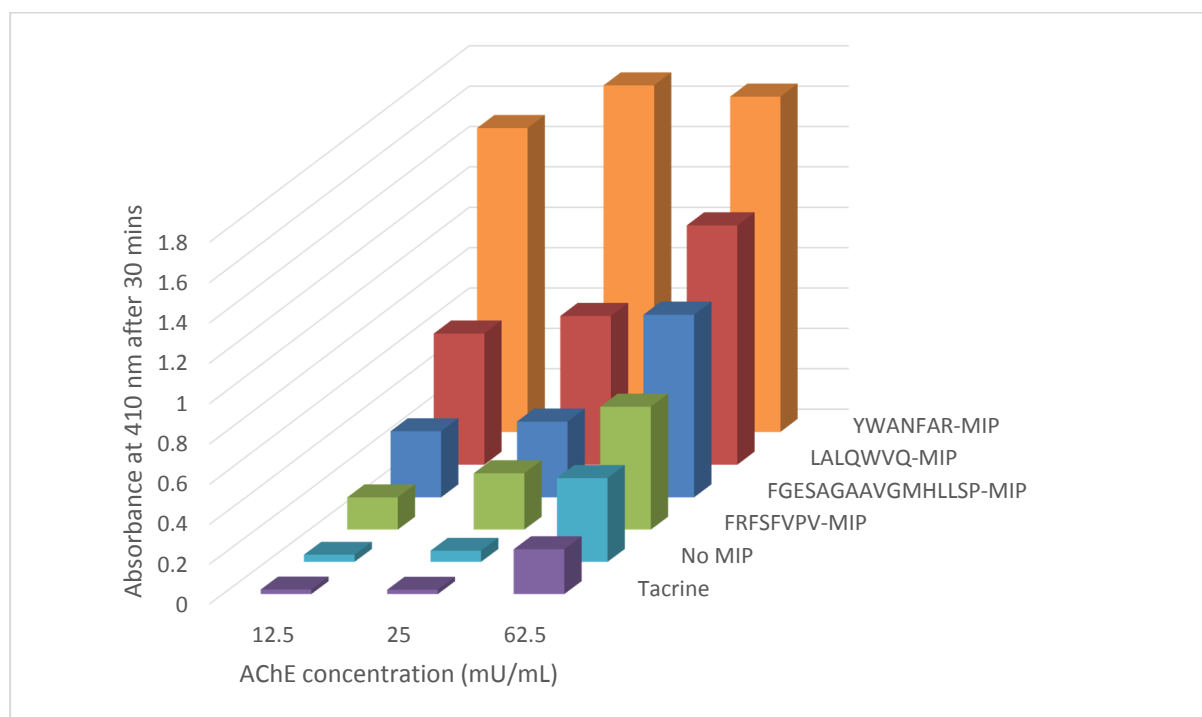


Figure 38. Direct measure of substrate conversion by enzyme alone and in the presence of FRFSFVPV-MIP.

Three trends emerge by comparing these experiments: firstly, the order of activation is consistent—YWANFAR-MIP clearly has the greatest effect, followed by LALQWVQ-MIP, FGESAGAASVGMHLLSP-MIP and FRFSFVPV-MIP. Secondly, as expected, the rate of reaction is proportional to enzyme concentration. Lastly, the degree of activation increases as enzyme concentration is diminished—this again is to be expected, as the proportion of activated enzyme will be greater at lower AChE concentrations. The increase in rate due to YWANFAR-MIP is close to 50-fold at both 12.5 and 25 mU mL⁻¹, indicating that this is the maximum degree of activation possible. Whilst this increase in rate may seem unlikely for such an efficient enzyme, the specificity constant for hAChE (1.32 x 10⁸ M⁻¹ s⁻¹) is still lower than that of a kinetically perfect enzyme (10⁸ to 10¹⁰ M⁻¹ s⁻¹), suggesting it may be possible to increase AChE’s rate from 10- to 100-fold higher than the native rate,²⁵⁴ which is in agreement with our observations.



Epitope	Relative rate (12.5 mU/mL)	Relative rate (25.0 mU/mL)	Relative rate (62.5 mU/mL)
YWANFAR-MIP	5524%	6355%	336%
LALQWVQ-MIP	1929%	1774%	243%
FGESAGAAVGMHLLSP-MIP	767%	572%	161%
FRFSFVPV-MIP	433%	461%	117%
No MIP	100%	100%	100%
Tacrine	62%	40%	59%

Figure 39. Effect of varying enzyme concentration on MIP-induced activation.

Originally, due to their size, it was expected that MIPs would inhibit AChE through steric occlusion of substrate access to the active centre, similar to fasciculin.²⁵⁵ It is possible that MIPs generated against other epitopes may indeed have this effect, especially those imprinted against sequences within the PAS; however, attempts to discover other epitopes common to both EeAChE and hAChE were unsuccessful, and for this reason efforts were focused on enzyme activation. Due to the highly optimised structure of the active site, it seems unlikely that any rearrangement of residues as a result of allosteric binding would be beneficial to the enzyme activity, and so it was hypothesised that the activation effects observed were a result of alteration to the deep gorge leading to the enzyme active site, thus making it more easily accessible to substrate or for product removal. In an attempt to observe such a conformational change, a titration of MIP against AChE was performed and changes to the protein's secondary structure observed by circular dichroism (Figure 40). A noticeable shallowing of the trough from 200-240 nm was evident as a result of increasing MIP concentration. This suggests that the presence of MIP is potentially loosening or flexing the structure of the protein. As AChE is known to have a flexible structure,²⁵⁶⁻²⁵⁸ it could be that the polymer is fixing the protein into a more favourable conformation. It is also possible to predict that the entrance of a substrate molecule into the active site and the exit of products might create a traffic limitation to the catalytic turnover rate. Being a metastable, flexible protein, it has been suggested that substrate displacement is promoted via “breathing”

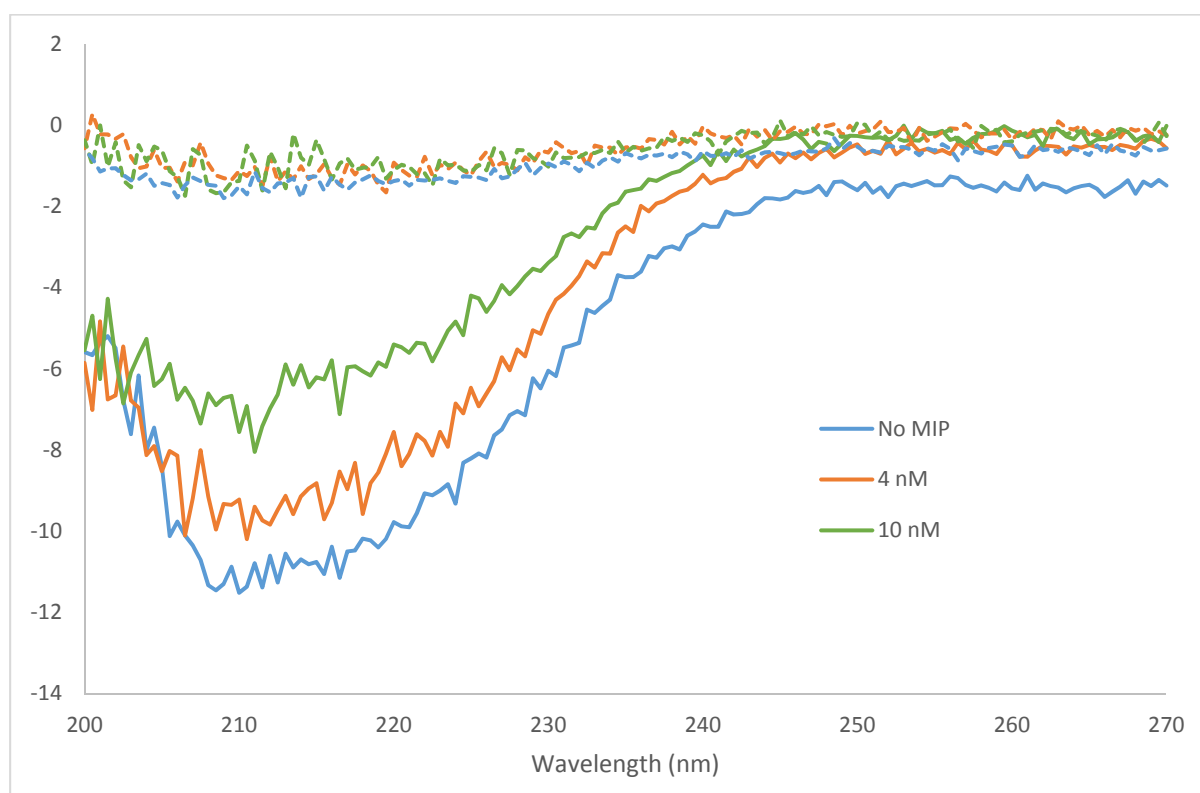


Figure 40. Circular dichroism spectra of AChE with increasing concentration of FGE-MIP. Dashed lines correspond to control measurements of MIP without protein.

motions, leading to an increase in diameter of the gorge to allow shuttling of molecules to the active site.²⁵⁹ This motion would involve contributions from a large fraction of the protein, and so binding of a relatively large MIP particle would be expected to influence the kinetics of such a process greatly. On the basis of molecular dynamics, it has also been proposed that products could leave the active site through a “back door”, transiently opened by concerted movements within the protein.²⁶⁰ Again, it would be expected that any change in conformation resulting from binding would have an influence on such processes.

4.5. Prevention and regeneration following inhibition

As it was believed the mechanism of activation was not involving interaction with the active site itself, it was unclear how MIP binding would affect inhibitors of AChE. For reversible AChE inhibitors, improving the accessibility to the active site through MIP binding could increase the potency of the inhibitor, or the degree of activation could counter the inhibitory effect entirely. In the case of irreversible inhibitors—specifically OP compounds—the same argument of improving accessibility resulting in more potent inhibition is true. However, an increase in reactivation through cleavage of the phosphoester-serine bond is also possible in this scenario^{198, 261}, and so once again the application of activating MIP could protect the enzyme activity from these inhibitors. Tacrine was employed as a reversible inhibitor of AChE. Instead of acting at the catalytic site, tacrine produces allosteric inhibition by binding to the hydrophobic anionic region on the enzyme’s surface.²⁶² When pre-incubated with MIP, the inhibitory effects of tacrine on AChE were completely negated (Figure 41). Whilst an interesting result, it

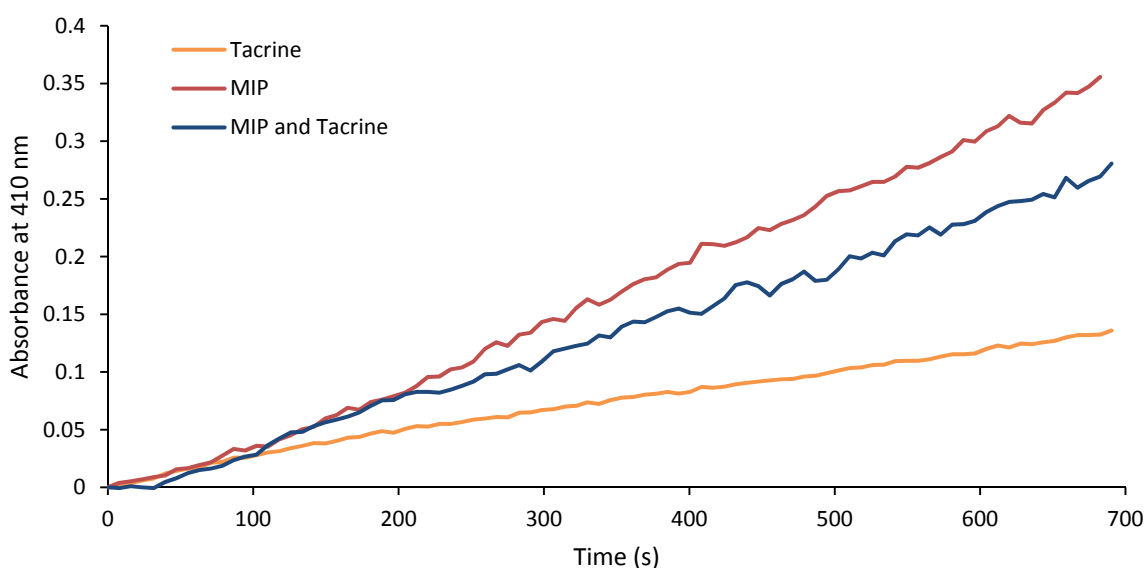


Figure 41. MIP providing protection of enzymatic activity from inhibition by tacrine

does not shed light on the mechanism of action of the MIP, and reversible inhibitors do not pose much of a practical threat. Of more interest is the response of AChE-MIP complexes to irreversible inhibitors, and so malathion, a widely used OP pesticide, was tested (Figure 42).

To test the ability of MIPs to prevent malathion from acting upon AChE, a pre-incubation for 15 minutes was performed prior to addition of malathion and substrate. The regenerative ability of MIPs was assessed in a similar manner; however, AChE was incubated instead with malathion prior to addition of MIP and substrate. Encouragingly, all MIPs appear to have a beneficial effect on retaining and restoring the enzyme activity; in the cases of LAL- and FGE-MIP the influence of malathion, which reduced the activity to as low as 15% of the native enzyme, was almost entirely negated.

It is unclear through which mechanism MIPs are countering the OP agent, although these results do lead us to believe an influence is being made on the active site itself, rather than just a change in accessibility as previously believed. Looking specifically at

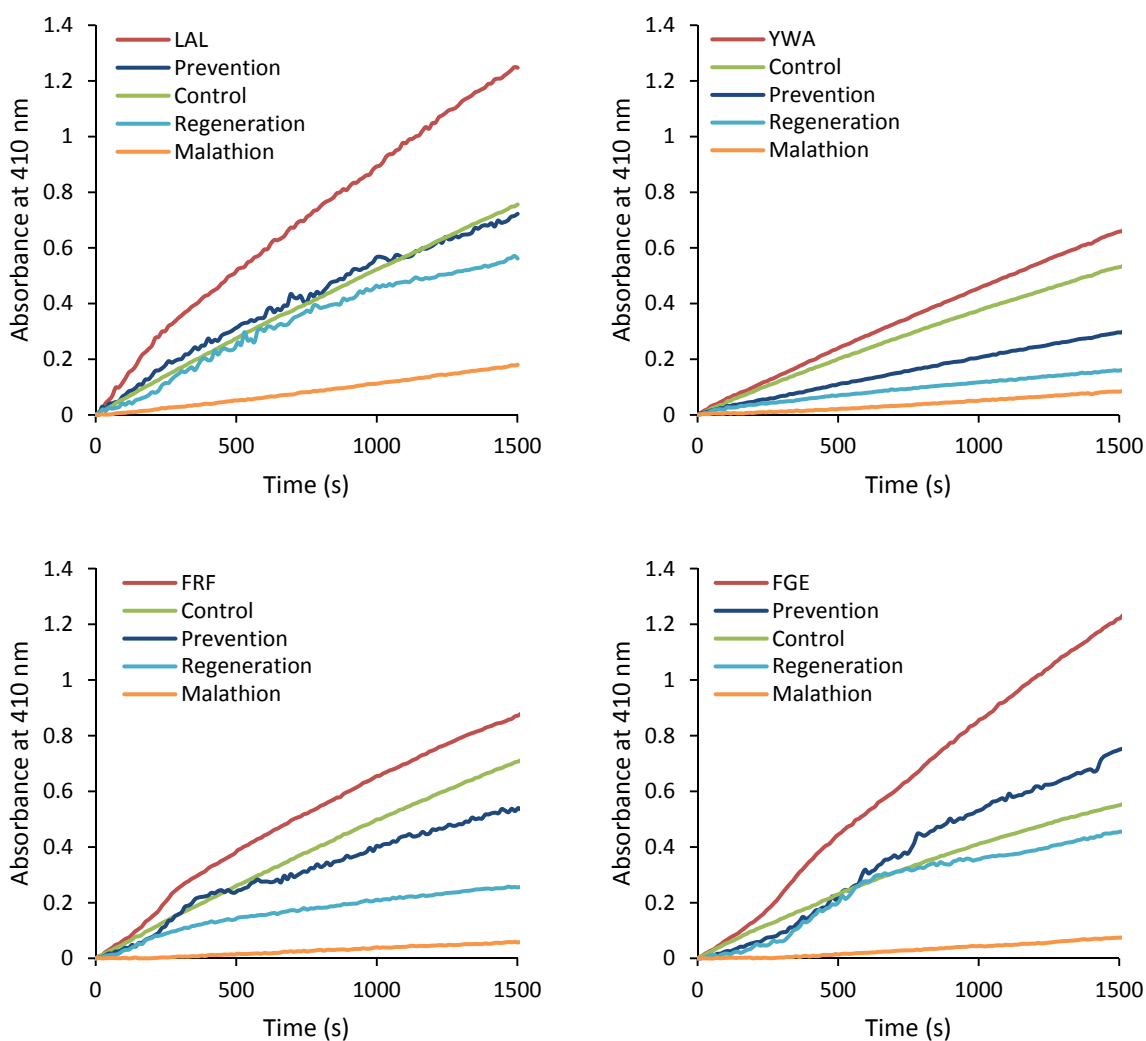


Figure 42. Prevention and regeneration of AChE by MIPs following inhibition from malathion.

the results obtained for FGE, the increase in rate between the control (no MIP or OP added, green curve) and enzyme with MIP (FGE, red curve) is roughly two-fold. If the MIP were simply activating the remaining enzyme which had not already been inactivated by malathion, we would expect a similar increase in rate between the malathion treated (yellow curve) and regeneration (light blue curve) experiments, however we instead see six-fold increase in rate between these two experiments. This suggests that the MIP is actively countering the effects of the OP, rather than just acting on free enzyme.

Focusing on the active site serine and its role in acetylcholine hydrolysis and OP inhibition it is possible to hypothesise how an alteration of the active site residues could explain both increase in rate of hydrolysis and decrease in “aging” of Ser-OP conjugates (Figure 43). Enzyme inactivation by OPs is a two-step process, with an intermediate Ser-OP conjugate following the initial reaction. This conjugate can then undergo two different hydrolysis reactions, with the leaving group determining the fate of the enzyme. If the Ser-OP bond is hydrolysed the enzyme is regenerated; however cleavage of the alternative phosphoester bond leads to strengthening of the Ser-OP bond, a process known as “aging”, which can no longer be hydrolysed and is considered irreversible inhibition of the enzyme. Any change to the conformation of active site residues which could potentially weaken the Ser-OP bond of this intermediate conjugate could therefore make the cleavage of this bond preferential to that of the phosphoester, and thus lead to a greater proportion of regeneration as opposed to aging. A weaker Ser-OAc bond brought about through the same conformational changes in the active site would also facilitate an easier final step in the enzyme’s catalytic function, and could thus contribute to the increase in reaction rate observed in the presence of MIP.

Further experiments are necessary in order to assess the potential of MIPs as a broad spectrum therapeutic against a range of OPs at clinically relevant concentrations, however these initial findings are encouraging. With the promising properties of MIPs for biological application and the need for new treatment options against OP intoxication, in vivo studies are being actively pursued.

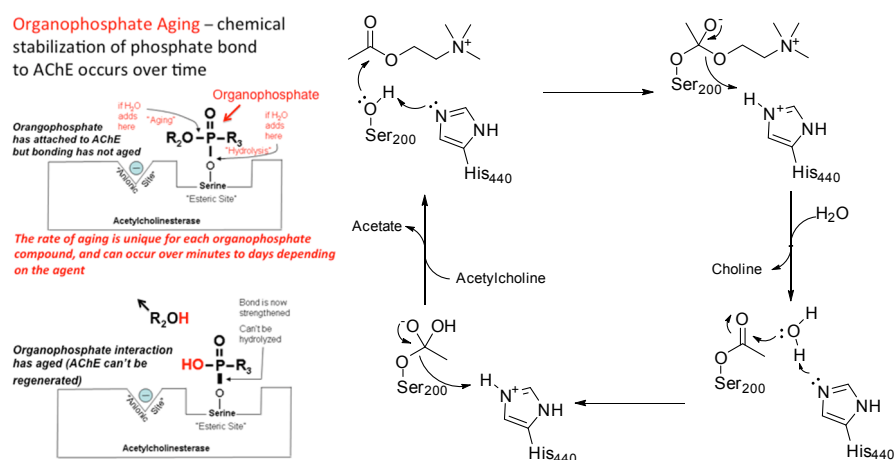


Figure 43. Roles of active site serine in hydrolysis and OP inactivation.

4.6. Sandwich MINA for the detection of AChE

Having extensively investigated the AChE-MIP interaction, attention was turned to assay development. Whilst FPMIA performed better when compared to MINA for peptides, the large increase in molecular weight associated with detection of a protein was expected to greatly reduce the change in polarisation as a result of a binding interaction, thus compromising the assay's sensitivity. MINA was therefore a more promising prospect, and also offered potential to aid in the problem of poor selectivity often observed with protein recognition through adaptation to a sandwich format. Furthermore, successful sandwich formation would further validate the site specificity of epitope imprinted MIPs for the target protein. To achieve this, magnetic template used in the standard MINA protocol was replaced with mMIPs by incorporating mNPs into the polymer itself (Figure 44). In this way two independent binding events are required in order to see a change in response as a result of addition of analyte.

With four separate epitopes identified for AChE, there are 12 potential sandwich complexes which can be utilised for detection. Potential problems with complex formation may arise through steric occlusion between two epitopes which are spatially close to one another, or through epitope binding sites no longer being recognised by a second MIP following an induced conformational change resulting from association of

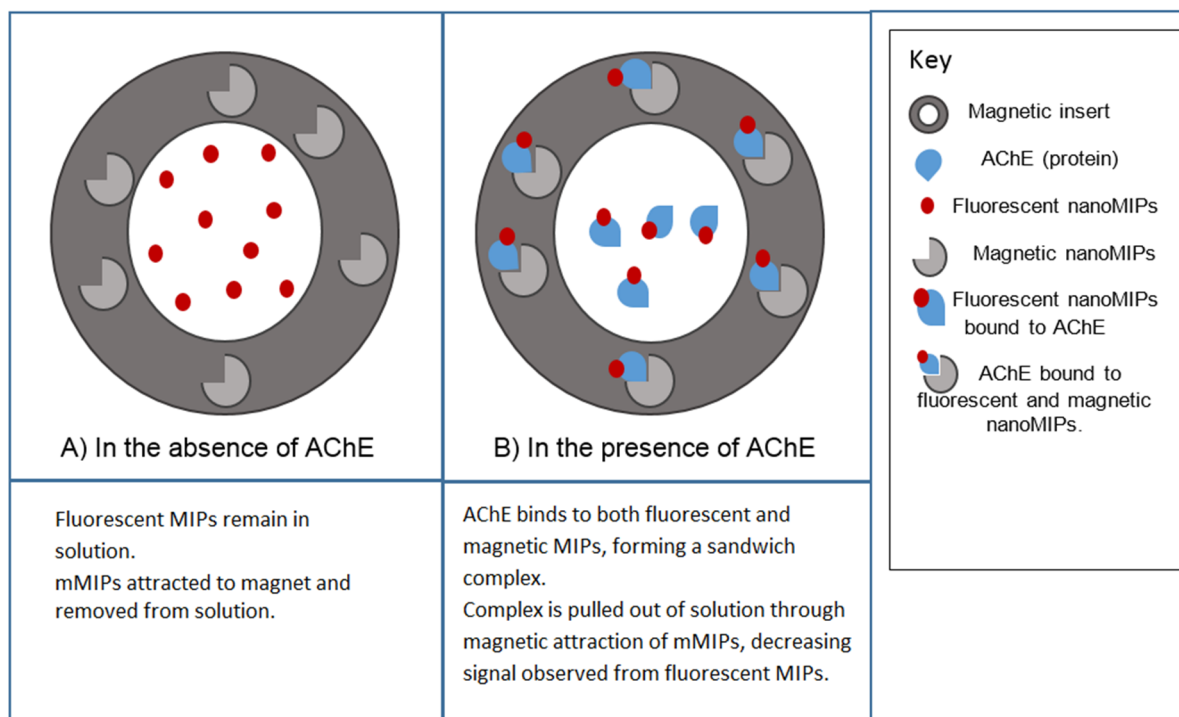


Figure 44. Sandwich MINA utilising both fluorescent and magnetic MIPs.

the first MIP. In order to assess all combinations, conditions were optimised for one set of MIPs, and then all MIPs tested under the same conditions. The epitope-imprinted MIPs selected for initial tests were YWA-MIP and FRF-MIP, as the position of these epitopes were furthest apart and therefore less likely to suffer from steric occlusion (Figure 34).

As was the case with MINA, selecting the correct concentrations of each assay component was the first challenge. This was even more difficult in a sandwich format, as all 3 components were required to be present in order to see any change in response at all (Figure 45 (iv)). If the concentration of fluorescent MIP is too low (Figure 45 (i)) mMIP and AChE may still bind and be removed from the solution through magnetic attraction to the microplate insert, however a change in signal will not be observed as there will be no change in fluorescence intensity. If the concentration is too high however the same is also true, an excess of fluorescent MIP will reduce the possible percentage decrease in fluorescence as a result of complex formation and will therefore make it more difficult to observe this change. Likewise in the case of mMIPs concentration being too low (Figure 45 (ii)), fluorescent MIP and protein may still bind with one another but the complex formed will not be removed from the solution due to the absence of mMIP, resulting in no observable change in signal. The final component, AChE, is also important to have in the right concentration range. If too low no complex can be formed (Figure 45 (iii)), however if in excess the chance of complex formation will also be reduced, as MIPs will be more likely to bind to free AChE than to an AChE-MIP complex.

Stock solutions (0.1 mg mL^{-1}) of magnetic and fluorescent MIPs were prepared. Fluorescent MIP was diluted 10-fold until the signal to noise was unacceptable, and the resulting concentration range ($1 - 100 \text{ } \mu\text{g mL}^{-1}$) also prepared for mMIPs. Each concentration of fluorescent and magnetic MIP was tested against a dilution series of AChE ($0.035 - 35 \text{ nM}$). Optimal results were observed using 0.1 mg mL^{-1} of both MIPs, with a Z' of 0.81 for the final assay. (Figure 46) The fluorescence decreased with

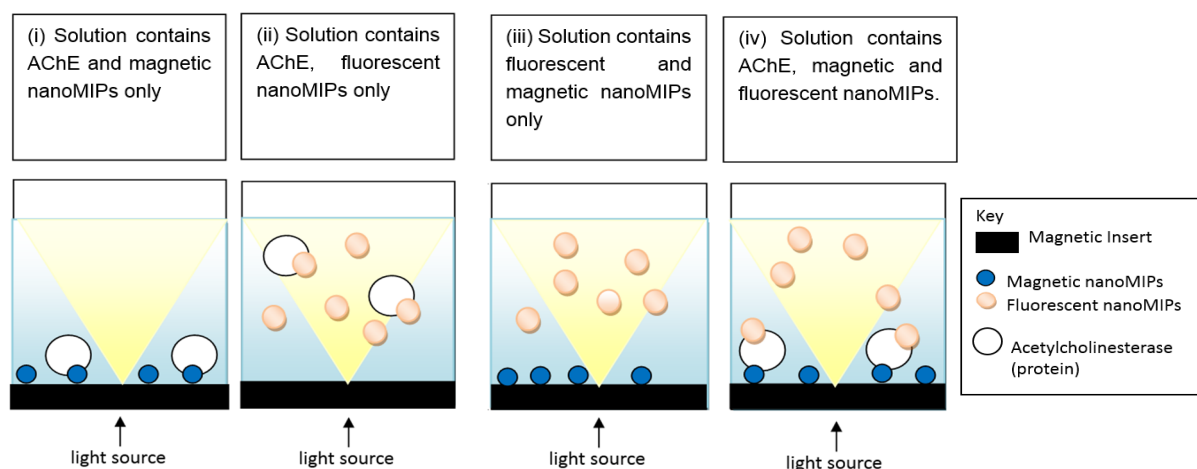


Figure 45. The possible outcomes from sandwich MINA, demonstrating the necessity of all three assay components to be present at the correct concentrations.

increasing AChE concentration, indicating the sandwich complex was being formed and fluorescent MIP was being pulled to the magnetic insert as a result. Experiments were repeated using other combinations of MIPs to assess their suitability (Figure 47). Promising results were obtained for 10 out of 12 possible combinations. All data were fit to 4 parameter logistic regressions with an average Z' of 0.70 for the entire dataset. As a proof of concept, the results indicate that simultaneous site-specific binding is achievable through epitope imprinting, and can be exploited for protein detection in a sandwich assay format.

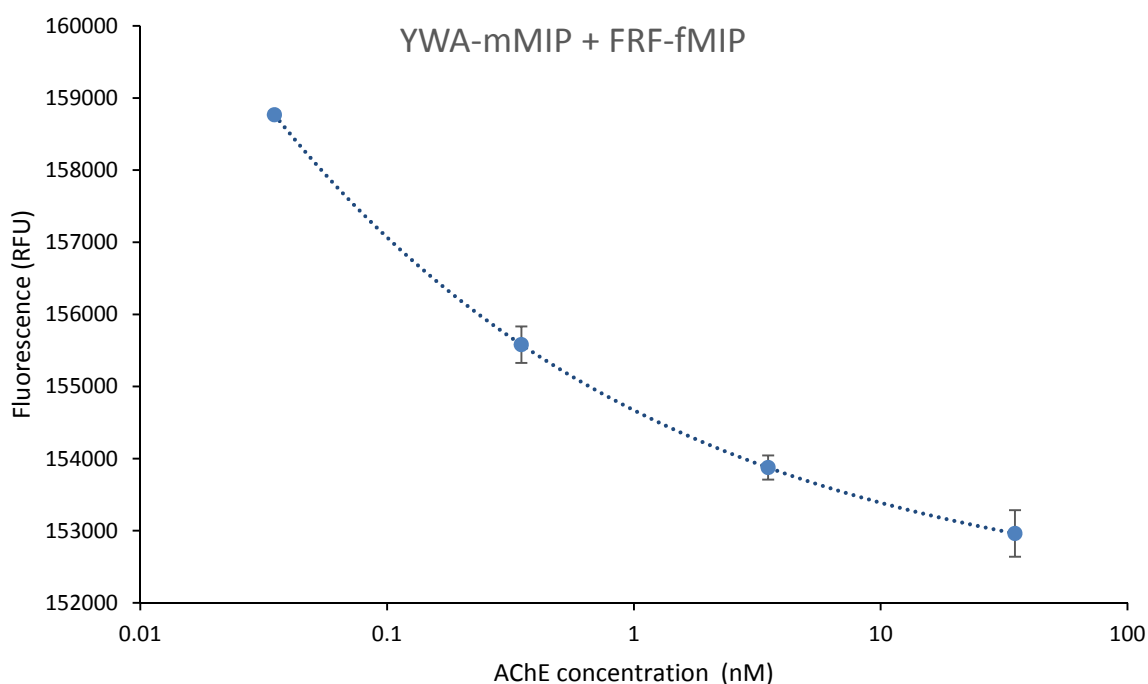
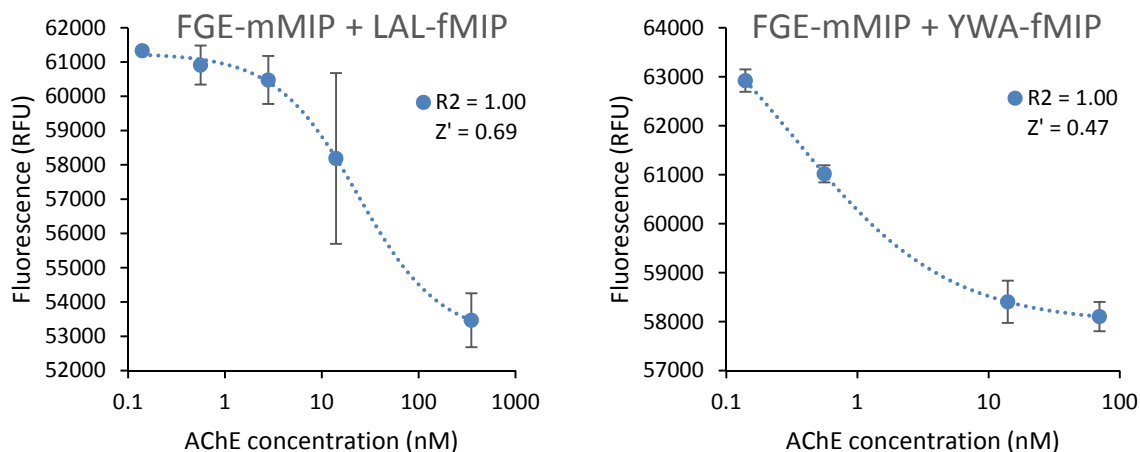


Figure 46. Sandwich MINA for AChE using fluorescent FRF-MIPs and YWA-mMIPs. $R^2 = 1$, $Z' = 0.81$.



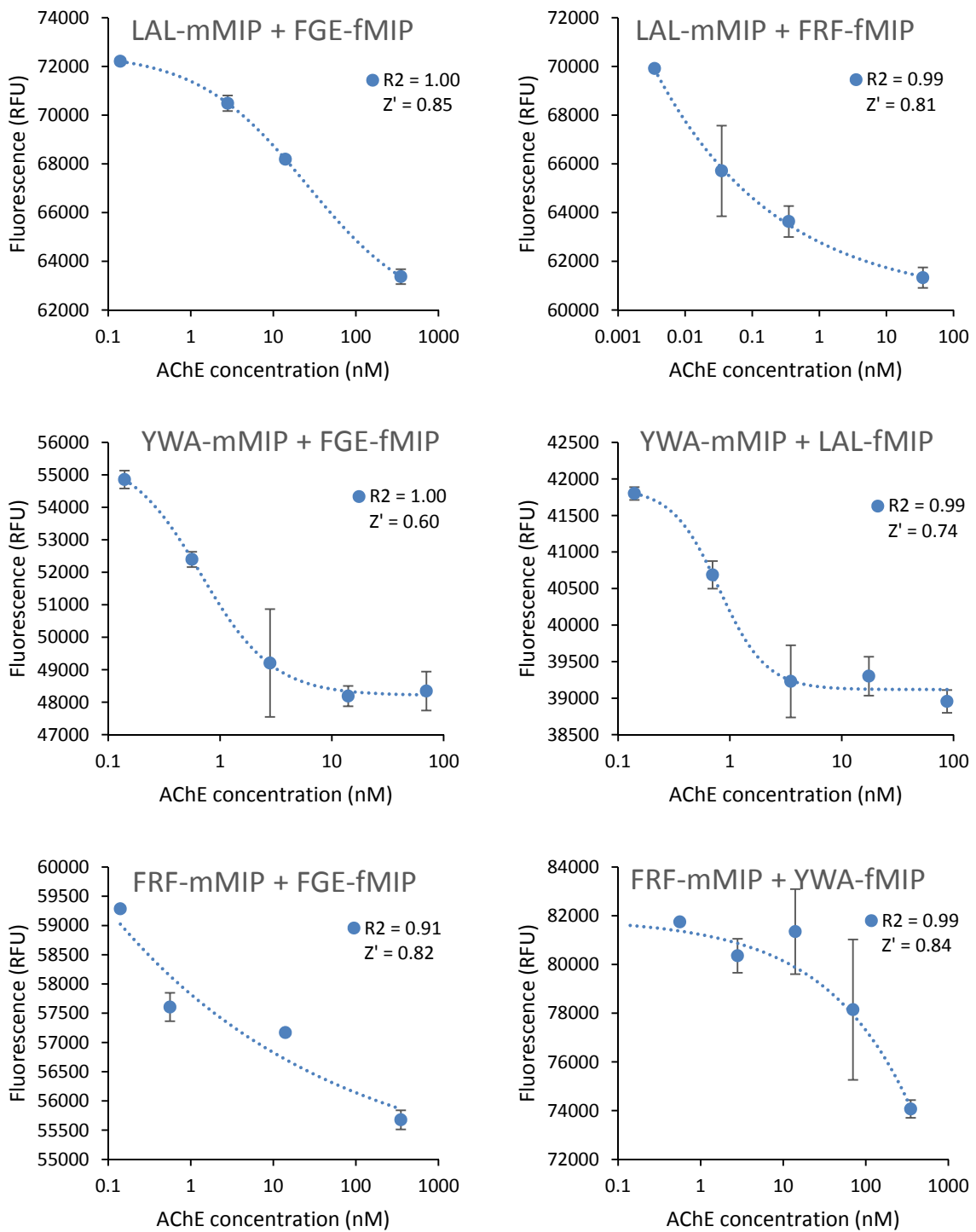


Figure 47. Sandwich MINAs utilising different combinations of fluorescent and magnetic MIPs.

4.7. Conclusions

Through a combination of solution-based whole protein imprinting and MS, utilising the protection offered by MIPs against proteolysis of the bound protein fragments, seven epitopes were identified for EeAChE. Of these, four were selected due to their presence also in hAChE and used as templates for solid-phase imprinting. The resulting epitope-imprinted MIPs retained affinity for the native enzyme, demonstrating nanomolar binding constants. The epitope-imprinted MIPs were subsequently utilised in the development of a sandwich MINA, providing validation of site-specific binding to the target protein. Positive results were obtained for the majority of MIPs tested, with an average Z' of 0.70 for the developed assays.

When assessed for their impact on enzyme activity, MIPs were found to enhance the enzyme's catalytic rate up to 60-fold. The MIPs ability to protect the enzyme and reverse the effects of a common OP pesticide was therefore tested, with the AChE-MIP complexes able to completely withstand inhibition. This presents an exciting opportunity to demonstrate the application of MIPs as potential therapeutics. Considering the promising properties of MIPs for biological application and the need for new treatment options against OP intoxication *in vivo* studies are being actively pursued.

CHAPTER 5: FINAL CONCLUSIONS AND FUTURE WORK

The research presented aimed to address the challenges regarding the imprinting of biological macromolecules, and to explore suitable assay formats for the detection of such targets. In doing so, the intention was to develop a reliable and rapid strategy to advance from target identification to production of a functional assay for any analyte of interest.

Initial work focused on development of a screening procedure for optimisation of polymer compositions. The protocol utilised 96-well filtration microplates, solid-phase synthesis with affinity separation, and a fluorescent reporter monomer. This allowed the simultaneous evaluation of 32 different monomer compositions in triplicate, generating information regarding the affinity and selectivity introduced through a variety of monomers. Optimal monomer compositions were selected from the screening results and demonstrated greater retention for the solid phase, indicative of a stronger binding affinity. The affinity distribution of MIPs collected with 60°C water was confirmed using SPR to be within the nanomolar range of dissociation constants, which is adequate for application to binding assays. Although not observed as part of this study, in the event that MIPs synthesised using the solid-phase protocol do not demonstrate appreciable binding, the developed screening method will provide a useful tool for optimising compositions for enhanced affinity.

Having concluded that MIPs suitable for application to binding assays could be readily synthesised, attention was turned to assay development. Two formats for the detection of peptides were explored, the first utilising fluorescence polarisation as a signalling method and the second relying upon the removal of fluorescent MIP from a sample solution following binding to a magnetic conjugate of the analyte. Both assays generated encouraging preliminary results demonstrating Z' values of 0.80 and 0.85 for FPMIA and MINA respectively. Whilst there is clearly potential for both formats thorough validation still needs to be performed through multiple repetitions and cross-selectivity experiments before they can be considered for application outside of an academic environment. Most importantly, as only a single peptide has been used as analyte for

each assay future work should be focused upon confirmation of the universal nature of these assay formats through application to a variety of analytes.

The final piece of this work was to consolidate the knowledge gained throughout the project and apply these techniques to the development of an assay for the detection of a protein. This involved a novel approach for identification of imprintable epitopes on the surface of the chosen model protein (AChE), utilising MS analysis of peptide sequences protected by MIPs from proteolysis following solution-based whole protein imprinting. Of the identified epitopes, four were chosen as templates for generation of MIPs with site-specific recognition for their respective epitope sequences on the surface of AChE. The specificity for different sites on the protein's surface was exploited by adaptation of MINA to a sandwich format for a more selective and sensitive assay than otherwise possible. Of the 12 possible combinations of epitope imprinted MIPs 10 successfully formed sandwich complexes with AChE. The resulting assays had an average Z' of 0.70 and working ranges over three orders of magnitude in most examples. As was the case regarding the developed peptide assays, future work should focus on validation of these preliminary results and application of this assay development strategy to other target proteins to evaluate its suitability as a generic procedure for obtaining practical assays for proteins.

Investigating the effect of binding interactions of epitope imprinted MIPs with AChE as part of the aforementioned assay development also revealed an exciting possibility for therapeutic application of MIPs. When assessed for their impact on enzyme activity, MIPs were found to enhance the enzyme's catalytic rate up to 60-fold. The MIPs ability to protect and regenerate AChE following exposure to a common OP pesticide was therefore tested, with the AChE-MIP complexes able to completely withstand inhibition. Further experiments are necessary in order to assess the potential of MIPs as a broad spectrum therapeutic against a range of OPs at clinically relevant concentrations; however, these initial findings are encouraging. With the promising properties of MIPs for biological application and the need for new treatment options against OP intoxication, *in vivo* studies are being actively pursued.

The work described in this thesis addresses the original objective to demonstrate an assay development process which can be used for the detection of peptides and proteins. As it stands however, whether the assays developed as part of this project can be considered universal formats for any analyte of interest yet to be determined. In the opinion of the author these strategies provide the most promise for delivering the goal of a generic assay platform, and the procedures and formats described here are currently undergoing further development by colleagues for other analytes of interest. MINA in particular is emerging as a popular assay, with examples of assays for small molecules beginning to appear in the literature to complement those developed here for peptides and proteins, providing strong evidence that this format may well be suitable for any analyte.

CHAPTER 6: EXPERIMENTAL

6.1. General information

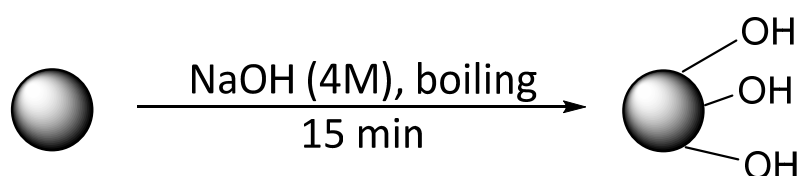
All chemicals used were purchased from commercial sources and used without further purification unless otherwise stated. All chemicals were stored under conditions outlined in the manufacturer's instructions. Anhydrous solvents were dried and stored under nitrogen, under pre-activated 4 Å molecular sieves. Spheringlass A-Glass 2429 microspheres used as solid phase for template immobilisation were obtained from Blagden Chemicals, UK. Filtration plates and vacuum manifold utilised for small scale polymer composition screening were purchased from Porvair Sciences, UK. 96 well black non-binding microplates used for FP and MINA (μ Clear bottom for MINA) experiments were acquired from Greiner Bio One. Microplates for MINA were modified in-house: magnetic sheets with self-adhesive backing were purchased from Polarity Magnets, UK, and cut into an annular shape using a JD4060 laser cutting machine from Mantech UK. Solvent evaporation took place under low pressure on a Buchi vacuum rotary evaporator, and a Labconco FreeZone 2.5 lyophiliser was used for the freeze-drying of peptides and nanoparticles.

Fluorescence, FP and absorbance microplate measurements were performed using a Hidex Sense microplate reader. Optical setups were optimised dependent upon the fluorophore/chromophore and concentrations used. Autofocus was used for each measurement with buffer selected for background measurements and the highest concentration of fluorophore/chromophore selected for signal measurements, with the focal point responsible for the largest signal to noise chosen for subsequent reading of the microplate. Excitation and emission apertures were modified if necessary to avoid signal saturation.

6.2. Preparation of template-derivatised solid phase

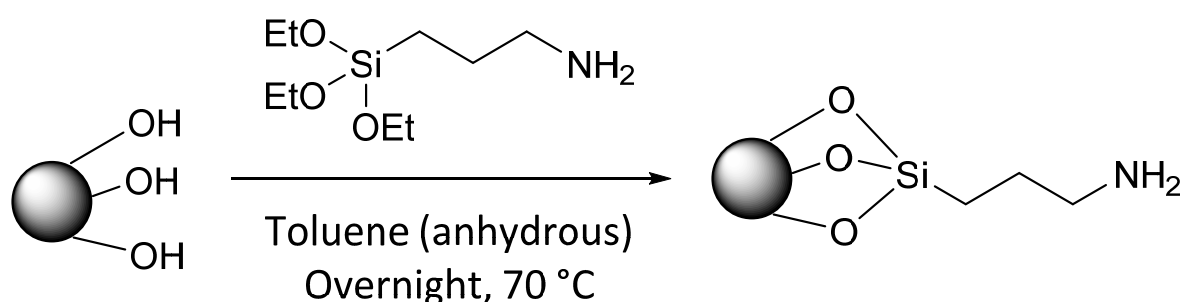
The quantities given in the following protocols are those typically used, however all steps involved in derivatisation of the solid phase are scalable, dependent upon the quantity of MIP required or template available.

6.2.1. Activation of glass microspheres



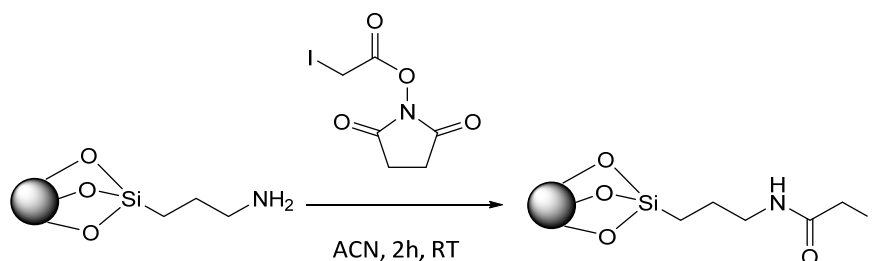
Glass microspheres (200 g) were boiled in sodium hydroxide (4 M, 160 mL) for 15 minutes prior to washing with 3 volumes (500 mL) of water. The beads were subsequently placed in a solution of sulphuric acid (50%, 160 mL) for 30 minutes before again washing with water (500 mL) and phosphate buffered saline (PBS, 500 mL), ensuring the final pH is between 6–8. Further washing with acetone (500 mL) was performed before drying under vacuum and placing the beads in an oven (150 °C) for 30 minutes.

6.2.2. Silanisation of glass microspheres

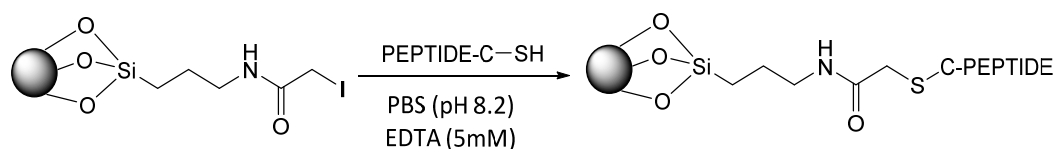


Activated glass microspheres (200 g) were incubated in a solution of toluene (80 mL, anhydrous) with (3-aminopropyl)triethoxysilane (1.6 mL) and 1,2-bis(triethoxysilyl)ethane (0.270 mL) overnight at 70 °C. Beads were subsequently washed with 3 volumes of methanol and 5 volumes of acetone to remove any residual silane, before drying under vacuum and further oven drying for 30 minutes at 150 °C.

6.2.3. Immobilisation of peptides

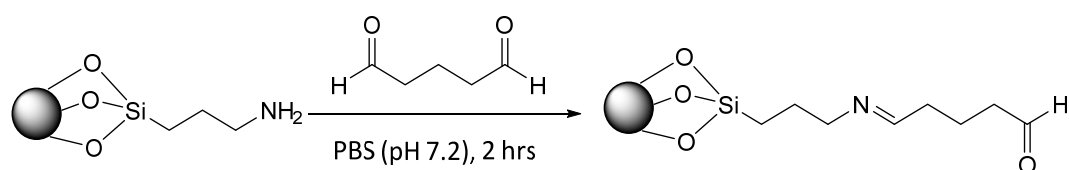


SIA (10 mg) was added to silanised solid phase (120 g) in anhydrous acetonitrile (50 ml) and incubated for 2h under exclusion of light, before washing with acetonitrile (5 x 50 mL).

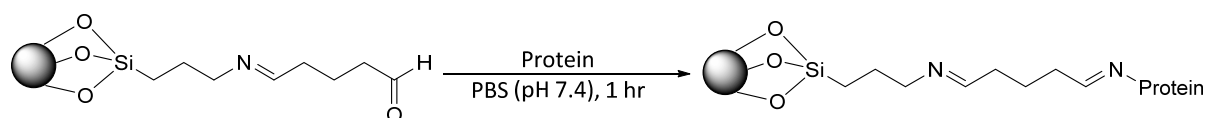


Thiol buffer (pH 8.2) consisting of PBS (50 mL) and ethylenediaminetetraacetic acid (74 mg) was degassed and purged with nitrogen prior to addition of peptide (5 mg). Incubation with SIA-functionalised solid phase (120 g) was allowed overnight with exclusion of light, followed by washing with water (1.5 L) and drying under vacuum.

6.2.4. Immobilisation of proteins



Silanised solid-phase (40 g) was incubated in a solution of glutaraldehyde (1.12 mL) in PBS (16 mL, pH 7.4) for two hours before washing with water (8 x 16 mL).



Glutaraldehyde-functionalised solid phase (40 g) was incubated in a solution of protein (8.0 mg) in PBS (16 mL, pH 7.4) for 1 hour before washing with water (12 x 16 mL).

6.3. Solid phase synthesis of MIP NPs

As with the preparation of template-derived solid phase, the synthesis of MIP nanoparticles is also a scalable process—for example, for the small scale synthesis screening with filtration microplates, only 50 mg of solid phase is used per synthesis. The quantities given below are therefore those employed for a typical synthesis.

Polymerisation mixture consisting of NIPAM (39 mg, 344.64 μmol), BIS (2 mg, 12.97 μmol), TBAm (33 mg, 259.47 μmol dissolved in 1 mL ethanol), AAc (100 μL of a 22 $\mu\text{L mL}^{-1}$ solution in water, 31.92 μmol), APMA (5.80 mg, 33 μmol), and if fluorescent MIPs are desired, *N*-fluoresceinylacrylamide (2.5 mg dissolved in 1 mL ethanol), was dissolved in water (100 mL) and purged with nitrogen for 30 minutes. Following this, the polymerisation mixture was added to template-derivatised beads (60 g) and polymerisation initiated using a solution of APS (30 mg/500 μL water, 131.47 μmol) and TEMED (30 μL , 70.03 μmol). The polymerisation was allowed to proceed for 60 minutes, before quenching of the reaction by allowing oxygen into the system. The beads were subsequently washed with water (9 x 30 mL) at room temperature to remove unreacted monomer and low affinity polymer before eluting high-affinity nanoparticles with hot water (100 mL) at 60 °C.

6.4. Analysis of the size of MIP NPs

Nanoparticle size was determined by DLS using a Zetasizer Nano (Nano-S) from Malvern Instruments Ltd. (Malvern, UK) and images obtained using a JEOL JEM-2100 LaB6 TEM. Prior to DLS measurements samples were subjected to sonication for 2 minutes, and measurements performed at 25 °C. Samples for TEM were prepared by placing 10 μL of the MIP NPs dispersion, previously sonicated for 2 min and filtered through a 1.2 μm glass fibre syringe filter, onto a carbon coated copper grid. The sample was left to dry overnight under a hood before imaging.

6.5. MIP affinity measurements by SPR

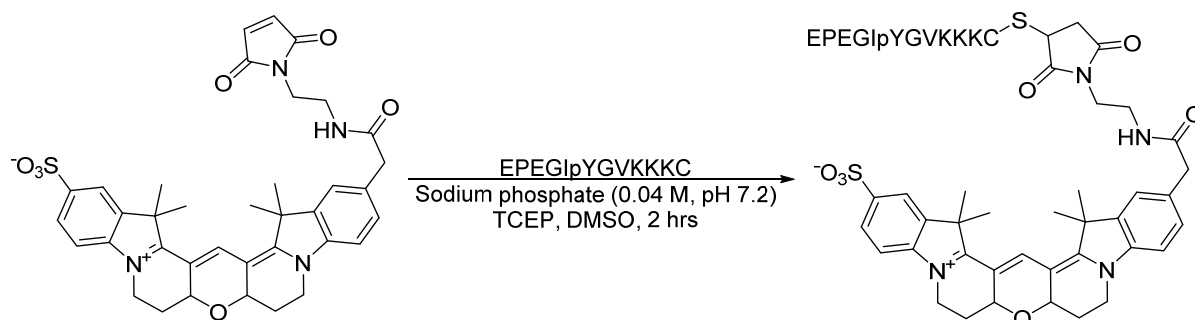
SPR experiments were performed using a MP-SPR Navi 220A NAALI (BioNavis). Bare gold sensor chips were incubated overnight with 11-mercaptoundecanoic acid (22 mg in ethanol (10 mL)) to afford a carboxyl functionalised surface and were rinsed with ethanol and dried under nitrogen immediately before use. All MIPs were immobilised using amine-coupling chemistry. The surfaces of flow cells one and two were activated for 7 min with a 1:1 mixture of NHS (0.1 M) and EDC (0.4 M) at a flow rate of 30 $\mu\text{L min}^{-1}$. MIPs (10-200 $\mu\text{g ml}^{-1}$ in 10 mM sodium acetate, pH 5.0) were then immobilised on flow cell 2, with a control polymer immobilised on flow cell 1 to serve as a reference surface. Both surfaces were subsequently blocked with a 7 min injection of ethanolamine (1 M, pH 8.0). To collect kinetic binding data analyte was injected over both flow cells at a rate of 15 $\mu\text{L min}^{-1}$ at 25 °C, using ultrapure water as running buffer and for all analyte dilutions. A kinetic titration injection strategy was employed, with analyte allowed to associate and dissociate for 14 and 5 mins respectively, before a final dissociation of 120 mins. All data were fit to a 1:1 interaction model using Tracedrawer 1.8 software, with χ^2 values used to determine the goodness of fit.

6.6. Small scale synthesis screen with filtration microplates

The standard polymerisation protocol was adapted to be performed in a single well of a 96 well microplate. Each polymerisation mixture (1 mL) was prepared with the functional monomer compositions modified as outlined in Table 2. These were then dispensed (100 μL per well) in triplicate into wells containing functionalised solid phase (50 mg), before initiating the polymerisation with APS and TEMED and leaving for 1 hour at room temperature. The monomer solution was then removed from each well by fitting the microplate into a vacuum manifold, and the solid phase washed with water (10 x 100 μL) to remove unreacted monomer and low-affinity polymer. After fluorescence measurements, further washing was performed in the same fashion using water at 60 °C to emulate the elution process of high-affinity MIPs, before again taking fluorescence measurements.

The quantity of MIP still bound to immobilised template was measured using the fluorescence introduced to the polymers through *N*-fluoresceinylacrylamide. A filter set with excitation of 485/10 nm and emission of 520/14 nm was used, with a dichroic mirror at 505 nm.

6.7. Fluorescent labelling of EPEGIpYGV-KKK-C



EPEGIpYGV-KKK-C (81 μg , 60 nmol) was dissolved in water (188 μL , 0.32 mM) and diluted with labelling buffer (63 μL , 0.2 M sodium phosphate, pH 7.2, containing 0.04 M TCEP). Cy3B maleimide (0.5 mg, 0.73 μM) was dissolved in DMSO (60 μL) before adding to the reaction vial and incubating for 120 minutes at room temperature. The labelled peptide was separated from the remaining free dye through precipitation with ice-cold diethyl ether. The solution was then centrifuged for 15 mins (14000 rpm), the supernatant removed and the pellet washed with further ice cold ether before dissolving in acetonitrile/water for purification by HPLC.

Analytical and semi-preparative HPLC were performed using a DIONEX UltiMate 3000 (model 310 UV detector, 230 pumps with a gradient controller, and 410 autosampler). This utilised a Phenomenex Gemini-NX C-18 110 \AA AXIA packed column with dimensions of 250 x 21.20 mm and flow of 0.5 mL min^{-1} with injection volume of 20 μL for analytical HPLC, and dimensions of 150 x 4.60 mm and flow of 1.6 mL min^{-1} with a variable injection volume of up to 2 mL for semi-prep HPLC. A two-solvent system was used for the collection of data: water with 0.1% trifluoroacetic acid and acetonitrile with 0.1% trifluoroacetic acid. UV detection was measured across two channels of 214 nm and 559 nm for both analytical and semi-prep HPLC. A gradient of 5-50% acetonitrile over 30 minutes was used for the collection of pure peptide and 5-100% acetonitrile over 20 minutes for the analysis of crude and pure peptides. Successful labelling was confirmed using a Voyager-DE-STR-MALDI-TOF Mass Spectrometer. Excitation and emission spectra of the labelled peptide were acquired in ultrapure water using a FluoroMax-2 spectrofluorometer from 400-700 nm using 1 nm steps.

6.8. FPMIA for EPEGIpYGV-KKK-C

A filter set with excitation of 560/40 nm and emission of 620/10 nm with a dichroic mirror at 600 nm was deemed optimal for the Cy3b conjugate. 100 flashes and a G factor of 1 were used for all measurements. Solutions of tracer (1.13 nM) and analyte were prepared in ultrapure water before addition of MIP (100 $\mu\text{g mL}^{-1}$) and dispensing of samples into a black non-binding 96 well microplate in triplicate.

6.9. Preparation of template-derivatised mNPs

N-[3-(trimethoxysilyl)propyl]ethylenediamine (2.5 mL) and 1,2-bis(triethoxysilyl)ethane (60 μL) were diluted in a 5% water in ethanol (v/v, 50 mL), and the pH adjusted to 4.5 – 5.5 with acetic acid. Iron oxide mNPs (Fe_3O_4 , 1 g, 50-100 nm) were added to the prepared silane solution and sonicated for 4 hours. The mNPs were subsequently washed with ethanol (10 x 50 mL) and acetone (50 mL) before curing by incubation at 110 °C to afford the silanised mNPs.

SIA (10 mg) was added to silanised mNPs (200 mg) in anhydrous acetonitrile (25 mL) and incubated for 2h under exclusion of light, before washing with acetonitrile (5 x 25 mL). Thiol buffer (pH 8.2) consisting of PBS (25 mL) and ethylenediaminetetraacetic acid (37 mg) was degassed and purged with nitrogen prior to addition of peptide (5 mg). Incubation with SIA-functionalised mNPs (200 mg) was allowed overnight with exclusion of light, followed by washing with water (750 mL) and drying under vacuum.

6.10. MINA for FRFSFVPV-GG-C

Template-derivatised mNPs (0.125 mg mL^{-1}) were incubated with fluorescently labelled MIPs (0.15 mg mL^{-1}) in phosphate buffer (0.25 mM, pH 7.6) for 1 hour. The supernatant was removed and replaced with analyte (0.01 – 100 μM) in HBS buffer (5 mM, pH 7.4). Samples were dispensed into modified magnetic microplates in triplicate and the fluorescence measured. A filter set with excitation of 490/20 nm and emission of 535/20 nm with a dichroic mirror at 505 nm were used for all measurements.

6.11. Epitope mapping of AChE

The target protein for identification of surface peptide sequences was acetylcholine esterase, an enzyme from electric eel *Electrophorus electricus* (Sigma, C-3389). AChE (0.7 mL, 2.2 mg mL⁻¹ in PBS) was mixed with deoxygenated monomeric mixture (10 mL), consisting of NIPAm (19.5 mg), BIS (3 mg), TBAm (15 mg), AAc (50 µL of a 22 µL mL⁻¹ solution in H₂O), and APMA (3 mg) dissolved in PBS (50 mL) and purged with nitrogen for 20 min. Polymerisation was initiated by addition of APS (100 µL, 120 mg mL⁻¹) and TEMED (6 µL, 15 µL mL⁻¹), and allowed for 1 h at room temperature (20 °C). To remove unreacted functional monomers and low-affinity particles PBS (10 mL) was added to the polymerised samples and incubated for 10 min, prior to filtration through a 50 kDa centrifuge filter for 30 mins at 3500 rpm. MIP nanoparticles bound to protein were reconstituted in PBS (5 mL) containing trypsin (0.5 mg, bovine pancreas, Sigma, T9201) and incubated at room temperature for 36 h. Free fragments of digested AChE and trypsin were removed by centrifugation of the samples using a 50 kDa centrifuge cartridge for 15 min at 3500 rpm followed by washing with PBS (2 x 5 mL). The peptides bound to MIPs were separated from polymers using hot water (2 x 1 mL), lyophilised and reconstituted in 0.1% formic acid/3% acetonitrile.

Peptides were initially loaded onto a Waters 2G-V/M Symmetry C18 trap column (180 µm x 20 mm, 5 µm) to desalt and chromatographically focus the peptides prior to elution onto a Waters Acquity HSS T3 analytical UPLC column (75 µm x 250 mm, 1.8 µm). Single pump trapping was used with 99.9% solvent A and 0.1% solvent B at flow rate of 5 µL/min for 3 min. Solvent A was LC-MS grade water containing 0.1% formic acid and solvent B was acetonitrile containing 0.1% formic acid. For the analytical column the flow rate was set at 0.3 µL/min and the temperature maintained at 40 °C. The 50 min run time gradient elution was initiated as the peptides were eluted from the trap column. The following gradient was used: 0 min — 3% B, 30 min — 40% B, 32 min — 85% B, 40 min — 85% B and 41 min — 3% B. The NanoAcquity UPLC was coupled to a Waters Synapt G2 HDMS mass spectrometer. The instrument was operated in positive electrospray ionisation mode. The capillary voltage was set at 2.4 kV and cone voltage at 30 V. PicoTip emitters (New Objective, US, 10µm internal diameter) were used for the nanostage probe. A helium gas flow of 180 mL/min and ion mobility separator nitrogen gas flow of 90 mL/min with a pressure of 2.5 mbar were used. The IMS wave velocity was set at 650 m/s and the IMS wave height at 40 V. During the HDMSE acquisition a low collision induced dissociation energy of 4 V was applied across the transfer ion guide. For the high collision induced dissociation energy acquisition a ramp of 20 to 40 V was applied. Argon was used as the collision induced dissociation gas. Lockspray provided mass accuracy throughout the chromatographic run using [Glu1]-Fibrinopeptide with 785.8427 *m/z*. The data was acquired using

MassLynx 4.1. All raw data were processed using ProteinLynx Global SERVER (Waters Corporation, Milford, Massachusetts, USA). ProteinLynx Global SERVER was used to assemble the data for alignment, peak picking, peptide and protein identification and limited upstream statistics. Data was searched against Uniprot *Electrophorus electricus* database (downloaded December 2016).

6.12. Structural modelling of AChE

The peptide sequence for AChE of *Electrophorus electricus* was obtained from the UniProt²⁴⁸ website (<http://www.uniprot.org/>) using the UniProt Knowledgebase as the UniProt Knowledgebase code O42275 (<http://www.uniprot.org/uniprot/O42275>) and saved in FASTA format. The 3D structure of the peptide sequence was created using the structure prediction program I-TASSER^{246, 263-265} (<http://zhanglab.ccmb.med.umich.edu/I-TASSER/>). The peptide sequence was added in FASTA format and sent to the I-TASSER On-line Server. Five PDB structures were generated and downloaded from the On-line Server and the C-score values were obtained. Only one structure had a positive C-score of +0.28 (the other four ranged from -1.41 to -2.62) and this structure was used as the 3D structure on the peptide sequence as an I-TASSER model and compared with the PDB ID: 4EY4 (www.rcsb.org). 4YE²⁴⁶ was chosen as this was the most accurate structure available for hAChE from X-RAY diffraction with the highest resolution of 2.16 Å for comparison with the I-TASSER model.

6.13. Circular dichroism measurements

Circular dichroism spectra were acquired using a Chirascan spectrometer from Applied Photophysics. AChE (0.6 µM) and MIP (4, 10 nM) in deionized water were added to a 1 mm pathlength cuvette and the signal allowed to stabilize. 6 scans were then performed and averaged from 200-270 nm using 0.5 nm steps.

6.14. Enzyme activity assays

Activity assays were adapted from the protocol booklet provided by Abcam (ab138871). Stock solutions were prepared as described in the assay kit. AChE (100 µL) was incubated with each MIP (100 µL) for 15 minutes before addition of 50 µL to wells in triplicate. 5,5'-dithio-bis-(2-nitrobenzoic acid) and acetylthiocholine were combined before simultaneous addition to each of the test wells (50 µL) to initiate the reaction.

Measurements were run continuously using a Hidex Sense microplate reader at OD=410 \pm 5 nm for 2000 s. In regeneration and prevention experiments, tacrine and malathion were added to final well concentrations of 50 nM and 300 μ M, respectively.

6.15. Synthesis of mMIPs

Iron oxide mNPs (Fe_3O_4 , 1 g, 50-100 nm) were dispersed in toluene (anhydrous, 45 mL) and 3-(trimethoxysilyl) propyl methacrylate (5 mL) added under stirring. This mixture was subsequently incubated under sonication for 4 hours. The synthesised iron oxide mNPs were separated from the solution through magnetic attraction and washed with toluene (6 x 50 mL) before drying under vacuum. The afforded acrylate functionalised mNPs (200 mg) were then included in the polymerisation mixture and MIPs synthesised as previously described.

6.16. Sandwich MINA for AChE

Both MIP solutions were sonicated for five minutes before use. A mixture of fluorescent and magnetic nanoMIPs (both 0.1 mg mL⁻¹) was prepared and added to a dilution series of AChE samples at the desired concentration range. MIP-AChE sample solutions were then dispensed into modified magnetic microplate wells in triplicate and the fluorescence measured. A filter set with excitation of 490/20 nm and emission of 535/20 nm with a dichroic mirror at 505 nm were used for all measurements.

CHAPTER 7: REFERENCES

1. C. Alexander, H. S. Andersson, L. I. Andersson, R. J. Ansell, N. Kirsch, I. A. Nicholls, J. O'Mahony and M. J. Whitcombe, *J. Mol. Recognit.*, 2006, **19**, 106-180.
2. A. G. Mayes and M. J. Whitcombe, *Adv. Drug Delivery Rev.*, 2005, **57**, 1742-1778.
3. K. Mosbach, *Trends Biochem. Sci.*, 1994, **19**, 9-14.
4. J. Wackerlig and P. A. Lieberzeit, *Sens. Actuators, B*, 2015, **207**, 144-157.
5. M. J. Whitcombe, N. Kirsch and I. A. Nicholls, *J. Mol. Recognit.*, 2014, **27**, 297-401.
6. G. Wulff, *Angew. Chem., Int. Ed. Engl.*, 1995, **34**, 1812-1832.
7. S. Ansari and M. Karimi, *Talanta*, 2017, **164**, 612-625.
8. T. Kubo and K. Otsuka, *TrAC, Trends Anal. Chem.*, 2016, **81**, 102-109.
9. L. Uzun and A. P. F. Turner, *Biosens. Bioelectron.*, 2016, **76**, 131-144.
10. S. Li, M. Zhu, M. J. Whitcombe, Sergey A. Piletsky and A. P. F. Turner, in *Molecularly Imprinted Catalysts*, Elsevier, Amsterdam, 2016, pp. 1-17.
11. P. Luliński, *Mater. Sci. Eng., C*, 2017, **76**, 1344-1353.
12. T. S. Bedwell and M. J. Whitcombe, *Anal. Bioanal. Chem.*, 2016, **408**, 1735-1751.
13. G. Vlatakis, L. I. Andersson, R. Muller and K. Mosbach, *Nature*, 1993, **361**, 645-647.
14. L. I. Andersson, R. Müller, G. Vlatakis and K. Mosbach, *Proc. Natl. Acad. Sci. U. S. A.*, 1995, **92**, 4788-4792.
15. L. I. Andersson, *Anal. Chem.*, 1996, **68**, 111-117.
16. H. Bengtsson, U. Roos and L. I. Andersson, *Anal. Commun.*, 1997, **34**, 233-235.
17. K. Haupt, A. Dzgoev and K. Mosbach, *Anal. Chem.*, 1998, **70**, 628-631.
18. S. A. Piletsky, E. V. Piletskaya, A. V. El'skaya, R. Levi, K. Yano and I. Karube, *Anal. Lett.*, 1997, **30**, 445-455.
19. P. Turkewitsch, B. Wandelt, G. D. Darling and W. S. Powell, *Anal. Chem.*, 1998, **70**, 2025-2030.
20. L. Ye, P. A. G. Cormack and K. Mosbach, *Anal. Commun.*, 1999, **36**, 35-38.
21. I. Surugiu, L. Ye, E. Yilmaz, A. Dzgoev, B. Danielsson, K. Mosbach and K. Haupt, *Analyst*, 2000, **125**, 13-16.
22. I. Surugiu, B. Danielsson, L. Ye, K. Mosbach and K. Haupt, *Anal. Chem.*, 2001, **73**, 487-491.
23. L. Ye and K. Mosbach, *J. Am. Chem. Soc.*, 2001, **123**, 2901-2902.
24. R. J. Ansell, D. Kriz and K. Mosbach, *Curr. Opin. Biotechnol.*, 1996, **7**, 89-94.

25. B. Selligren, *J. Chromatogr. A*, 1994, **673**, 133-141.
26. H. Kempe and M. Kempe, *Macromol. Rapid Commun.*, 2004, **25**, 315-320.
27. A. G. Mayes and K. Mosbach, *Anal. Chem.*, 1996, **68**, 3769-3774.
28. L. Zhang, G. Cheng and C. Fu, *React. Funct. Polym.*, 2003, **56**, 167-173.
29. J. Haginaka, H. Takehira, K. Hosoya and N. Tanaka, *J. Chromatogr. A*, 1999, **849**, 331-339.
30. A. Abouzarzadeh, M. Forouzani, M. Jahanshahi and N. Bahramifar, *J. Mol. Recognit.*, 2012, **25**, 404-413.
31. S. Boonpangrak, V. Prachayasittikul, L. Bülow and L. Ye, *J. Appl. Polym. Sci.*, 2006, **99**, 1390-1398.
32. O. Brüggemann, K. Haupt, L. Ye, E. Yilmaz and K. Mosbach, *J. Chromatogr. A*, 2000, **889**, 15-24.
33. Y. Jin, M. Jiang, Y. Shi, Y. Lin, Y. Peng, K. Dai and B. Lu, *Anal. Chim. Acta*, 2008, **612**, 105-113.
34. J. Li, B. Zu, Y. Zhang, X. Guo and H. Zhang, *J. Polym. Sci., Part A: Polym. Chem.*, 2010, **48**, 3217-3228.
35. M. Liu, Y. Li, J. Han and X. Dong, *J. Sep. Sci.*, 2014, **37**, 1118-1125.
36. Y. Liu, K. Hoshina and J. Haginaka, *Talanta*, 2010, **80**, 1713-1718.
37. T. Mausia, D. De Smet, Q. Guorun, C. Van Peteghem, D. Zhang, A. Wu and S. De Saeger, *Anal. Lett.*, 2011, **44**, 2633-2643.
38. C. Miura, N. Funaya, H. Matsunaga and J. Haginaka, *J. Pharm. Biomed. Anal.*, 2013, **85**, 288-294.
39. G. Pan, Y. Zhang, Y. Ma, C. Li and H. Zhang, *Angew. Chem. Int. Ed.*, 2011, **50**, 11731-11734.
40. S. Pardeshi, R. Dhodapkar and A. Kumar, *Food Chem.*, 2014, **146**, 385-393.
41. M. Seifi, M. Hassanpour Moghadam, F. Hadizadeh, S. Ali-Asgari, J. Aboli and S. A. Mohajeri, *Int. J. Pharm.*, 2014, **471**, 37-44.
42. R. C. Stringer, S. Gangopadhyay and S. A. Grant, *Anal. Chim. Acta*, 2011, **703**, 239-244.
43. J. Wang, P. A. G. Cormack, D. C. Sherrington and E. Khoshdel, *Angew. Chem. Int. Ed.*, 2003, **42**, 5336-5338.
44. K. Yoshimatsu, J. LeJeune, D. A. Spivak and L. Ye, *Analyst*, 2009, **134**, 719-724.
45. W. Zhang, N. Tan, X. Jia, G. Wang, W. Long, X. Li, S. Liao and D. Hou, *Mater. Sci. Eng., C*, 2015, **53**, 166-174.
46. C. Zhao, J. Dai, Z. Zhou, X. Dai, Y. Zou, P. Yu, T. Zou, C. Li and Y. Yan, *J. Appl. Polym. Sci.*, 2014, **131**, n/a-n/a.
47. J. Cao, X. Zhang, X. He, L. Chen and Y. Zhang, *Chem. Asia. J.*, 2014, **9**, 526-533.
48. J. Liu, L. Zhang, L. Li Han Song, Y. Liu, H. Tang and Y. Li, *J. Sep. Sci.*, 2015, **38**, 1172-1178.
49. S. R. Carter and S. Rimmer, *Adv. Mater.*, 2002, **14**, 667-670.
50. D. Y. Ko, H. J. Lee and B. Jeong, *Macromol. Rapid Commun.*, 2006, **27**, 1367-1372.
51. R. Liu, G. Guan, S. Wang and Z. Zhang, *Analyst*, 2011, **136**, 184-190.
52. N. Pérez, M. J. Whitcombe and E. N. Vulfson, *J. Appl. Polym. Sci.*, 2000, **77**, 1851-1859.
53. N. Pérez, M. J. Whitcombe and E. N. Vulfson, *Macromolecules*, 2001, **34**, 830-836.

54. N. Pérez-Moral and A. G. Mayes, *Langmuir*, 2004, **20**, 3775-3779.
55. Z. Zhang, L. Liu, H. Li and S. Yao, *Appl. Surf. Sci.*, 2009, **255**, 9327-9332.
56. R. E. Fairhurst, C. Chassaing, R. F. Venn and A. G. Mayes, *Biosens. Bioelectron.*, 2004, **20**, 1098-1105.
57. M. R. Halhalli, C. S. A. Aureliano, E. Schillinger, C. Sulitzky, M. M. Titirici and B. Sellergren, *Polym. Chem.*, 2012, **3**, 1033-1042.
58. H. He, G. Fu, Y. Wang, Z. Chai, Y. Jiang and Z. Chen, *Biosens. Bioelectron.*, 2010, **26**, 760-765.
59. Y. Li, W.-H. Zhou, H.-H. Yang and X.-R. Wang, *Talanta*, 2009, **79**, 141-145.
60. B. Sellergren, B. Rückert and A. J. Hall, *Adv. Mater.*, 2002, **14**, 1204-1208.
61. X. Shen and L. Ye, *Chem. Commun.*, 2011, **47**, 10359-10361.
62. T. Zhou, X. Shen, S. Chaudhary and L. Ye, *J. Appl. Polym. Sci.*, 2014, **131**, n/a-n/a.
63. T. Zhou, K. Zhang, T. Kamra, L. Bulow and L. Ye, *J. Mater. Chem. B*, 2015, **3**, 1254-1260.
64. M. M. Titirici, A. J. Hall and B. Sellergren, *Chem. Mater.*, 2002, **14**, 21-23.
65. E. Yilmaz, K. Haupt and K. Mosbach, *Angew. Chem. Int. Ed.*, 2000, **39**, 2115-2118.
66. D. Vaihinger, K. Landfester, I. Kräuter, H. Brunner and G. E. M. Tovar, *Macromol. Chem. Phys.*, 2002, **203**, 1965-1973.
67. N. Pérez-Moral and A. G. Mayes, *Anal. Chim. Acta*, 2004, **504**, 15-21.
68. S. Wei, A. Molinelli and B. Mizaikoff, *Biosens. Bioelectron.*, 2006, **21**, 1943-1951.
69. K. Yoshimatsu, K. Reimhult, A. Krozer, K. Mosbach, K. Sode and L. Ye, *Anal. Chim. Acta*, 2007, **584**, 112-121.
70. H. Kempe and M. Kempe, *Anal. Chem.*, 2006, **78**, 3659-3666.
71. B. Tse Sum Bui and K. Haupt, *J. Mol. Recognit.*, 2011, **24**, 1123-1129.
72. S. H. Cheong, S. McNiven, A. Rachkov, R. Levi, K. Yano and I. Karube, *Macromolecules*, 1997, **30**, 1317-1322.
73. S.-H. Cheong, A. E. Rachkov, J.-K. Park, K. Yano and I. Karube, *J. Polym. Sci., Part A: Polym. Chem.*, 1998, **36**, 1725-1732.
74. Y. Long, J. Y. N. Philip, K. Schillén, F. Liu and L. Ye, *J. Mol. Recognit.*, 2011, **24**, 619-630.
75. K. R. Noss, A. D. Vaughan and M. E. Byrne, *J. Appl. Polym. Sci.*, 2008, **107**, 3435-3441.
76. A. E. Rachkov, S.-H. Cheong, A. V. El'skaya, K. Yano and I. Karube, *Polym. Adv. Technol.*, 1998, **9**, 511-519.
77. G. Orellana Moreleda, S. Aparicio Lara, M. Moreno Bondi and E. Benito Peña, *Spanish Patent ES 2197811*, 2004.
78. E. Benito-Peña, M. C. Moreno-Bondi, S. Aparicio, G. Orellana, J. Cederfur and M. Kempe, *Anal. Chem.*, 2006, **78**, 2019-2027.
79. J. L. Urraca, M. C. Moreno-Bondi, G. Orellana, B. Sellergren and A. J. Hall, *Anal. Chem.*, 2007, **79**, 4915-4923.
80. C.-H. Lu, W.-H. Zhou, B. Han, H.-H. Yang, X. Chen and X.-R. Wang, *Anal. Chem.*, 2007, **79**, 5457-5461.
81. J. Matsui, T. Sodeyama, K. Tamaki and N. Sugimoto, *Chem. Commun.*, 2006, DOI: 10.1039/B604354B, 3217-3219.
82. K. Sreenivasan, *J. Appl. Polym. Sci.*, 2001, **82**, 889-893.

83. R. Suedee, T. Srichana, T. Chuchohome and U. Kongmark, *J. Chromatogr. B*, 2004, **811**, 191-200.
84. R. Suedee, V. Seechamnaturakit, A. Sukswan and B. Canyuk, *Int. J. Mol. Sci.*, 2008, **9**, 2333.
85. C. E. Hunt, P. Pasetto, R. J. Ansell and K. Haupt, *Chem. Commun.*, 2006, DOI: 10.1039/B516194K, 1754-1756.
86. X.-A. Ton, V. Acha, K. Haupt and B. Tse Sum Bui, *Biosens. Bioelectron.*, 2012, **36**, 22-28.
87. N. W. Turner, C. I. Holdsworth, A. McCluskey and M. C. Bowyer, *Aust. J. Chem.*, 2012, **65**, 1405-1412.
88. P. K. Ivanova-Mitseva, A. Guerreiro, E. V. Piletska, M. J. Whitcombe, Z. Zhou, P. A. Mitsev, F. Davis and S. A. Piletsky, *Angew. Chem. Int. Ed.*, 2012, **51**, 5196-5199.
89. W. Wan, M. Biyikal, R. Wagner, B. Sellergren and K. Rurack, *Angew. Chem. Int. Ed.*, 2013, **52**, 7023-7027.
90. Y. Zhao, Y. Ma, H. Li and L. Wang, *Anal. Chem.*, 2012, **84**, 386-395.
91. M.-H. Lee, J. L. Thomas, Y.-C. Chen, W.-T. Chin and H.-Y. Lin, *Microchim. Acta*, 2013, **180**, 1393-1399.
92. H. Liu, L. Ren, G. Fang, H. Li and S. Wang, *Anal. Methods*, 2013, **5**, 5677-5683.
93. S. Wang, Z. Xu, G. Fang, Y. Zhang, B. Liu and H. Zhu, *J. Agric. Food. Chem.*, 2009, **57**, 4528-4534.
94. G. Fang, J. Lu, M. Pan, W. Li, L. Ren and S. Wang, *Food Anal. Methods*, 2011, **4**, 590-597.
95. J.-P. Wang, W.-W. Tang, G.-Z. Fang, M.-F. Pan and S. Wang, *J. Chin. Chem. Soc.*, 2011, **58**, 463-469.
96. L. Meng, X. Qiao, Z. Xu, J. Xin and L. Wang, *Food Anal. Methods*, 2012, **5**, 1229-1236.
97. D. Zhao, X. Qiao, Z. Xu, R. Xu and Z. Yan, *J. Immunoassay Immunochem.*, 2013, **34**, 16-29.
98. X. Du, F. Zhang, H. Zhang, Y. Wen and T. Saren, *Food Agric. Immunol.*, 2014, **25**, 411-422.
99. Q. Sun, L. Xu, Y. Ma, X. Qiao and Z. Xu, *J. Sci. Food Agric.*, 2014, **94**, 102-108.
100. C. Shi, X. Liu, L. Song, X. Qiao and Z. Xu, *Food Anal. Methods*, 2015, **8**, 2496-2503.
101. X. Bi and Z. Liu, *Anal. Chem.*, 2014, **86**, 959-966.
102. A. Poma, A. Guerreiro, M. J. Whitcombe, E. V. Piletska, A. P. F. Turner and S. A. Piletsky, *Adv. Funct. Mater.*, 2013, **23**, 2821-2827.
103. I. Chianella, A. Guerreiro, E. Moczko, J. S. Caygill, E. V. Piletska, I. M. P. De Vargas Sansalvador, M. J. Whitcombe and S. A. Piletsky, *Anal. Chem.*, 2013, **85**, 8462-8468.
104. X. Hu, G. Li, M. Li, J. Huang, Y. Li, Y. Gao and Y. Zhang, *Adv. Funct. Mater.*, 2008, **18**, 575-583.
105. N. Griffete, H. Frederich, A. Maître, S. Ravaine, M. M. Chehimi and C. Mangeney, *Langmuir*, 2012, **28**, 1005-1012.
106. C. Guo, C. Zhou, N. Sai, B. Ning, M. Liu, H. Chen and Z. Gao, *Sens. Actuators, B*, 2012, **166**, 17-23.
107. F. Liu, S. Huang, F. Xue, Y. Wang, Z. Meng and M. Xue, *Biosens. Bioelectron.*, 2012, **32**, 273-277.

108. X. Wang, Z. Mu, R. Liu, Y. Pu and L. Yin, *Food Chem.*, 2013, **141**, 3947-3953.
109. F. Xue, T.-r. Duan, S.-y. Huang, Q.-h. Wang, M. Xue and Z.-h. Meng, *J. Nanomaterials*, 2013, **2013**, 5-5.
110. Y. Zhang, Z. Pan, Y. Yuan, Z. Sun, J. Ma, G. Huang, F. Xing and J. Gao, *PCCP*, 2013, **15**, 17250-17256.
111. N. Casis, C. Busatto, M. M. Fidalgo de Cortalezzi, S. Ravaine and D. A. Estenoz, *Polym. Int.*, 2015, **64**, 773-779.
112. J. Hou, H. Zhang, Q. Yang, M. Li, L. Jiang and Y. Song, *Small*, 2015, **11**, 2738-2742.
113. N. Sai, Y. Wu, Z. Sun, G. Huang and Z. Gao, *Talanta*, 2015, **144**, 157-162.
114. W. Bai, N. A. Gariano and D. A. Spivak, *J. Am. Chem. Soc.*, 2013, **135**, 6977-6984.
115. L. Wang and Z. Zhang, *Sens. Actuators, B*, 2008, **133**, 40-45.
116. W. Liu, Y. Guo, J. Luo, J. Kou, H. Zheng, B. Li and Z. Zhang, *Spectrochim. Acta, Part A*, 2015, **141**, 51-57.
117. R. V. Shutov, A. Guerreiro, E. Moczko, I. P. de Vargas-Sansalvador, I. Chianella, M. J. Whitcombe and S. A. Piletsky, *Small*, 2014, **10**, 1086-1089.
118. J. Ye, Y. Chen and Z. Liu, *Angew. Chem. Int. Ed.*, 2014, **53**, 10386-10389.
119. D. Wang, N. Gan, H. Zhang, T. Li, L. Qiao, Y. Cao, X. Su and S. Jiang, *Biosens. Bioelectron.*, 2015, **65**, 78-82.
120. S. Chen, N. Gan, H. Zhang, F. Hu, T. Li, H. Cui, Y. Cao and Q. Jiang, *Anal. Bioanal. Chem.*, 2015, **407**, 2499-2507.
121. M. Peeters, P. Csipai, B. Geerets, A. Weustenraed, B. van Grinsven, R. Thoelen, J. Gruber, W. De Ceuninck, T. J. Cleij, F. J. Troost and P. Wagner, *Anal. Bioanal. Chem.*, 2013, **405**, 6453-6460.
122. M. Peeters, S. Kobben, K. L. Jiménez-Monroy, L. Modesto, M. Kraus, T. Vandenryt, A. Gaulke, B. van Grinsven, S. Ingebrandt, T. Junkers and P. Wagner, *Sens. Actuators, B*, 2014, **203**, 527-535.
123. K. Bers, K. Eersels, B. van Grinsven, M. Daemen, J. F. J. Bogie, J. J. A. Hendriks, E. E. Bouwmans, C. Püttmann, C. Stein, S. Barth, G. M. J. Bos, W. T. V. Germeraad, W. De Ceuninck and P. Wagner, *Langmuir*, 2014, **30**, 3631-3639.
124. K. Eersels, B. van Grinsven, M. Khorshid, V. Somers, C. Püttmann, C. Stein, S. Barth, H. Diliën, G. M. J. Bos, W. T. V. Germeraad, T. J. Cleij, R. Thoelen, W. De Ceuninck and P. Wagner, *Langmuir*, 2015, **31**, 2043-2050.
125. K. Eersels, B. van Grinsven, T. Vandenryt, K. L. Jiménez-Monroy, M. Peeters, V. Somers, C. Püttmann, C. Stein, S. Barth, G. M. J. Bos, W. T. V. Germeraad, H. Diliën, T. J. Cleij, R. Thoelen, W. D. Ceuninck and P. Wagner, *Phys. Status Solidi A*, 2015, **212**, 1320-1326.
126. C. Nantasenamat, H. Li, C. Isarankura-Na-Ayudhya and V. Prachayasittikul, *Chemom. Intell. Lab. Syst.*, 2012, **116**, 128-136.
127. J. Hu, X. Mao, S. Cao and X. Yuan, *Polym. Sci., Ser. A*, 2010, **52**, 328-339.
128. D. S. Janiak and P. Kofinas, *Anal. Bioanal. Chem.*, 2007, **389**, 399-404.
129. D. R. Kryscio, M. Q. Fleming and N. A. Peppas, *Macromol. Biosci.*, 2012, **12**, 1137-1144.
130. D. R. Kryscio, M. Q. Fleming and N. A. Peppas, *Biomed. Microdevices*, 2012, **14**, 679-687.
131. E. Verheyen, J. P. Schillemans, M. van Wijk, M.-A. Demeniex, W. E. Hennink and C. F. van Nostrum, *Biomaterials*, 2011, **32**, 3008-3020.

132. S. Li, S. Cao, M. J. Whitcombe and S. A. Piletsky, *Prog. Polym. Sci.*, 2014, **39**, 145-163.
133. M. J. Whitcombe, I. Chianella, L. Larcombe, S. A. Piletsky, J. Noble, R. Porter and A. Horgan, *Chem. Soc. Rev.*, 2011, **40**, 1547-1571.
134. A. Rachkov and N. Minoura, *Biochim. Biophys. Acta, Protein Struct. Mol. Enzymol.*, 2001, **1544**, 255-266.
135. X. Bi and Z. Liu, *Anal. Chem.*, 2014, **86**, 12382-12389.
136. X. Tu, P. Muhammad, J. Liu, Y. Ma, S. Wang, D. Yin and Z. Liu, *Anal. Chem.*, 2016, **88**, 12363-12370.
137. P. Muhammad, X. Tu, J. Liu, Y. Wang and Z. Liu, *ACS Appl. Mater. Interfaces*, 2017, **9**, 12082-12091.
138. J. Xu, K. Haupt and B. Tse Sum Bui, *ACS Appl. Mater. Interfaces*, 2017, **9**, 24476-24483.
139. F. Lanza and B. Sellergren, *Anal. Chem.*, 1999, **71**, 2092-2096.
140. T. Takeuchi, D. Fukuma and J. Matsui, *Anal. Chem.*, 1999, **71**, 285-290.
141. A. Rachkov and N. Minoura, *J. Chromatogr. A*, 2000, **889**, 111-118.
142. H. R. Culver and N. A. Peppas, *Chem. Mater.*, 2017, **29**, 5753-5761.
143. Y. Hoshino, T. Kodama, Y. Okahata and K. J. Shea, *J. Am. Chem. Soc.*, 2008, **130**, 15242-15243.
144. F. Canfarotta, A. Poma, A. Guerreiro and S. Piletsky, *Nat. Protoc.*, 2016, **11**, 443.
145. M. Baker, *Nature*, 2015, **521**, 274-276.
146. A. Bradbury and A. Pluckthun, *Nature*, 2015, **518**, 27-29.
147. K. Groff, J. Brown and A. J. Clippinger, *Biotechnol. Adv.*, 2015, **33**, 1787-1798.
148. NRC, *National Academy Press, Washington, D.C.*, 1999.
149. J. A. Ubersax and J. E. Ferrell Jr, *Nat. Rev. Mol. Cell Biol.*, 2007, **8**, 530.
150. M. Mann, S.-E. Ong, M. Grønborg, H. Steen, O. N. Jensen and A. Pandey, *Trends Biotechnol.*, 2002, **20**, 261-268.
151. H. C. Harsha and A. Pandey, *Mol. Oncol.*, 2010, **4**, 482-495.
152. Y. Li-Rong, I. H. J. and V. T. D., *Proteomics: Clin. Appl.*, 2007, **1**, 1042-1057.
153. C. Sun and R. Bernards, *Trends Biochem. Sci.*, 2014, **39**, 465-474.
154. A. S. Banks, F. E. McAllister, J. P. Camporez, P. J. Zushin, M. J. Jurczak, D. Laznik-Bogoslavski, G. I. Shulman, S. P. Gygi and B. M. Spiegelman, *Nature*, 2015, **517**, 391-395.
155. Y. Y. Bahk, M. Ahsan-Ul-Bari and Y. J. Kim, *J. Microbiol. Biotechnol.*, 2013, **23**, 279-288.
156. M. H. Flight, *Nat Rev Drug Discov*, 2013, **12**, 739.
157. M. Steger, F. Tonelli, G. Ito, P. Davies, M. Trost, M. Vetter, S. Wachter, E. Lorentzen, G. Duddy, S. Wilson, M. A. Baptista, B. K. Fiske, M. J. Fell, J. A. Morrow, A. D. Reith, D. R. Alessi and M. Mann, *Elife*, 2016, **5**.
158. S. Hartmann, A. J. Ridley and S. Lutz, *Front Pharmacol*, 2015, **6**, 276.
159. R. Kumar, V. P. Singh and K. M. Baker, *J Mol Cell Cardiol*, 2007, **42**, 1-11.
160. J. D. Clark, M. E. Flanagan and J.-B. Telliez, *J. Med. Chem.*, 2014, **57**, 5023-5038.
161. R. Galien, *Pharmacol Rep*, 2016, **68**, 789-796.
162. A. Pandey, A. V. Podtelejnikov, B. Blagoev, X. R. Bustelo, M. Mann and H. F. Lodish, *Proc Natl Acad Sci U S A*, 2000, **97**, 179-184.
163. K. Marcus, D. Immler, J. Sternberger and H. E. Meyer, *Electrophoresis*, 2000, **21**, 2622-2636.

164. M. O. Collins, L. Yu and J. S. Choudhary, *Proteomics*, 2007, **7**, 2751-2768.
165. J. Chen, S. Shinde, P. Subedi, C. Wierzbicka, B. Sellergren, S. Helling and K. Marcus, *J. Chromatogr. A*, 2016, **1471**, 45-50.
166. L. Bllaci, S. B. Torsetnes, C. Wierzbicka, S. Shinde, B. Sellergren, A. Rogowska-Wrzesinska and O. N. Jensen, *Anal. Chem.*, 2017, **89**, 11332-11340.
167. C. Wierzbicka, S. B. Torsetnes, O. N. Jensen, S. Shinde and B. Sellergren, *RSC Adv.*, 2017, **7**, 17154-17163.
168. C. Wierzbicka, K. Gajoch, O. N. Jensen and B. Sellergren, *Submitted for publication*, 2017.
169. C. Wierzbicka, M. Liu, D. Bauer, K. Irgum and B. Sellergren, *J. Mater. Chem. B*, 2017, **5**, 953-960.
170. D. S. Smith and S. A. Eremin, *Anal. Bioanal. Chem.*, 2008, **391**, 1499-1507.
171. Amersham-Biosciences, *Fluorescence screening reagents guide*.
172. Amersham-Biosciences, *Amersham Cy3B mono-reactive dye Product Booklet*.
173. G. T. Hermanson, *Bioconjugate Techniques*, Elsevier Science, 2010.
174. S. S. Piletsky, A. E. G. Cassa, E. V. Piletska, J. Czulak and S. A. Piletsky, *Submitted for publication*, 2018.
175. R. Mahajanb, M. Rouhia, S. Shindea, T. Bedwell, S. Piletsky, I. Nicholls and B. Sellergren, *Submitted for publication*, 2018.
176. J. Massoulié, L. Pezzementi, S. Bon, E. Krejci and F.-M. Vallette, *Prog. Neurobiol.*, 1993, **41**, 31-91.
177. I. Silman and J. L. Sussman, *Chem. Biol. Interact.*, 2008, **175**, 3-10.
178. J. Sussman, M. Harel, F. Frolow, C. Oefner, A. Goldman, L. Toker and I. Silman, *Science*, 1991, **253**, 872-879.
179. Z. Radić, E. Reiner and P. Taylor, *Mol. Pharmacol.*, 1991, **39**, 98-104.
180. A. Ordentlich, D. Barak, C. Kronman, N. Ariel, Y. Segall, B. Velan and A. Shafferman, *J. Biol. Chem.*, 1995, **270**, 2082-2091.
181. L. E. Hebert, P. A. Scherr, L. A. Beckett and et al., *JAMA*, 1995, **273**, 1354-1359.
182. A. Burns and S. Iliffe, *BMJ*, 2009, **338**.
183. S. Ahmadi-Abhari, M. Guzman-Castillo, P. Bandosz, M. J. Shipley, G. Muniz-Terrera, A. Singh-Manoux, M. Kivimäki, A. Steptoe, S. Capewell, M. O'Flaherty and E. J. Brunner, *BMJ*, 2017, **358**.
184. *US Pat.*, 9,377,466, 2016.
185. M. Hashimoto, E. Rockenstein, L. Crews and E. Masliah, *NeuroMol. Med.*, 2003, **4**, 21-35.
186. C. Hock, U. Konietzko, J. R. Streffer, J. Tracy, A. Signorell, B. Müller-Tillmanns, U. Lemke, K. Henke, E. Moritz, E. Garcia, M. A. Wollmer, D. Umbricht, D. J. F. de Quervain, M. Hofmann, A. Maddalena, A. Papassotiropoulos and R. M. Nitsch, *Neuron*, 2003, **38**, 547-554.
187. J. M. Orgogozo, S. Gilman, J. F. Dartigues, B. Laurent, M. Puel, L. C. Kirby, P. Jouanny, B. Dubois, L. Eisner, S. Flitman, B. F. Michel, M. Boada, A. Frank and C. Hock, *Neurology*, 2003, **61**, 46-54.
188. M. Pfeifer, S. Boncristiano, L. Bondolfi, A. Stalder, T. Deller, M. Staufenbiel, P. M. Mathews and M. Jucker, *Science*, 2002, **298**, 1379.
189. E. K. Perry, R. H. Perry, G. Blessed and B. E. Tomlinson, *Neuropathol. Appl. Neurobiol.*, 1978, **4**, 273-277.
190. E. K. Perry, B. E. Tomlinson, G. Blessed, K. Bergmann, P. H. Gibson and R. H. Perry, *Br. Med. J.*, 1978, **2**, 1457-1459.

191. V. N. Talesa, *Mech Ageing Dev*, 2001, **122**, 1961-1969.
192. R. M. Lane, S. G. Potkin and A. Enz, *Int. J. Neuropsychopharmacol.*, 2006, **9**, 101-124.
193. R. J. Polinsky, *Clin Ther*, 1998, **20**, 634-647.
194. B. Reisberg , R. Doody , A. Stöffler , F. Schmitt , S. Ferris and H. J. Möbius N. *Engl. J. Med.*, 2003, **348**, 1333-1341.
195. L. S. Schneider, *J Clin Psychiatry*, 1996, **57 Suppl 14**, 30-36.
196. B. K. Alldredge, R. L. Corelli, M. E. Ernst, B. J. Guglielmo, P. A. Jacobson, W. A. Kradjan and B. R. Williams, *Koda-Kimble and Young's applied therapeutics: The clinical use of drugs*, 2013.
197. J. R. Reigart and J. R. Roberts, *Recognition and Management of Pesticide Poisonings*, 1999.
198. K. M. George, T. Schule, L. E. Sandoval, L. L. Jennings, P. Taylor and C. M. Thompson, *J. Biol. Chem.*, 2003, **278**, 45512-45518.
199. K.-H. Krause, C. van Thriel, P. A. De Sousa, M. Leist and J. G. Hengstler, *Arch. Toxicol.*, 2013, **87**, 1877-1881.
200. S. P. Singh, A. D. Aggarwal, S. S. Oberoi, K. K. Aggarwal, A. S. Thind, D. S. Bhullar, D. S. Walia and P. S. Chahal, *J Forensic Leg Med*, 2013, **20**, 14-18.
201. C. Barras, *New Sci.*, 2018, **237**, 7-7.
202. D. A. Jett and D. T. Yeung, *Proc. Am. Thorac. Soc.*, 2010, **7**, 254-256.
203. M. Peplow, *Chem. Eng. News*, 2018, **96**, 3-3.
204. Y. Rosman, A. Eisenkraft, N. Milk, A. Shiyovich, N. Ophir, S. Shrot, Y. Kreiss and M. Kassirer, *Ann. Intern. Med.*, 2014, **160**, 644-648.
205. H. Thiermann, F. Worek and K. Kehe, *Chem. Biol. Interact.*, 2013, **206**, 435-443.
206. F. Worek, T. Wille, M. Koller and H. Thiermann, *Chem. Biol. Interact.*, 2013, **203**, 125-128.
207. P. Masson, *Toxicol. Lett.*, 2011, **206**, 5-13.
208. R. R. Chapleau, P. J. Robinson, J. J. Schlager and J. M. Gearhart, *Theor. Biol. Med. Modell.*, 2014, **11**, 42.
209. R. R. Chapleau, C. A. McElroy, C. D. Ruark, E. J. Fleming, A. B. Ghering, J. J. Schlager, L. D. Poepelman and J. M. Gearhart, *J. Biomol. Screening*, 2015, **20**, 1142-1149.
210. Y. Bourne, L. Renault, S. Essono, G. Mondielli, P. Lamourette, D. Boquet, J. Grassi and P. Marchot, *PLoS ONE*, 2013, **8**, e77226.
211. C. E. Olson, V. Chhajlani, J. T. August and E. D. Schmell, *Arch. Biochem. Biophys.*, 1990, **277**, 361-367.
212. M. H. Remy, Y. Frobert and J. Grassi, *Eur. J. Biochem.*, 1995, **231**, 651-658.
213. A. E. Reyes, D. R. Perez, A. Alvarez, J. Garrido, M. K. Gentry, B. P. Doctor and N. C. Inestrosa, *Biochem. Biophys. Res. Commun.*, 1997, **232**, 652-655.
214. N. C. Inestrosa, A. Alvarez, C. A. Pérez, R. D. Moreno, M. Vicente, C. Linker, O. I. Casanueva, C. Soto and J. Garrido, *Neuron*, 1996, **16**, 881-891.
215. J. H. Kim, G. N. Choi, J. H. Kwak, H. R. Jeong, C.-H. Jeong and H. J. Heo, *Food Sci. Biotechnol.*, 2011, **20**, 311-318.
216. Y. Shen, R. Sheng, J. Zhang, Q. He, B. Yang and Y. Hu, *Biorg. Med. Chem.*, 2008, **16**, 7646-7653.
217. G. V. De Ferrari, M. A. Canales, I. Shin, L. M. Weiner, I. Silman and N. C. Inestrosa, *Biochemistry*, 2001, **40**, 10447-10457.

218. Y. Bourne, P. Taylor, P. E. Bougis and P. Marchot, *J. Biol. Chem.*, 1999, **274**, 2963-2970.
219. G. Johnson and S. Moore, *The Peripheral Anionic Site of Acetylcholinesterase: Structure, Functions and Potential Role in Rational Drug Design*, 2006.
220. J. K. Atwal, Y. Chen, C. Chiu, D. L. Mortensen, W. J. Meilandt, Y. Liu, C. E. Heise, K. Hoyte, W. Luk, Y. Lu, K. Peng, P. Wu, L. Rouge, Y. Zhang, R. A. Lazarus, K. Scearce-Levie, W. Wang, Y. Wu, M. Tessier-Lavigne and R. J. Watts, *Sci. Transl. Med.*, 2011, **3**, 84ra43-84ra43.
221. C. Saraiva, C. Praça, R. Ferreira, T. Santos, L. Ferreira and L. Bernardino, *J. Controlled Release*, 2016, **235**, 34-47.
222. X. Gao, J. Qian, S. Zheng, Y. Changyi, J. Zhang, S. Ju, J. Zhu and C. Li, *ACS Nano*, 2014, **8**, 3678-3689.
223. D. T. Wiley, P. Webster, A. Gale and M. E. Davis, *Proc. Natl. Acad. Sci. U. S. A.*, 2013, **110**, 8662-8667.
224. S. D. Kong, J. Lee, S. Ramachandran, B. P. Eliceiri, V. I. Shubayev, R. Lal and S. Jin, *J. Controlled Release*, 2012, **164**, 49-57.
225. S.-H. Cha, J. Hong, M. McGuffie, B. Yeom, J. S. VanEpps and N. A. Kotov, *ACS Nano*, 2015, **9**, 9097-9105.
226. N. O. Fischer, C. M. McIntosh, J. M. Simard and V. M. Rotello, *Proc. Natl. Acad. Sci. U. S. A.*, 2002, **99**, 5018-5023.
227. B. Sellergren, *Nat. Chem.*, 2010, **2**, 7.
228. A. Cutivet, C. Schembri, J. Kovensky and K. Haupt, *J. Am. Chem. Soc.*, 2009, **131**, 14699-14702.
229. A. Guerreiro, A. Poma, K. Karim, E. Moczko, J. Takarada, I. P. de Vargas-Sansalvador, N. Turner, E. Piletska, C. S. de Magalhães, N. Glazova, A. Serkova, A. Omelianova and S. Piletsky, *Adv. Healthcare Mater.*, 2014, **3**, 1426-1429.
230. C. Jinxing, Z. Kun, L. Shan, W. Mozhen, A. Anila and G. Xuewu, *Part. Part. Syst. Charact.*, 2017, **34**, 1600260.
231. Y.-J. Liao, Y.-C. Shiang, C.-C. Huang and H.-T. Chang, *Langmuir*, 2012, **28**, 8944-8951.
232. H. Zhang, J. Jiang, H. Zhang, Y. Zhang and P. Sun, *ACS Macro Letters*, 2013, **2**, 566-570.
233. Y. Hoshino, H. Koide, T. Urakami, H. Kanazawa, T. Kodama, N. Oku and K. J. Shea, *J. Am. Chem. Soc.*, 2010, **132**, 6644-6645.
234. F. Canfarotta, A. Waters, R. Sadler, P. McGill, A. Guerreiro, D. Papkovsky, K. Haupt and S. Piletsky, *Nano Res.*, 2016, **9**, 3463-3477.
235. Z. Wu, J. Hou, Y. Wang, M. Chai, Y. Xiong, W. Lu and J. Pan, *Int. J. Pharm.*, 2015, **496**, 1006-1014.
236. H. M. Berman, P. E. Bourne and J. Westbrook, *Curr. Proteomics*, 2004, **1**, 49-57.
237. J. Ponomarenko, H.-H. Bui, W. Li, N. Fusseder, P. E. Bourne, A. Sette and B. Peters, *BMC Bioinf.*, 2008, **9**, 514-514.
238. X.-M. Zhang, G. Liu and M.-J. Sun, *Brain Res.*, 2000, **868**, 157-164.
239. *GB Pat.*, GB1704823.2, 2017.
240. S. Bon, M. Vigny and J. Massoulié, *Proc. Natl. Acad. Sci. U. S. A.*, 1979, **76**, 2546-2550.
241. X. M. Zhang, G. Liu and M. J. Sun, *Brain Res.*, 2001, **895**, 277-282.
242. A. Poma, A. Guerreiro, S. Caygill, E. Moczko and S. Piletsky, *RSC Adv.*, 2014, **4**, 4203-4206.

243. J. Yang, R. Yan, A. Roy, D. Xu, J. Poisson and Y. Zhang, *Nat. Methods*, 2015, **12**, 7-8.
244. S. N. Abramson, M. H. Ellisman, T. J. Deerinck, Y. Maulet, M. K. Gentry, B. P. Doctor and P. Taylor, *J. Cell Biol.*, 1989, **108**, 2301-2311.
245. R. A. Ogert, M. K. Gentry, E. C. Richardson, C. D. De Al, S. N. Abramson, C. R. Alving, P. Taylor and B. P. Doctor, *J. Neurochem.*, 1990, **55**, 756-763.
246. H. M. Berman, J. Westbrook, Z. Feng, G. Gilliland, T. N. Bhat, H. Weissig, I. N. Shindyalov and P. E. Bourne, *Nucleic Acids Res.*, 2000, **28**, 235-242.
247. E. Boutet, D. Lieberherr, M. Tognolli, M. Schneider, P. Bansal, A. J. Bridge, S. Poux, L. Bougueleret and I. Xenarios, in *Plant Bioinformatics: Methods and Protocols*, ed. D. Edwards, Springer New York, New York, NY, 2016, DOI: 10.1007/978-1-4939-3167-5_2, pp. 23-54.
248. T. U. Consortium, *Nucleic Acids Res.*, 2015, **43**, D204-D212.
249. S. Simon and J. Massoulié, *J. Biol. Chem.*, 1997, **272**, 33045-33055.
250. J. L. Sussman and I. Silman, *Curr. Opin. Struct. Biol.*, 1992, **2**, 721-729.
251. H. Dvir, I. Silman, M. Harel, T. L. Rosenberry and J. L. Sussman, *Chem. Biol. Interact.*, 2010, **187**, 10-22.
252. G. L. Ellman, *Arch. Biochem. Biophys.*, 1958, **74**, 443-450.
253. D. Dingova, J. Leroy, A. Check, V. Garaj, E. Krejci and A. Hrabovska, *Anal. Biochem.*, 2014, **462**, 67-75.
254. R. A. Alberty and G. G. Hammes, *J. Phys. Chem.*, 1958, **62**, 154-159.
255. M. Harel, G. J. Kleywegt, R. B. G. Ravelli, I. Silman and J. L. Sussman, *Structure*, **3**, 1355-1366.
256. Y. Bourne, J. Grassi, P. E. Bougis and P. Marchot, *J. Biol. Chem.*, 1999, **274**, 30370-30376.
257. J. M. Bui and J. Andrew McCammon, *Chem. Biol. Interact.*, 2008, **175**, 303-304.
258. J. P. Colletier, B. Sanson, F. Nachon, E. Gabellieri, C. Fattorusso, G. Campiani and M. Weik, *J. Am. Chem. Soc.*, 2006, **128**, 4526-4527.
259. T. Shen, K. Tai, R. H. Henchman and J. A. McCammon, *Acc. Chem. Res.*, 2002, **35**, 332-340.
260. Y. Xu, J.-P. Colletier, M. Weik, G. Qin, H. Jiang, I. Silman and J. L. Sussman, *Biophys. J.*, 2010, **99**, 4003-4011.
261. M. B. Čolović, D. Z. Krstić, T. D. Lazarević-Pašti, A. M. Bondžić and V. M. Vasić, *Curr. Neuropharmacol.*, 2013, **11**, 315-335.
262. A. Abdu, *Acta Neurol. Scand.*, 1992, **85**, 69-74.
263. A. Roy, A. Kucukural and Y. Zhang, *Nat. Protoc.*, 2010, **5**, 725.
264. J. Yang and Y. Zhang, *Nucleic Acids Res.*, 2015, **43**, W174-W181.
265. Y. Zhang, *BMC Bioinf.*, 2008, **9**, 40.